AD_____

Award Number:W81XWH-09-1-0209

TITLE: Role of Cyclin E as an Early Event in Ovarian Carcinogenesis

PRINCIPAL INVESTIGATOR: Christine Walsh, M.D., M.S.

CONTRACTING ORGANIZATION: Cedars-Sinai Medical Center
Los Angeles, CA 90048-9004

REPORT DATE: April 2012

TYPE OF REPORT: Annual Summary

PREPARED FOR: U.S. Army Medical Research and Materiel Command
Fort Detrick, Maryland 21702-5012

REPORT DOCUMENTATION PAGE

Form Approved
OMB No. 0704-0188

1. REPORT DATE *(DD-MM-YYYY)*	2. REPORT TYPE	3. DATES COVERED *(From - To)*
April 2012	Annual Summary	1 April 2009 - 31 March 2012

4. TITLE AND SUBTITLE
Role of Cyclin E as an Early event in Ovarian Carcinogenesis

5a. CONTRACT NUMBER

5b. GRANT NUMBER
W81XWH-09-1-0209

5c. PROGRAM ELEMENT NUMBER

6. AUTHOR(S)
Christine Walsh, M.D., M.S.

5d. PROJECT NUMBER

5e. TASK NUMBER

5f. WORK UNIT NUMBER

7. PERFORMING ORGANIZATION NAME(S) AND ADDRESS(ES)

Cedars-Sinai Medical Center

Los Angeles, CA 90048-9004

8. PERFORMING ORGANIZATION REPORT NUMBER

9. SPONSORING / MONITORING AGENCY NAME(S) AND ADDRESS(ES)
U.S. Army Medical Research
And Materiel Command
Fort Detrick, Maryland
21702-5012

10. SPONSOR/MONITOR'S ACRONYM(S)

11. SPONSOR/MONITOR'S REPORT NUMBER(S)

12. DISTRIBUTION / AVAILABILITY STATEMENT
Approved for public release; distribution unlimited

13. SUPPLEMENTARY NOTES

14. ABSTRACT
At the genetic level, ovarian cancer is characterized by a large degree of genetic instability. High copy-number amplification at the *CCNE1* (cyclin E) gene locus is the single most notable recurrent change, occurring in about 20% of tumors. We have hypothesized that *CCNE1* gene amplification is an initiating event in the carcinogenic process of a subset of epithelial ovarian cancers. We have made progress towards testing our hypothesis of cyclin E-induced ovarian cancer initiation in a mouse model. We have also demonstrated the mechanisms underlying the synergistic cytotoxicity of ovarian cancer cells to combination treatment with bortezomib and a natural dietary phytochemical indole-3-carbinole (I3C). The translational relevance could be in the re-introduction of bortezomib to the therapeutic armamentarium against ovarian cancer if the in vitro results replicate in humans.

15. SUBJECT TERMS
Cyclin E, RB, bortezomib, Indole-3-Carbinol, mouse model, ovarian cancer initiation

16. SECURITY CLASSIFICATION OF:			17. LIMITATION OF ABSTRACT	18. NUMBER OF PAGES	19a. NAME OF RESPONSIBLE PERSON
a. REPORT	b. ABSTRACT	c. THIS PAGE			USAMRMC
U	U	U	UU	59	19b. TELEPHONE NUMBER *(include area code)*

Table of Contents

Page

INTRODUCTION

We are interested in defining the genetic changes that initiate and drive the aggressive behavior of epithelial ovarian malignancies. In a pilot study looking at the genetic changes occurring across the whole genome of high-grade papillary serous ovarian cancers, we identified *cyclin E* as an interesting candidate gene. We found high-copy number amplification of the *cyclin E* gene locus to be the single most notable recurrent genetic event. Furthermore, epidemiological evidence links the subset of cyclin E overexpressing epithelial ovarian cancers to an increased number of lifetime ovulatory cycles and the "incessant ovulation" theory of ovarian cancer causality. Experimental systems have shown deregulation of cyclin E levels to result in chromosomal instability, a hallmark feature of epithelial ovarian cancers. This led us to hypothesize that cyclin E deregulation is an important initial event in ovarian carcinogenesis. We proposed three specific aims: (1) to characterize the genetic events induced along with cyclin E amplification and overexpression; (2) to determine the role of cyclin E and its collaborating genetic events in ovarian cancer initiation; and (3) to define the subset of ovarian cancers with impaired cyclin E inhibition and to determine whether these tumors demonstrate an enhanced response to targeted therapy. Here, we report research accomplishments from the three years of the study.

BODY

Specific Aim 1: To characterize the genetic events induced along with cyclin E amplification and overexpression.

Task 1: DNA analysis for genetic events occurring with cyclin E gene amplification using anatomical samples.

Upon screening 72 ovarian cancer cases on a frozen tumor tissue microarray for *CCNE1* gene amplification using fluorescence in-situ hybridization (FISH), we identified 11 cases with a cluster pattern of cyclin E. These samples also underwent gene expression profiling on an Agilent Human 1A VS Chip. Together, these studies found a high correlation between *CCNE1* gene amplification and cyclin E overexpression. We planned to have these 11 samples arrayed with the Affymetrix 250K *Nsp* oligonucleotide microarray to determine the genetic events that occur commonly among ovarian cancer samples with *CCNE1* gene amplification. However, we put this task on hold as our collaborator generated Agilent array CGH data on 128 ovarian cancer samples from our tumor bank. Of these, 20 tumors demonstrated focal amplification of the *CCNE1* gene locus. Using Agilent DNA Analytics 4.0 software, we analyzed the eight tumors with the highest *CCNE1* gene amplification levels for common amplifications and deletions.

Amplified in > 50% of 8 tumors:

- **Chr 1:** *NDUFS5, MACF1*
- **Chr 2:** *ITGB5, MUC13, AB033063, CCDC48, BC122540, GP9, RAB43, ISY1, CNBP, COPG, H1FX*

- **Chr 3:** *SCHIP1, IL12A, AK097161, BC033011, IFT80, KHL24, YEATS2, MAP6D1, PARL, ABCC5*
- **Chr 8:** *ZMAT4*
- **Chr 9:** *PKN3, ZDHHC12, ZER1, TBC1D13, ENDOG, CCBL1, LRRC8A*
- **Chr 14:** *COCH, STRN3*
- **Chr 19:** *CACNA1A, AX721153, BC017035, ZNF100, ZNF43, AB062076, AK094793, POP4, PLEKHF1, CCNE1*
- **Chr 20:** *AK097804, BC023657, AB2099990, COMMD7, DNMT3B, MAPRE1*

Deleted in ≥ 50% of 8 tumors:

- **Chr 5:** *NDUFA12L, ADAMTS6*

We further characterized an additional 106 ovarian cancers by performing immunohistochemistry (IHC) and FISH analysis on corresponding formalin-fixed, paraffin-embedded tissues in order to make correlations between cyclin E expression and amplification. We specifically chose to analyze a subset of tumors for which microarray gene expression data had already been generated.

Cyclin E Immunohistochemistry: Formalin-fixed, paraffin-embedded tissue sections were stained for cyclin E using a standard IHC protocol. Briefly, slides were de-paraffinized, rehydrated, and treated with a citrate-based, high pH antigen retrieval solution at high temperature to unmask antigens (Antigen Unmasking Solution, Vector Labs, Burlingame, CA). The slides were then placed in a hydrogen peroxide bath to quench endogenous peroxidase activity, blocked with normal horse serum, and incubated with mouse monoclonal anti-cyclin E antibody (Vector Labs; catalog #: VP-C396). The antibody was used at a 1:50 dilution for one hour at room temperature. All subsequent steps were carried out using the Vectastain ABC Kit (Mouse IgG) (Vector Labs) followed by final staining using ImmPACT DAB Peroxidase Substrate (Vector Labs) and counterstaining with hematoxylin. After tissue sections were stained and analyzed, we observed varying levels of cyclin E staining in our samples (Fig. 1).

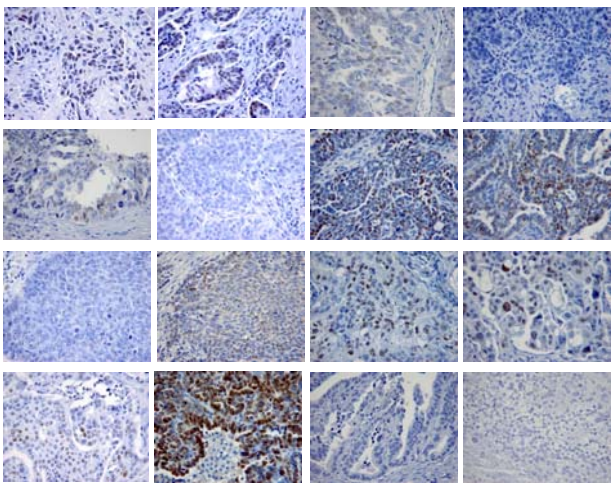

Figure 1. Cyclin E IHC of papillary serous ovarian carcinoma tissue. Tissue samples were stained using a standard IHC protocol. The cyclin E antibody used in the experiment was diluted 1:50 and incubated with tissue sections for 1 hour at room temperature. Slides were analyzed under a microscope and images were captured under a 40X objective lens.

Since varying levels of cyclin E staining were observed, the slides were scored by two individuals simultaneously using a dual-scoped microscope. The percent of the tumor cells staining positive was also determined. If no staining was observed, the section was given a score of 0. Sections that did show staining were scored as 1, 2 or 3 depending on the staining intensity (Fig. 2). Several sections had a variation in staining intensity within tumor cells and were thus scored as 1 to 2, or 2 to 3 (Fig. 2). The number of sections stained at each intensity is shown in Table 1.

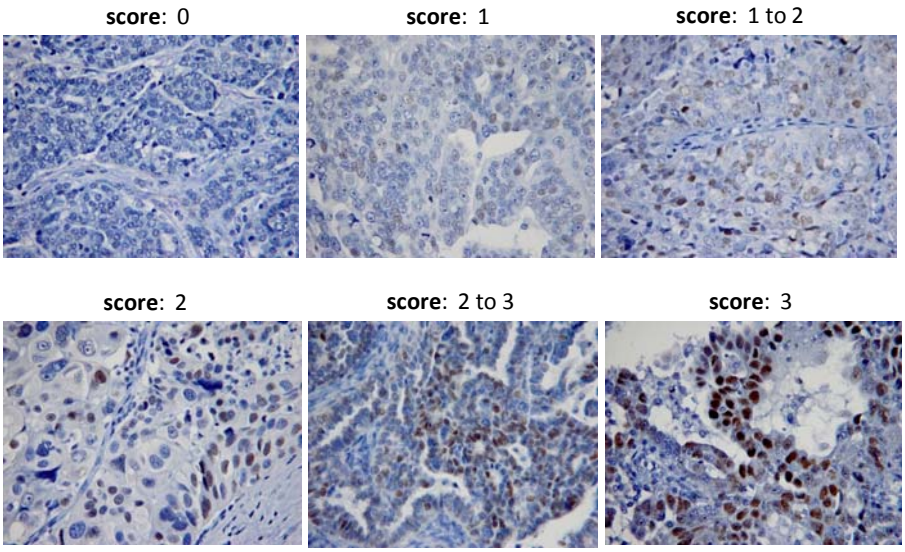

Figure 2. Scoring of cyclin E IHC sections. Stained tissue sections were observed under the microscope and scored as either 0 (no staining visible), 1, 1 to 2, 2, 2 to 3, or 3.

SCORE	0	1	1 to 2	2	2 to 3	3	
# slides	40	18	32	5	9	2	Total: 106

Table 1. Cyclin E IHC scores for papillary serous ovarian cancer cases

Fluorescent in-situ hybridization: The additional 106 human ovarian cancer cases were analyzed for cyclin E amplification using FISH analysis. First, a cyclin E FISH probe was prepared using the bacterial artificial chromosome (BAC) clone RPCI11.C-345J21. Cyclin E-specific primers were used in a PCR reaction to confirm the expression of cyclin E by the BAC clone (Fig. 3). A ~300 bp PCR product corresponding to cyclin E was detected.

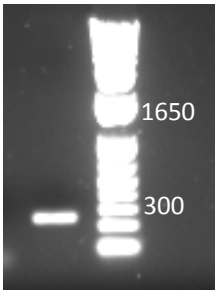

Figure 3. PCR of BAC clone to confirm expression of cyclin E. DNA isolated from BAC clone RPCI11.C-345J21 was used in a PCR reaction using cyclin E-specific primers. The PCR reaction was analyzed by gel electrophoresis and a cyclin E-specific band was detected at ~300 bp.

After confirming that the BAC clone did indeed express cyclin E, a nick translation reaction was performed to incorporate a red-dUTP label to the DNA. The labeling reaction was carried out overnight at 15°C and the following day, part of the reaction was analyzed by gel electrophoresis to determine the probe size (Fig. 4). The DNA smear was detected in the 250-300 bp range, as expected for an efficient labeling reaction. The remaining reaction was incubated with COT-1 DNA and ethanol-precipitated before re-suspension of the DNA pellet with hybridization buffer.

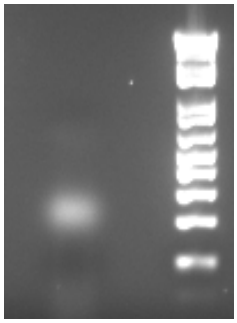

Figure 4. Nick translation labeling of cyclin E BAC with red-dUTP. To prepare the cyclin E FISH probe, 1 µg of BAC DNA was incubated with red-dUTP, dNTPs, nick translation buffer, and nick translation enzyme in an overnight reaction at 15°C. The following day, 5 µl of the translation reaction was analyzed by gel electrophoresis. The DNA smear was detected between 250-300 bp confirming that the reaction was efficient.

To perform the FISH analysis, slide sections were de-paraffinized, treated with a protease solution, denatured, and hybridized overnight with the red-dUTP-labeled cyclin E probe. The sections were then washed and analyzed by fluorescence microscopy to detect cyclin E and control probe signals. As a trial run, FISH was performed on a sample slide of blood cells using the red-dUTP lab-labeled cyclin E probe along with a commercially-available red-labeled cyclin E probe (Fig. 5). As seen, both probes specifically detected the cyclin E locus (red signal), indicating that the lab-labeled probe worked well as a FISH probe and could be used in further experiments.

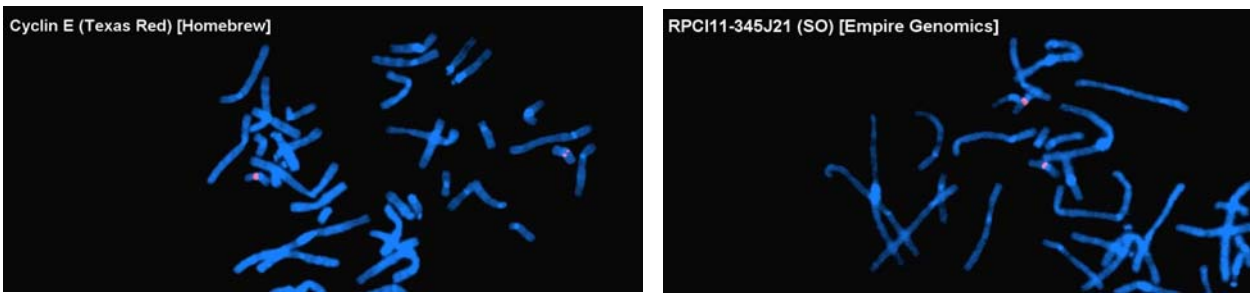

Figure 5. Cyclin E FISH of normal blood DNA. The lab-labeled cyclin E FISH probe (left panel) and a commercially-available cyclin E FISH probe (right panel) were used in a trial run FISH experiment to test the quality of the lab-labeled probe. Specific signals detecting the cyclin E gene locus were observed.

The next step in our cyclin E FISH optimization was to test our probe in OVCAR3 cells, an ovarian cancer cell line with known cyclin E amplification. OVCAR3 cells were grown

in culture on collagen and slides were prepared for FISH. A GFP-labeled, 19p telomere control probe was also added to the cyclin E probe mix. Cyclin E amplification was observed in OVCAR3 cells as indicated by strong RFP signals detected, often seen in a cluster pattern (Fig. 6). Compared to cyclin E, the GFP signal corresponding to the 19p control probe only showed two signals. These results indicated that the cyclin E probe was working properly and could detect gene amplification in a relevant cell line.

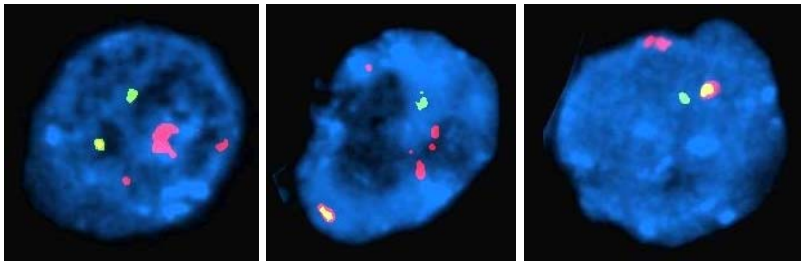

Figure 6. Cyclin E FISH in OVCAR3 cells. The cyclin E FISH probe and a control GFP-labeled 19p telomere control probe were used in a FISH analysis of OVCAR3 cells, an ovarian cancer cell line with known cyclin E amplification. Three different cells are shown and cyclin E amplification is seen with the red cluster pattern within each cell compared to the two GFP+ signals.

With FISH conditions optimized, we performed FISH analysis of our ovarian cancer samples. In collaboration with the clinical cytogenetics core at Cedars-Sinai Medical Center, the samples were stained with cyclin E and control probe. Within our sample set, we observed samples with no cyclin E amplication (score 0), low amplification or polysomy (score 1), high amplification (score 2), or very high amplification with signal clustering (score 3) (Fig. 7).

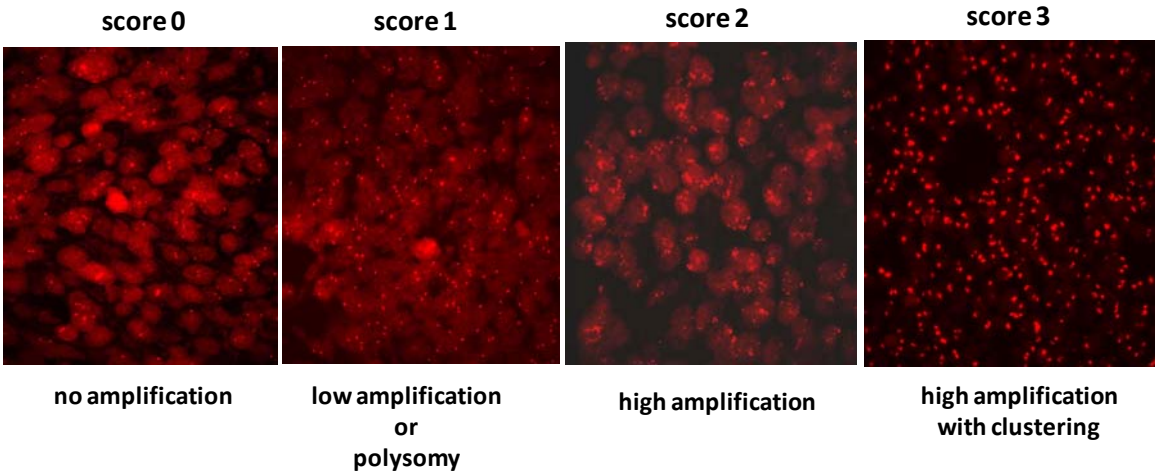

Figure 7: Scoring of cyclin E FISH slides. Papillary serous ovarian cancer specimens were analyzed by FISH for cyclin E amplification and scored. Samples displayed no amplification (score 0), low amplification or polysomy (score 1), high amplification (score 2), or high amplification with clustering (score 3).

In several samples, there was a distinct amplification of cyclin E in the tumor but not in the stroma, indicating that amplification was tumor-specific (Fig. 8). For many samples, there was also a correlation between cyclin E amplification and high cyclin E expression as determined by IHC (Fig. 16).

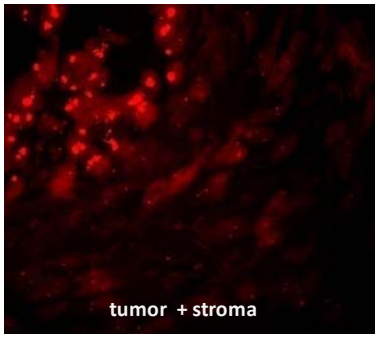

Figure 8. Cyclin E amplification in tumor but not in surrounding stroma. Cyclin E amplification is seen in the top left portion of the image in a cluster pattern. The surrounding stromal tissue, seen towards the right, shows no cyclin E amplification.

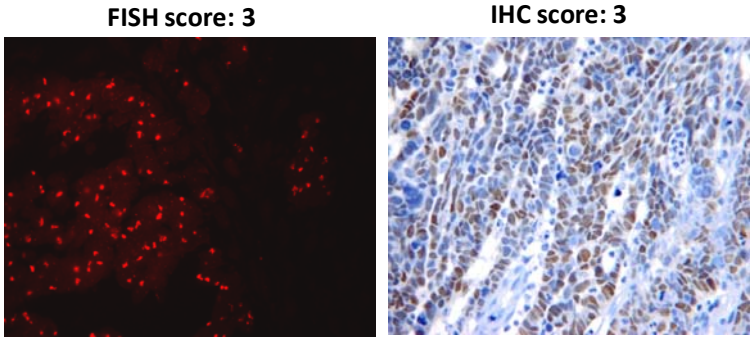

Figure 9. Cyclin E amplification correlates with cyclin E expression. The same papillary serous ovarian cancer case was analyzed by cyclin E FISH and IHC. Both methods indicate that cyclin E is amplified and has high protein expression levels.

The results obtained from FISH and IHC experiments were analyzed along with the corresponding gene expression profiling data from matched samples. We found correlation between the gene expression data (CCNE1 fold change) and only the highest levels CCNE1 gene amplification (on FISH) or cyclin E protein expression (IHC) (Figure 10).

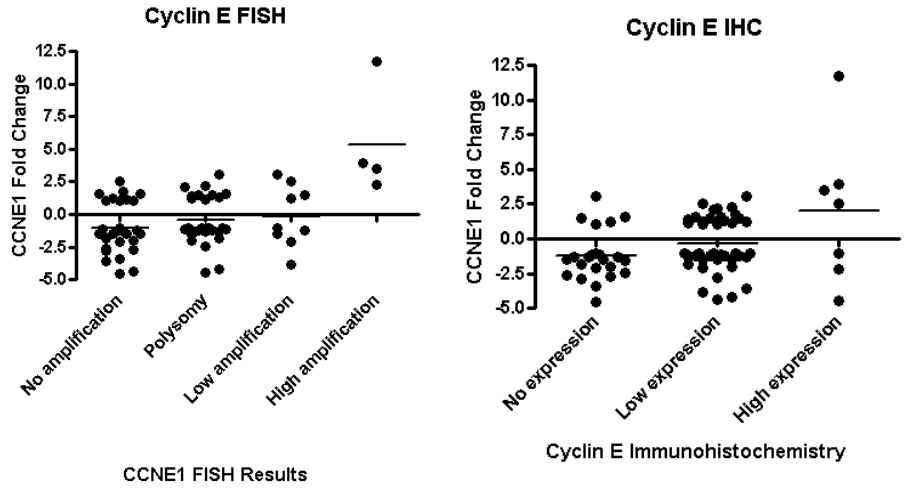

Figure 10. *CCNE1* fold change correlates with high CCNE1 gene amplification (FISH) and with high cyclin E protein expression (IHC). Lines demonstrate mean values.

Task 2: RNA analysis for gene pathways activated with cyclin E overexpression, using anatomical samples.

We have completed RNA isolation and gene expression profiling from 132 papillary serous ovarian cancer samples. We have performed an analysis to identify the genes that are upregulated with cyclin E overexpression. We found the majority of the genes are cell cycle genes functionally related to cyclin E and cell cycle progression. This is unlike Her2 in breast cancer, where the genes correlating with HER2 are located on the same amplicon. However, we found some correlated genes adjacent to *CCNE1*, including *C19orf1*, *C19orf12* and *ZNF587*.

Specific Aim 2: To determine the role of cyclin E and its collaborating genetic events in ovarian cancer initiation

Task 3: Mouse model to test ability of cyclin E and its collaborating genetic events to induce oncogenic activation

To test the cancer initiating potential of cyclin E overexpression, we used a mouse model which allows for introduction of collaborating genetic events to lead to transformation of mouse primary ovarian surface epithelial cells. Full-length cyclin E and a truncated cyclin E isoform have been expressed by a retroviral vector which allows for introduction of a gene of interest into a specific cell type or tissue.

Lower molecular weight isoforms of cyclin E have been described by Dr. K. Keyomarsi's group in Texas [1]. As many as five low molecular weight (LMW) isoforms of cyclin E exist in cancer tissues, while only the 50-kDa cyclin E form is expressed in normal tissues. The LMW isoforms have been described to have greater malignant potential.

Cyclin E cloning: We created the reagents to allow for introduction of the full-length cyclin E gene and truncated cyclin E isoforms into our mouse model. OVCAR5 cells were transfected with 2 µg pRC-CMV-cyclin E, pcDNA3-cyclin E FL, pcDNA3-cyclin E trunc 1, or pcDNA3-cyclin E trunc 2 using the BioT transfection reagent (Bioland Scientific, La Palma, CA). Whole cell lysates were collected and 25 µg of protein was analyzed by Western blot. Cyclin E protein expression was detected using an anti-cyclin E mouse monoclonal antibody (clone HE12, Santa Cruz Biotechnology, Santa Cruz, CA), followed by a fluorescently-conjugated secondary antibody for visualization using the LI-COR Odyssey Infrared Imaging System (LI-COR Biotechnology, Lincoln, NB). The pRC-CMV-cyclin E construct was provided by B. Weinberg and the pcDNA3-cyclin E constructs were provided by K. Keyomarsi (University of Texas).

For all three constructs, the cyclin E gene cassette was cloned into the EcoRI site of pcDNA3. The constructs were digested with EcoRI and the resulting DNA was analyzed by gel electrophoresis (Fig. 11), confirming the presence of FL-cyclin E (1.2 kb) and the LMW isoforms (<1.2 kb).

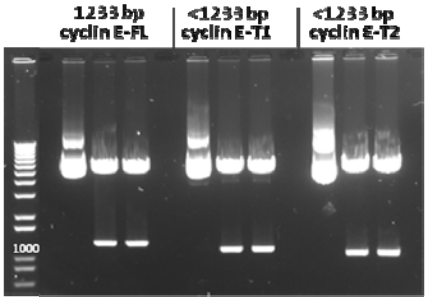

Figure 11: EcoRI digest of pcDNA3-cyclin E constructs. For each construct, 1.5 µg DNA was digested with EcoRI for 2 hours at 37°C. The resulting digest was analyzed by gel electrophoresis. For each construct, the first lane corresponds to "uncut" DNA as a control followed by two lanes of EcoRI-digested DNA. Once digested, the cyclin E-FL construct releases a 1.2 kb fragment whereas the T1 and T2 constructs reveal DNA fragments smaller than FL.

To analyze the protein expression of cyclin E FL, T1 and T2, the pcDNA3 constructs were over-expressed in OVCAR5 cells by transfection. Whole cell lysates were collected and the protein analyzed by Western blot (Fig. 12). The pRC-CMV-cyclin E construct expressed full-length cyclin E (50 kDa) in addition to the lower molecular weight isoforms (45 kDa, 35 kDa). The pcDNA3-cyclin E FL also expressed all isoforms, especially the 50 kDa protein. The pcDNA3-cyclin E trunc 1 and trunc 2 expressed the 45 and 35 kDa isoforms, respectively. The cyclin E expression cassettes from these constructs were recombined into the RCAS retroviral vector for introduction of the viral vector into our mouse model.

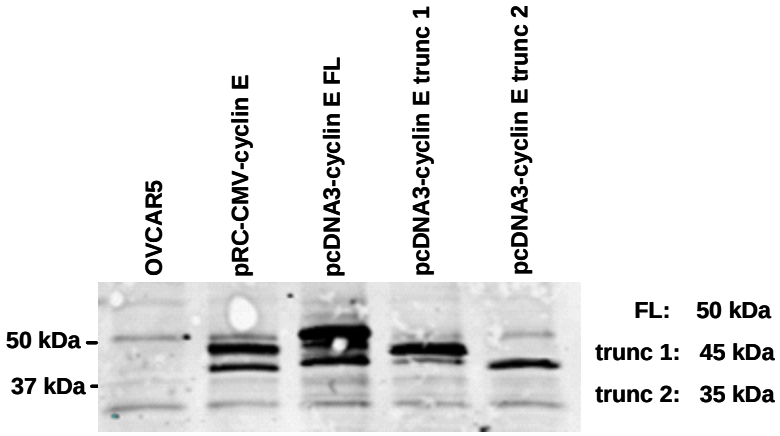

Figure 12. Western blot analysis of cyclin E expression. OVCAR5 cells were left untreated (lane 1) or transfected with 2 µg pRC-CMV-cyclin E, pcDNA3-cyclin E FL, pcDNA3-cyclin E trunc 1, or pcDNA3-cyclin E trunc 2 (lanes 2-5). Whole cell lysates were collected and 25 µg of protein was analyzed by Western blot for cyclin E expression.

Recombination Reaction with RCAS Vector: To introduce cyclin E FL, cyclin E T1 and cyclin E T2 into the RCAS vector, Gateway cloning was used. Although we had pcDNA3-cyclin E FL, we opted to use pDONR221 cyclin E FL instead. The pDONR221 vector is an entry clone containing *att*L sites which can be used in Gateway cloning to introduce a gene of interest into a vector containing *att*R sites, such as the RCAS vector. The recombination occurs in the presence of LR clonase to generate RCAS-

cyclin E FL (Fig. 13, *top panel*) and RCAS-cyclin E trunk 1 and RCAS-cyclin E trunk 2 (Fig 13, *bottom panel*).

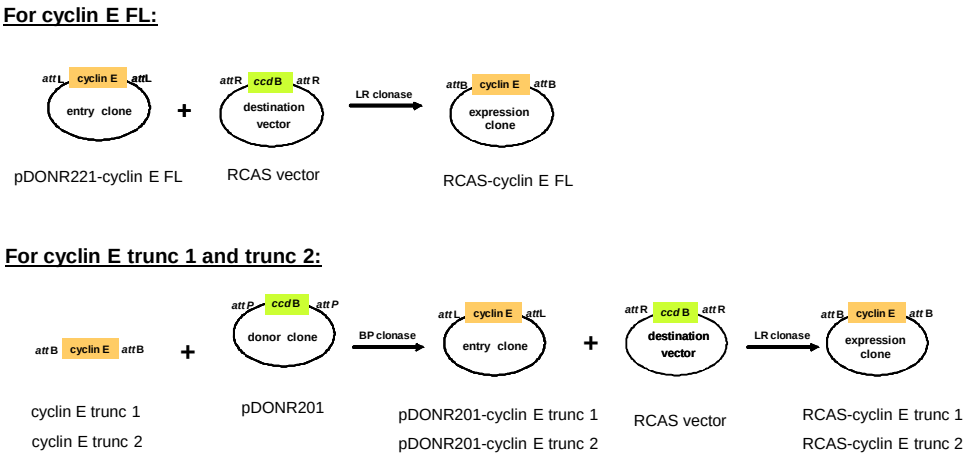

Figure 13. Recombination of cyclin E into RCAS destination vector. *(Top panel)* For cloning of cyclin E FL into the RCAS vector, the pDONR221-cyclin E FL entry clone was combined with RCAS in a LR reaction to generate RCAS cyclin E FL. *(Bottom panel)* For cloning of the LMW isoforms of cyclin E (T1 and T2) into RCAS, pcDNA3-cyclin E FL was used as a template and T1- or T2-specific primers containing flanking *att*B sites were used (not shown in diagram). The *att*B-cyclin E T1 and *att*B-cyclin E T2 PCR products were combined with the pDONR201 donor vector in a BP reaction to generate the entry clones pDONR201-cyclin E T1 and pDONR201-cyclin E T2. These constructs were then combined with the RCAS vector in a LR reaction to generate RCAS-cyclin E T1 and RCAS-cyclin E T2.

After recombination of cyclin E FL into the RCAS vector, several clones were sequenced to confirm the presence of the cyclin E gene. To test for cyclin E FL protein expression, OVCAR5 cells were either untreated or transfected with the RCAS vector alone or RCAS-cyclin E FL. Untreated cells and cells transfected with RCAS alone expressed only endogenous cyclin E whereas cells transfected with RCAS-cyclin E FL overexpressed cyclin E (Fig. 14). In all conditions, the 50 kDa band was present, although with RCAS-cyclin E FL, the 45 and 35 kDa isoforms were also over-expressed.

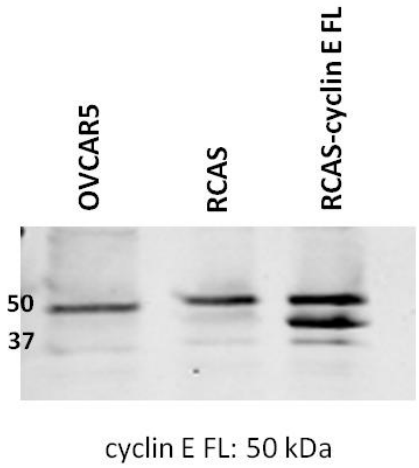

Figure 14. Western blot analysis of RCAS-cyclin E FL over-expression in OVCAR5 cells. OVCAR5 cells were either left untreated or transfected with 2 µg RCAS or RCAS-cyclin E FL. Whole cells lysates were collected and 30 µl of sample was analyzed by Western blot for cyclin E expression.

For enabling entry of the truncated isoforms into the RCAS vector, cyclin E T1 and cyclin E T2 were first PCR-amplified from pcDNA3-cyclin E FL using cyclin E isoform-specific primers (Fig. 15). Since entry into pDONR requires recombination between *att*B and *att*P sites, the isoform-specific PCR primers also contained *att*B recombination sites at their ends, allowing for the introduction of these sites to the amplified PCR products. The resulting PCR products were analyzed by gel electrophoresis (Fig. 15). Cyclin E T1 had an approximate size of 1500 base pairs (bp) whereas cyclin E T2 was slightly smaller at ~1200 bp. The PCR products were gel-purified and used in a recombination reaction with the pDONR201 vector to give rise to pDONR201-cyclin E T1 and pDONR201-cyclin E T2 (Fig.13, *bottom panel*). Subsequent clones were analyzed by sequencing and positive clones were combined in a LR reaction with the RCAS vector to generate RCAS-cyclin E T1 and RCAS-cyclin E T2.

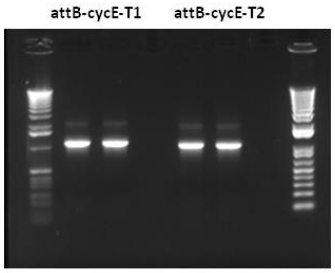

pcDNA3-cyclinE-EL used as template for attB PCR

Figure 15. Gel electrophoresis of *att*B-cyclin E T1 and *att*B-cyclin E T2 PCR products. The pcDNA3-cyclin E FL construct was used a template to amplify cyclin E T1 and cyclin E T2 using isoform-specific PCR primers containing *att*B recombination sites. The PCR products were analyzed by gel electrophoresis and gel purified. The *att*B-cyclin E T1 gene has a size of ~1500 bp and the *att*B-cyclin E T2 gene is ~1200 bp in length.

293T cells were left untreated or transfected with RCAS-cyclin E FL (as a control), RCAS-cyclin E T1, or RCAS-cyclin E T2. Whole cell lysates were collected and analyzed by Western blot for cyclin E protein expression (Fig. 16). RCAS-cyclin E FL highly expressed all cyclin E isoforms whereas RCAS-cyclin E T2 expressed high levels of the 35 kDa isoform. Despite analyzing three RCAS-cyclin E T1 clones, the construct did not over-express the 45 kDa isoform since only endogenous cyclin E was detected. This indicated that the efficient recombination of cyclin E T1 into RCAS had not occurred. The RCAS-cyclin E T2 construct efficiently over-expressed T2 as seen by the expression of the 35 kDa isoform of cyclin E. Further troubleshooting did not allow us to successfully clone cyclin E T1 into the RCAS vector.

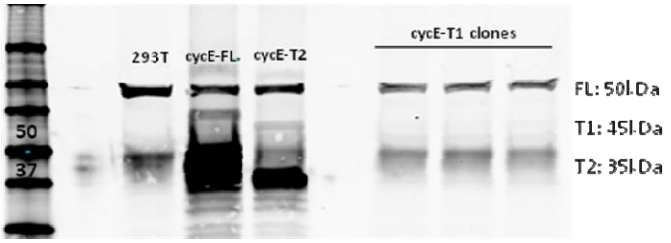

Figure 16. Western blot analysis of RCAS-cyclin E over-expression in 293T cells. 293T cells were either left untreated (293T lane) or transfected with 2 µg RCAS-cyclin E FL (as a positive control), RCAS-cyclin E T1, or RCAS-cyclin E T2. Whole cell lysates were isolated and 30 µl of the sample was analyzed by Western blot for cyclin E protein expression. Three different RCAS-cyclin E clones were analyzed. The large molecular weight band that appears in all lanes is a background band that is always detected when using this cyclin E antibody.

Generation of RCAS-cyclin E virus: The DF-1 chicken fibroblastic cell line was used for RCAS-cyclin E FL and RCAS-cyclin E trunc 2 transfection and subsequent virus production. DF-1 cells were maintained in DMEM supplemented with 10% FBS and 1% penicillin-streptomycin. Twenty micrograms of each construct was transfected into a 10-cm dish of DF-1 cells using Lipofectamine 2000 reagent (Invitrogen Corporation, Carlsbad, CA). The following day, the supernatant containing RCAS-cyclin E FL and RCAS-cyclin E trunc2 virus particles were collected and filtered through a 0.8 µm filter to remove cell debris. DF-1 cells stably expressing RCAS-myc, RCAS-Kras and RCAS-cre were previously established in the lab.

Concentration of the viral supernatant: DF-1 cells expressing RCAS viruses with different oncogenes were grown in 10-cm tissue culture dishes in DMEM with 10% FBS, and 1% antibiotics. Once cells were completely confluent, they were further expanded into eight 15-cm dishes. Upon confluency of the 15-cm dishes, the media was replaced with reduced serum Opti-MEM media overnight. The following day, the medium was collected and filtered through 0.8um filter to remove cell debris. The filtered supernatant was then incubated overnight at 4°C with Retro-X Concentrator (Clontech, Mountain View, CA) to concentrate virus. The following day, the samples were centrifuged at 4°C for 45 min at 3100 rpm. The supernatant was removed and the virus pellet was resuspended in Opti-MEM before storing at -80°C.

Mouse Model: We have crossed transgenic mice that express Keratin5-TVA (chicken retroviral keratin receptor that is expressed on the ovary) with conditional P53 mutant mice. K5-TVA mice have been crossed with 129S4-Trp53^{tm2Tyj} (P53 LSL R172H) mice, which carry a conditional point-mutant allele of the p53 gene that can be activated by Cre-mediated recombination. This line contains a LoxP site and a transcriptional / translational STOP sequence in intron 1 (making it functionally equivalent to a null mutation) and an R172H missense mutation in exon 5. The strain was maintained on a 129S4/SvJae background. Activation with Cre-recombinase leads to deletion of the transcriptional termination sequence (Lox-Stop-Lox) and expression of the oncogenic P53 protein. The genotyping strategy is illustrated in figure 17.

Primers:

T036 : 5'-agc tag cca cca tgg ctt gag taa gtc tgc a -3'
T035 : 5'-ctt gga gac ata gcc aca ctg -3'
T037 : 5'-tta cac atc cag cct ctg tgg -3'

Product Sizes:

T036/T035: 279 bp (Mut LSL)
T037/T035: 166 bp (Wild Type)

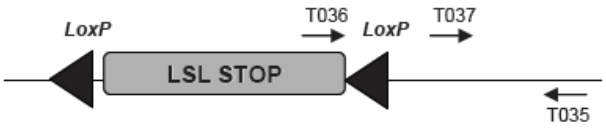

Figure 17. Genotyping strategy of P53 LSL R172H mice. The noted primers allow us to detect the wild type allele with T037 and T035, which amplify intron 1, and the mutant allele with T036 and T035, which amplifies the LSL element.

We genotyped mice with one-step PCR procedures using mouse tail tissues to isolate DNA from crude lysates. Mice that carry the K5-TVA transgene and the conditional mutant P53 allele were selected for further experiments. The RCAS-Cyclin E vector and Ad-Cre were introduced into the OSE of K5-TVA p53 LSL R172H mice to determine the oncogenic potential of cyclin E overexpression in the setting of P53 oncogenic expression.

Ovary isolation and infection of ovarian cells: Ovaries from newborn K5-TVA p53 LSL R172H pups were isolated using standard aseptic surgical procedures: The ovaries were separated from the bursa and transferred to a tissue culture dish containing DMEM (supplemented with 10% FBS and 1% antibiotics). The ovaries were allowed to grow in a CO2 incubator for 48 hr. After the cells were attached, the medium was then replaced with fresh viral supernatant.

The viral supernatant was used to replace the medium of growing ovarian cells. The infection of OSE cells was repeated every 12 hours for 5 days. The cells were then trypsinized and expanded.

Infection of ovarian cells in culture. The isolated ovaries were divided into five groups: each group was infected with a unique combination of viral supernatants from DF-1 cells producing RCAS viruses with different oncogenes.

The following combinations were used to infect the ovarian cells:

1) RCAS-cre (to activate expression of oncogenic P53)
2) RCAS-cre + RCAS-CyclinE
3) RCAS-cre + RCAS-CyclinE + RCAS-myc
4) RCAS-cre + RCAS-CyclinE + RCAS-Kras
5) RCAS-cre + RCAS-CyclinE + RCAS-Akt
6) RCAS-cre + RCAS-myc + RCAS-Kras (positive control)

The ovarian cells infected with any combination containing CyclinE successfully proliferated during the early passages, but starting from passage 3, they did not survive. The ovarian cells infected with only RCAS-cre did not passage well and died during early passages. Phenotypes of the infected ovarian cells were observed during the first days of infection (Fig. 18).

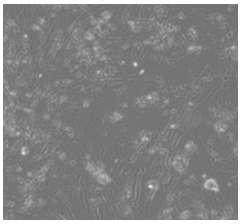

RCAS-cre

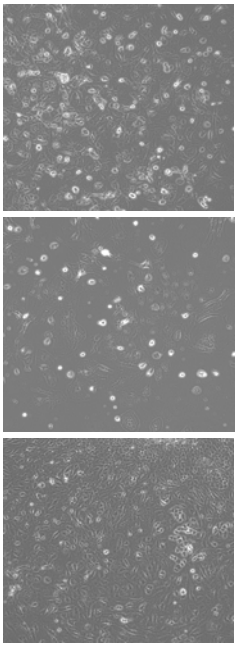

RCAS-CyclinE (+ cre)

RCAS-Cyclin E + RCAS-myc (+ cre)

RCAS-Myc + RCAS-Kras (+ cre) (positive control)

Figure 18. Phenotypes of mouse ovarian surface epithelial cells infected with RCAS virus causing overexpression of various combinations of oncogenes. The mouse OSE cells infected with RCAS-cre only (to activate the expression of oncogenic P53 did not survive in early passages. The mouse OSE cells infected with RCAS-cre + RCAS-Cyclin E appeared to have an initial growth advantage, but these cells eventually started to die after the third passage. Similarly, the cells infected with RCAS-cre + RCAS-myc + RCAS-Kras (our positive control) also started to die after the third passage.

The failed experiment was repeated again. This time, the mouse OSE cells were infected with concentrated viruses, but the same results were obtained: the infected cells did not survive after the early passages. Prior literature ("Induction of ovarian cancer by defined multiple genetic changes in a mouse model system", Sandra Orsulic, et al. *Cancer Cell* 2002) [2], suggests we should see transformation of ovarian surface epithelial cells after exposure to oncogenic expression of c-*myc* and K-*ras* in the setting of null P53 protein. Our experiment did not demonstrate this result when we overexpressed c-*myc* and K-*ras* in the setting of mutant P53 protein. This left us to conclude three possibilities as to why our experiment failed:

1) The viral supernatant was not adequately allowing for infection of the mouse OSE cells
2) The cre recombinase was not causing expression of the dominant negative mutated P53 protein
3) The mutant P53 protein of 129S4-Trp53^{tm2Tyj} mice was not sufficiently silencing normal P53 activity (compared to the null P53 condition) and this is causing cells to die upon exposure to oncogenic stress

To address the first possibility (the viral supernatant is not adequately allowing for infection of the mouse OSE cells), we generated RCAS-AP (alkaline phosphatase) virus in DF-1 cells. The isolated ovaries were infected with supernatant of the DF-1 cells

containing the RCAS-AP or the concentrated RCAS-AP virus for 3 days, replacing the medium with fresh RCAS-AP every day. The expression of Alkaline Phosphatase was determined using the Fast Violet B salt from Sigma-Aldrich AP kit, following the manufacturer's recommendations. Figure 19 demonstrates the OSE cells were positively stained with AP dye, confirming successful infection with RCAS virus.

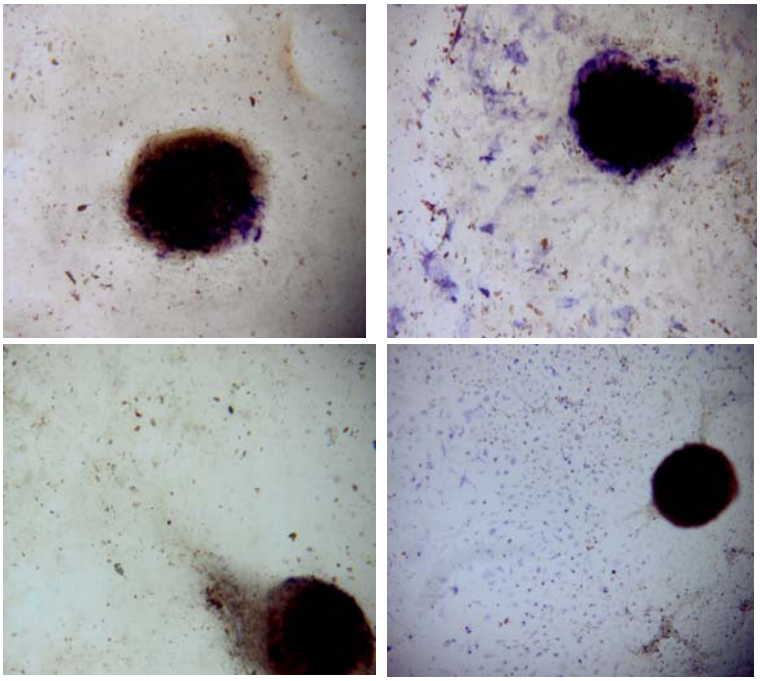

Figure 19. Expression of RCAS-AP (alkaline phosphatase) in mouse ovarian surface epithelial cells. The mouse ovaries are isolated and placed in a tissue culture dish containing DMEM. After 48 hours, the ovarian surface epithelial cells are found attached to the dish surrounding the ovary (dark spot). The medium was replaced with fresh viral supernatant containing RCAS-AP. The cells were fixed with 10% formalin for 10 minutes, washed with PBS and stained with Fast Violet B salt alkaline dye. The top left panel demonstrates the negative control. The top right panel demonstrates RCAS-AP infection through addition of viral supernatant. The bottom two panels demonstrate infection with concentrated RCAS-AP virus. The AP is expressed as a brown stain.

The second possibility explaining the failure of our experiment was that the cre-recombinase was not causing adequate expression of the P53 dominant negative mutated protein. To investigate this possibility, we tested the activity of RCAS-cre in the epithelial cells of K5-TVA 129S4-Trp53^{tm2Tyj} (p53 LSL R172H) mice. We found adequate cre activity, ruling out this possibility.

The third possibility was that we are not able to achieve a complete inactivation of p53 activity in the OSE cells of 129S4-Trp53^{tm2Tyj} (P53 LSL R172H) mice. Since the original mouse model experiments were done using the ovaries from transgenic mice generated from K5-TVA and p53 null parents, we repeated these experiments in mouse OSE cells with K5-TVA+/+ and p53-/- genotypes.

We used the Trp53^{tm1Tyj} mutant strain developed in the laboratory of Dr. Tyler Jacks at the Center for Cancer Research at the MIT. These mice have a targeted (knock-out) allele that was produced by a targeted neo insertion into the Trp53 locus. Homozygotes show no visible phenotype but develop tumors at 3 – 6 months of age. Heterozygotes develop tumors at 10 months of age. These mice were crossed with K5-TVA mice. The following information from the developer's lab (http://jaxmice.jax.org/strain/002101.html) was used to genotype our population of mice (fig. 20).

Expected Results:	Mutant = 600 bp Heterozygote = 400 bp and 600 bp Wild type = 400 bp

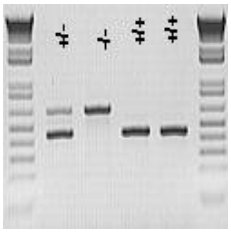

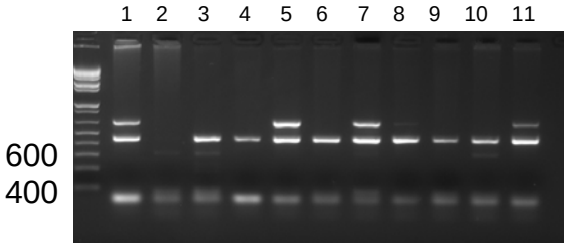

Figure 20. Genotype of P53 null mice. The top gel demonstrates the expected genotyping results for null (600 bp), heterozygote (400 bp and 600 bp), and wild type P53 mice (400 bp). The bottom gel demonstrates the genotyping results for the mice in our lab. Lanes 5, 7, and 11 demonstrate the heterozygote P53 null state in three mice.

The heterozygote p53 +/- mice (mouse 1 male and mice 5, 7 female) were crossed with the K5-TVA mice. The next generation of K5-TVA p53 +/- mice were bred together to generate K5-TVA p53 -/- offspring. The K5-TVA p53 +/- mice were also bred to the K5-TVA 129S4-Trp53^{tm2Tyj} (p53 LSL R172H) mice to generate mice with the K5-TVA P53 LSL R172H$^{Mut/-}$ genotype.

Ovaries were isolated from the female pups with the K5-TVA p53 -/- genotype and the K5-TVA P53 LSL R172H$^{Mut/-}$ genotype and the viral infections were repeated. Unfortunately, using this technique with the p53 null mice also resulted in experimental failure with failure of even our control cells to grow after approximately 3 passages.

This led us to suspect that there might be a problem with the infection technique using the RCAS virus. While continuing to troubleshoot this possibility, we also searched the literature for other techniques that would allow for us to proceed with our experiments without having to depend on RCAS infection. We found a method describing the isolation of mouse ovarian surface epithelial cell lines [3]. Our RCAS system was designed to specifically infect the ovarian surface epithelial cells without infecting the

stromal cells. We decided to use this described method of OSE cell isolation to accomplish the same purpose.

Isolation of mouse ovarian surface epithelial cells. Under aseptic conditions, we transferred the ovaries from 21 day old female p53-/- mice to a culture dish containing high-glucose Dulbecco's modified Eagle medium (GIBCO laboratories) supplemented with 10% fetal bovine serum (FBS), penicillin (100 U/ml) and streptomycin (100 J.lg/ml). The fallopian tubes and the connective tissue surrounding the ovaries were removed. The ovaries were washed three times with phosphate-buffered saline (PBS) and treated with 0.025% trypsin for 60 minutes. The ovaries were removed and growth medium (DMEM containing 4.5 g/L glucose, L-glutamine, sodium pyruvate, 10% FBS, 1% penicillin, 1% streptomycin, 10 ng/ml EGF, 500 ng/ml hydrocortisone, 10 ug/ml insulin) was added to the reaction solution to dilute the trypsin. The cell suspension was placed in a tissue culture dish at 5% CO_2 in 37º C humidified air.

Retroviral infection of p53-/- MOSE cells. After establishing the MOSE cell culture line, the cells were divided into seven groups to be infected with retrovirus generated in LynxA packaging cells. On day 1, LynxA cells were plated in 6-well plates at 2.5 x 10^5 cell/well in DMEM containing 10% FBS with no antibiotics. On day 2, LynxA cells at 70% confluency were transfected with one of the following conditions:

1. pBabe-puro (negative control)
2. pBabe-Cyclin E
3. pBabe-Myc
4. pBabe-K-ras
5. pBabe-myc + pBabe-K-ras (positive control)
6. pBabe-Cyclin E + pBabe-Myc
7. pBabe-Cyclin E + pBabe-K-ras

After transfection, cells were then incubated at 37º C overnight. On day 3, the medium was replaced with complete DMEM (+antibiotics, 1% pen/strep) and I uM dexamethasone. P53-/- MOSE cells were plated in 6-well plates at 2 x 10^5 cells/well in the complete DMEM medium containing insulin, EGF and hydrocortisone supplement.

On day 4, the medium from the LynxA cells (containing virus) was collected, centrifuged at 1000 rpm to pellet the cell debris and filtered through 45 um filters. Polybrene at 8 ug/ml was added to each viral soup specimen and the supernatant was added into the appropriate wells to infect the target MOSE cells. The plates containing the MOSE cells with 3 ml/well of viral soup were centrifuged at 1700 rpm for 1 hour at room temperature in order to increase the infection efficiency. Plates were then incubated at 5% CO_2 and 37º C overnight. On day 5, the medium was replaced with fresh complete DMEM containing the insulin, EGF and hydrocortisone supplement.

On day 6, the successfully infected p53-/- MOSE cells were selected with appropriate antibiotics (puromycin 5 mg/ml for pBabe-puro and pBabe-Cyclin E, balsticidine 5 ug/ml for pBabe-Myc and hygromycin 200 ug/ml for pBabe-K-ras). On day 7, the cells were

expanded into larger dishes and were further maintained in supplemented medium with the appropriate antibiotics.

Results of cyclin E overexpression in mouse ovarian surface epithelial cells. As of this report, we have performed multiple experiments with the two different mouse models to determine the effect of cyclin E overexpression on the potential for oncogenic transformation. In the first model, using the RCAS virus to introduce various combinations of oncogenes specifically to the epithelial ovarian cells of K5-TVA 129S4-Trp53^{tm2Tyj} (p53 LSL R172H) mice and the K5-TVA p53 -/- mice, we were not able to get even our positive control to work, leading us to conclude that there was some toxic effect in the media of the DF1 cells that led to experimental failure. This caused us to shift gears to use a different mouse model that involved the trypsinization of whole ovaries from p53-/- mice to isolate the mouse ovarian surface epithelial cells from the underlying stroma. This allowed for transfection of various combinations of oncogenes using the pBabe rather than the RCAS vector. Figure 21 demonstrates a representative result of this experiment. The pBabe-Myc + K-ras condition is our positive control and appears to have caused transformation of the MOSE cells. The pBabe-puro condition is our negative control. The pBabe-Cyclin E condition does not cause rapid transformation of the cells, as seen with the positive control, but the experiment is on-going.

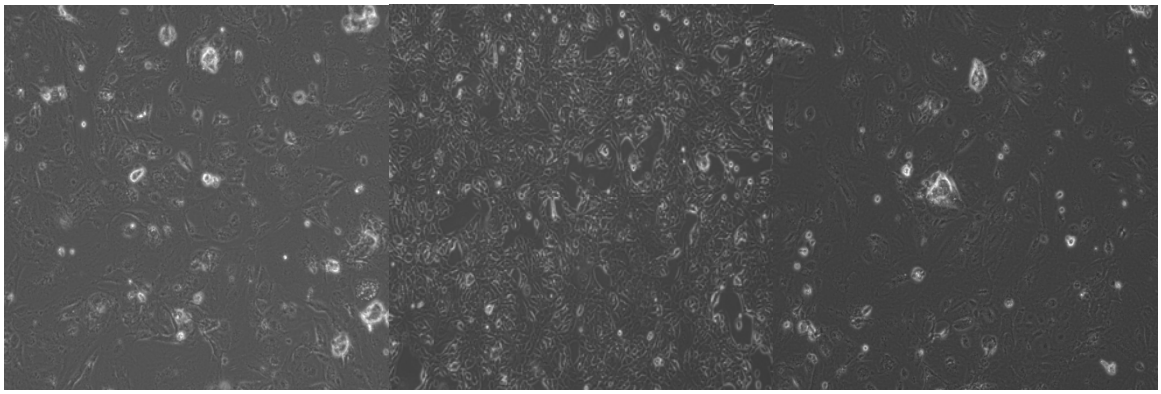

Figure 21. Phenotypes of mouse ovarian surface epithelial cells infected with pBabe retrovirus causing overexpression of various combinations of oncogenes. The MOSE cells overexpressing cyclin E do not appear to have undergone transformation, unlike the MOSE cells overexpressing the combination of Myc and K-ras (positive control).

Cells from the various experimental conditions were grown to confluency and then injected into the peritoneal cavity of female nude mice. At this time, there are 4 nude mice injected with Cyclin E overexpressing cells. We will continue to monitor these mice for the possible development of ovarian/peritoneal carcinomas over the subsequent months.

Specific Aim 3: To define the subset of ovarian cancers with impaired cyclin E inhibition and to determine whether these tumors demonstrate an enhanced response to targeted therapy

Task 4: Immunohistochemistry (IHC) for cyclin E, SKP2, P27 using anatomic samples

We performed immunohistochemistry for cyclin E in patient ovarian cancer samples (see results under task 1). We initially had difficulty in identifying an appropriate antibody for cyclin E that resulted in nuclear staining. After trouble-shooting multiple different antibodies, we found a mouse-monoclonal anti-cyclin E antibody from Vector Labs that performed well at a 1:50 dilution. Our analysis (task 1) showed a correlation between the highest levels of cyclin E IHC staining and *CCNE1* fold-change on microarray expression analysis. We were not able to successfully trouble-shoot the SKP2 or P27 antibodies for a similar analysis.

Task 5: DNA mutation analysis for FBXW7 mutations, using anatomical samples

In our pilot study, we identified thirteen samples with loss of heterozygosity at the *FBXW7* gene locus. The SCF-Fbw7 ubiquitin ligase system ensures tight control of cyclin E levels. Disruption of the Fbw7 tumor suppressor leads to genetic instability through deregulated cyclin E activity. The *FBXW7* gene has been found to be mutated in ovarian cancer cell lines, implicating its potential role in the pathogenesis of this malignancy. We planned to screen for mutations in the *FBXW7* gene in these 13 ovarian cancer samples. We did a search of publically available data from Sanger and the cancer genome atlas (TCGA). In the Sanger data, one *FBXW7* mutation (c.1417delA) was found in a single cell line (T-24) among a panel of 21 ovarian cancer cell lines. Sanger data also included sequencing in 183 clinical tumors (including breast, CNS, kidney, colon, lung, pancreas, pleura, salivary gland, skin, upper GI tract, and urinary tract) and found mutations in *FBXW7* in 2 (1%) of samples. No clinical ovarian cancer samples were included in the Sanger data, but the TCGA used NextGen sequencing and found no *FBXW7* mutations in 60 to 80 ovarian cancer samples. Based on this publically available data, *FBXW7* appears to be very infrequently mutated in multiple tumor types, including ovarian cancer. Therefore, we have not performed this task and have focused our attention on other areas that were likely to be of higher yield.

Task 6: In vitro proliferation assays, using 6 serous ovarian cancer cell lines with various cyclin E and SKP2 expression, and assessing for therapeutic response to the proteasome inhibitor, bortezomib

The goal of this task was to determine whether targeted therapies could be used to specifically inhibit ovarian cancers that overexpress cyclin E.

To accomplish this task, we assayed a panel of ovarian cancer cell lines to determine endogenous levels of cyclin E and SKP2. We found OVCAR3 cells to express high

levels of both proteins and OVCAR5 cell to express low levels of both proteins (figure 22). We used these two cell lines in further experiments. Additionally, we found OVCAR3 cells to have a genetic amplification of the *CCNE1* gene locus on chromosome 19, similar to the amplifications seen in clinical ovarian cancer cell lines (figure 23). This led us to conclude that OVCAR3 cells are a good model for studying therapeutic responses in the setting of cyclin E amplification and overexpression.

9A.

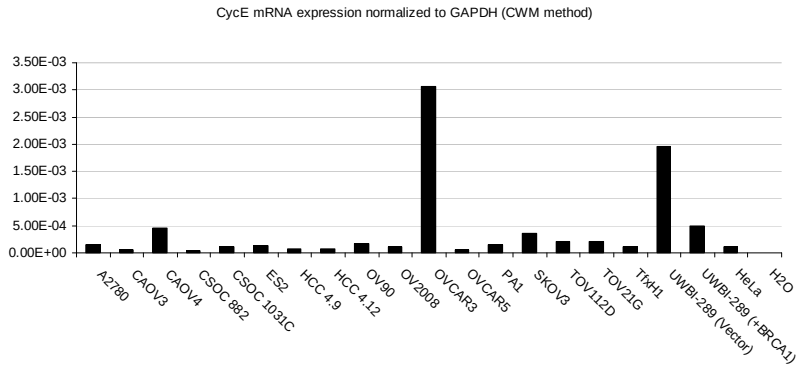

9B.

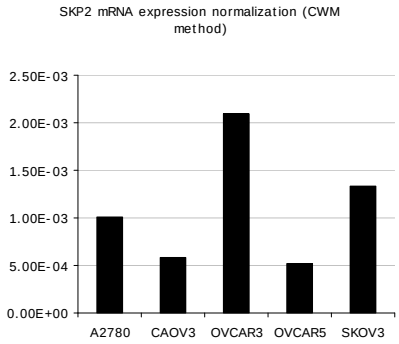

9C.

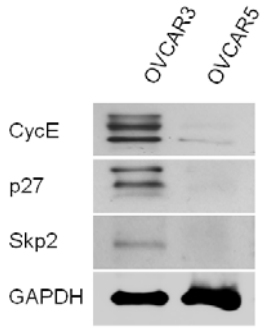

Figure 22. Cyclin E and SKP2 expression in panel of ovarian cancer cell lines. **9A.** Real time PCR demonstrating differing cyclin E expression levels in various ovarian cancer cell lines. **9B.** Real time PCR demonstrating differing SKP2 levels in various ovarian cancer cell lines. **9C.** Western blot demonstrating cyclin E, P27, SKP2 levels in OVCAR3 and OVCAR5.

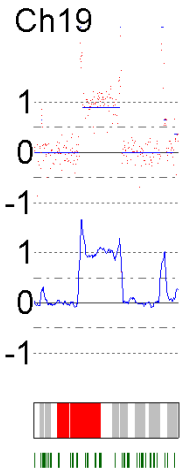

Figure 23. Amplification at the *CCNE1* gene locus on chromosome 19 in the OVCAR3 ovarian cancer cell line. Blue lines projecting above the "0" copy number line represents areas of genetic amplification. The broad area of copy number amplification contains the *CCNE1* gene.

Tumors with cyclin E deregulation were hypothesized to be attractive targets for therapy with SKP2 inhibitors. SKP2 is a ubiquitin ligase that targets P27kip1 for degradation. P27 is a powerful negative regulator of the cell cycle, preventing activation of cyclin E-cdk2 or cyclin D-cdk4 complexes and cell cycle progression at the G1 to S boundary. Therefore, inhibition of SKP2 could lead to upregulation of P27 levels and inhibition of aberrant cyclin E activity and inhibition of progression through the cell cycle. The proteasome inhibitor, bortezomib (Velcade), has been shown to inhibit the growth of colorectal tumor cell lines through upregulation of P27 and induction of apoptosis [4].

We tested the sensitivity of OVCAR3 and OVCAR5 ovarian cancer cell lines to the effects of bortezomib. Consistent with our hypothesis, we discovered that the cyclin E overexpressing OVCAR3 cells were indeed more sensitive to bortezomib (figure 24).

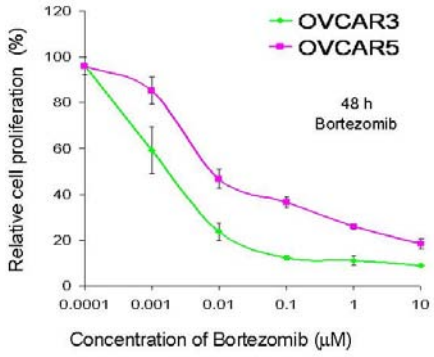

Figure 24. OVCAR3 (high cyclin E levels) cells are more sensitive to bortezomib than OVCAR5 cells (low cyclin E levels). Relative cell proliferation to various concentrations of bortezomib was measured by the MTT assay at 48 hours.

However, given the fact that OVCAR3 and OVCAR5 cells differ in many ways other than cyclin E levels, we set out to create a more informative model system. We transfected OVCAR5 cells to overexpress cyclin E or an empty control vector. We treated these cells with bortezomib and found no difference in their response (figure 25). Similar negative data were obtained with stable transfection in OVCAR5 cells, as well as with overexpression of cyclin E in other ovarian cancer cell lines such as SKPV3 and A2780 (data not shown). This led us to conclude that the differential effects demonstrated between OVCAR3 and OVCAR5 were not due to cyclin E levels.

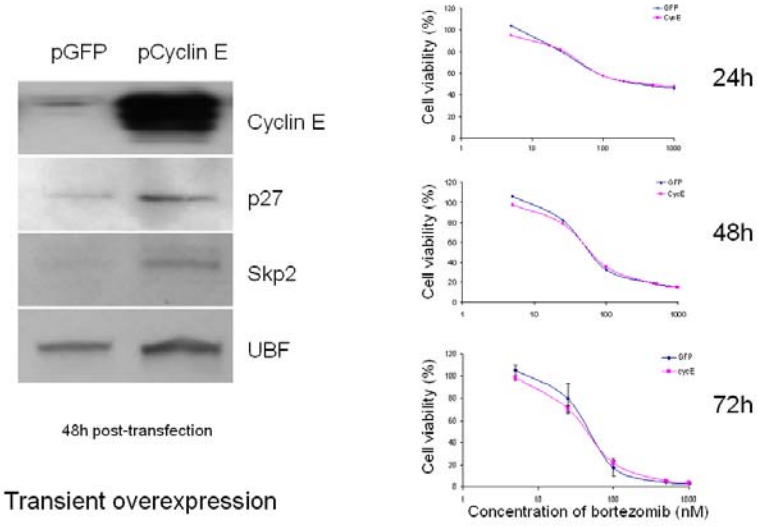

Figure 25. No difference in sensitivity to bortezomib between OVCAR5 cells transfected with empty vector (pGFP) or cyclin E (pCyclin E). Data are shown for transient overexpression of cyclin E.

In light of this data disproving our original hypothesis, we searched the literature for alternative agents that might be capable of differentially targeting cyclin E overexpressing cells. We found a report of a natural dietary phytochemical, indole-3-carbinole (I3C), that works as a natural elastase inhibitor and disrupts cyclin E activity [5]. The low molecular weight (LMW) isoforms of cyclin E are tumor-specific and cause increased cell proliferation, elevated kinase activity and increased clonogenicity. These LMW cyclin E isoforms are generated via proteolysis of the normal 50 kDa cyclin E form by the elastase enzyme, which itself can be selectively inhibited by I3C. I3C exhibits potent anti-carcinogenic properties and has been shown to shift the accumulation of cyclin E from the LMW to the 50 kDa isoform and to induce a G1 cell cycle arrest.

Considering the specific inhibitory properties of I3C and bortezomib in the processing and expression of cyclin E, we investigated the hypothesis that ovarian cancer overexpressing cyclin E may demonstrate an enhanced response to targeted combination therapy with I3C and bortezomib. We found synergistic cytotoxicity of I3C and bortezomib in both OVCAR3 and OVCAR5 cells, with greater sensitivity of each individual drug in OVCAR3 cells and greater synergistic effect of the drug combination in OVCAR5 cells (figure 26).

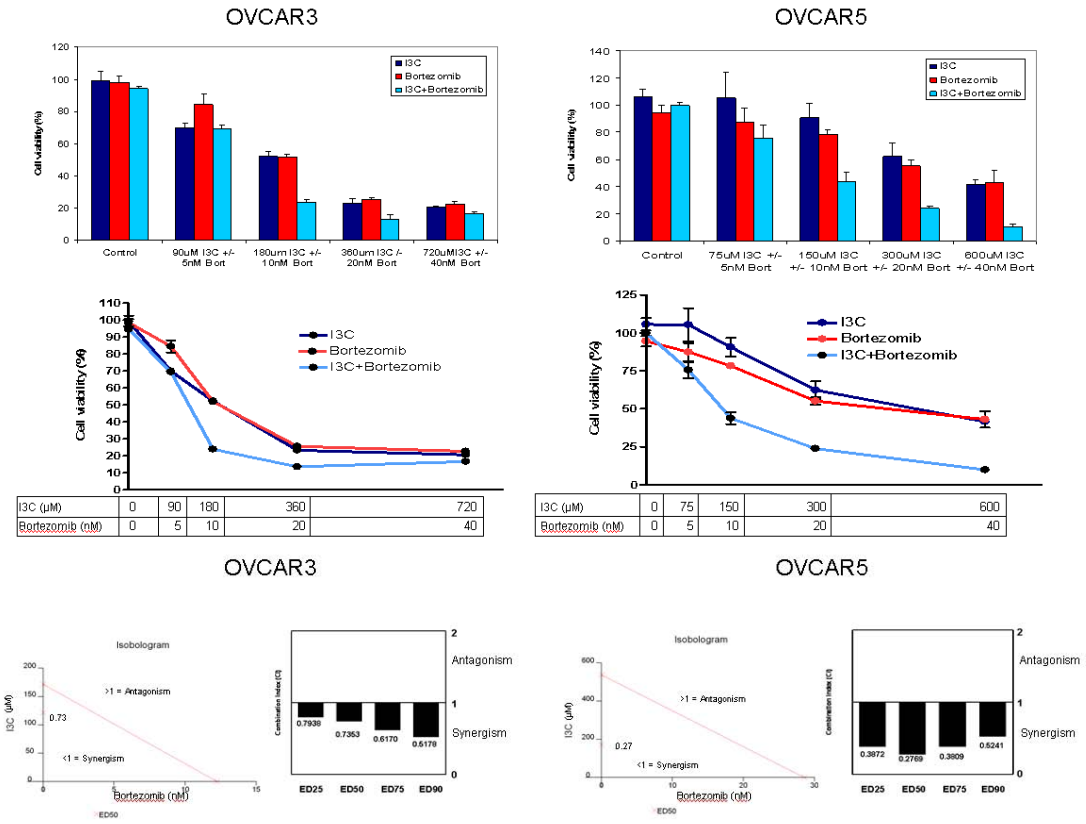

Figure 26. OVCAR3 cells are more sensitive to the effects of I3C and bortezomib alone and OVCAR5 cells are more sensitive to the combination treatment. Cell viability data are generated from Cell Titer-Glo Luminescent Cell Viability Assay (upper panel). Synergy data are determined by isobologram analysis using CalcuSyn software (lower panel).

We found that I3C and bortezomib have varying effects on the cell cycle in the two different cell lines (figure 27). I3C induces an S phase accumulation in OVCAR3 and a G1 arrest in OVCAR5 cells. Bortezomib induces a G2/M arrest in both cell lines, but this is more pronounced in the OVCAR5 cells. The combination of the two drugs causes a G2/M arrest and the accumulation of a sub-G1 population of cells that are undergoing apoptosis.

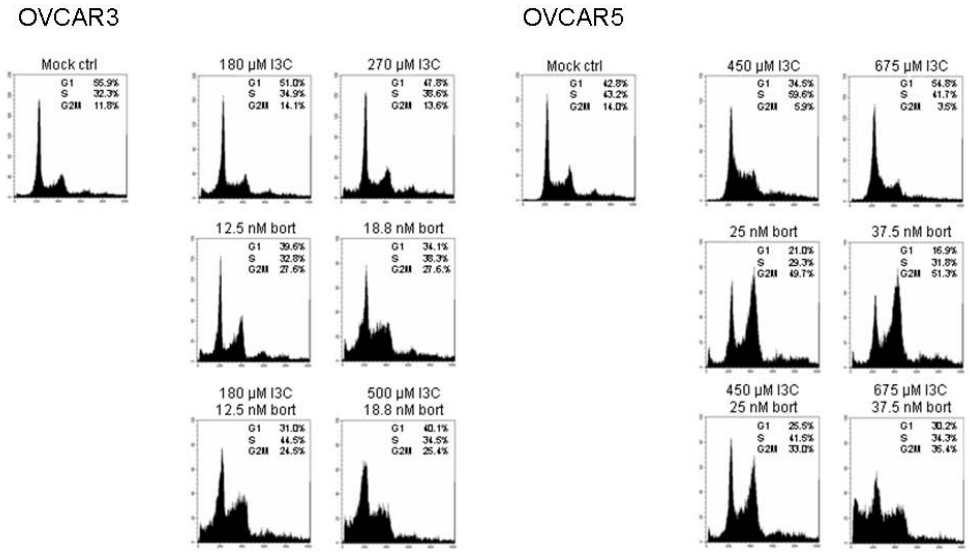

Figure 27. I3C and bortezomib alone and in combination alter the cell cycle and enhance apoptosis in OVCAR3 and OVCAR5 cells. For cell cycle analysis, cells were treated with the indicated concentrations of drugs and harvested 24 hours post treatment. Samples were fixed with 70% ethanol and labeled with propidium iodide (PI). Samples were analyzed for PI incorporation with a Becton Dickinson FACScan using ModFit LT software. The results were generated from multiple independent experiments performed in triplicate.

The combination of the two agents appeared to have a greater impact in inducting apoptosis in the OVCAR5 cells (figure 28).

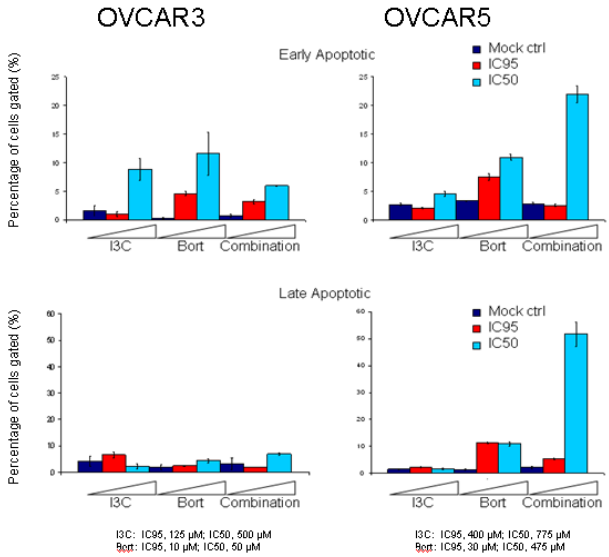

Figure 28. I3C and bortezomib induce apoptosis. The greatest effect is seen in OVCAR5 cells with a combination of drugs. FACS analysis of Annexin V and propidium iodide (PI) stained cells were used to discriminate between early and late apoptotic cells.

We performed western blotting analysis for proteins from various cellular pathways to interrogate the mechanisms for the observed data. We found a decrease in phospho-Rb levels with increasing drug concentration in both cell lines for single and combination treatment, with the effect being more pronounced in the OVCAR5 cells (figure 29). This data suggest an inhibitory effect of the drugs on progression through the cell cycle at the G1/S phase. P27kip1 levels are not altered and do not appear to be responsible for the observed effects.

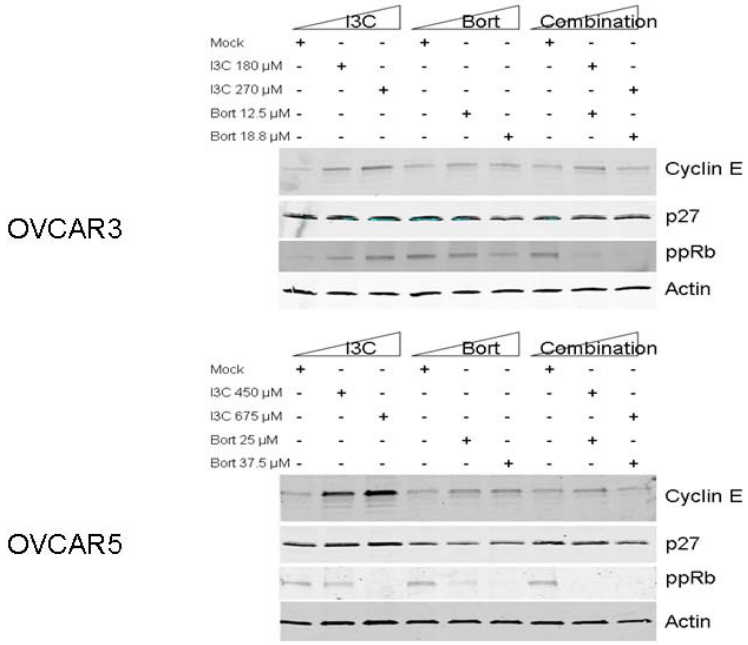

Figure 29. Decreased phosphor-Rb levels with increasing doses of I3C and bortezomib alone and in combination. Western blotting was used for protein expression analysis of OVCAR3 and OVCAR5 cells treated with the indicated agents for 24 hours.

This data was presented as a poster presentation at the 2010 AACR (American Association for Cancer Research meeting in Washington D.C., see appendix).

To determine the mechanism responsible for the synergistic effect of I3C and bortezomib, we performed RNA microarray analysis. Considering that both the apoptotic and synergistic effects of I3C and bortezomib were more robust in OVCAR5 cells compared to OVCAR3 cells at equipotent doses, we selected OVCAR5 cells for microarray analysis. We treated OVCAR5 cells with vehicle (mock), 675 µM I3C, 37.5 nM bortezomib or combination for 24 h, identical to the maximum concentrations used for our apoptosis and cell cycle studies. Three independent experiments were performed for a total of four triplicate conditions (12 samples). Total RNA was isolated as described for qRT-PCR analysis and the quality of RNA confirmed using an Agilent 2100 bioanalyzer. Probe labeling, microarray hybridization, washing and scanning were carried out as per manufacturer's instructions (Illumina).

Twelve samples were used to probe the Illumina HumanHT-12 v4 Expression BeadChip containing 47,231 human gene transcripts. Subsequent microarray analysis showed that our replicate samples from triplicate experiments share genes with similar gene

expression patterns that cluster close together. This data is represented as a dendrogram (Fig. 30), and demonstrates the reproducibility of our results.

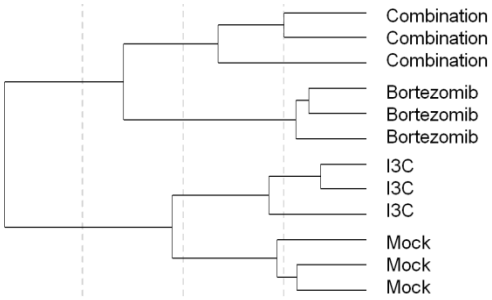

Figure 30. Dendrogram demonstrating data from triplicate experiments cluster closest to one another. OVCAR5 cells were treated with vehicle (mock), 675 µM I3C, 37.5 nM bortezomib or in combination for 24 h with subsequent RNA isolation and microarray gene expression analysis.

To filter our microarray data, we focused on significantly altered genes (p<0.0025) with log-fold changes >1.5 (upregulated) or <-1.5 (downregulated). While I3C treatment has significantly more differentially expressed genes (216 genes) in common with co-treatment compared to bortezomib (147 genes), the majority are unique to the combination condition (297 genes) (Fig. 31).

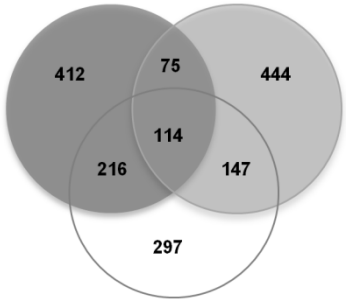

Figure 31. Venn diagram representing overlap between I3C and bortezomib treatment. Target genes with log-fold changes >0.4 or <-0.4 (p<0.0025) are presented.

In total, I3C/bortezomib treatment altered the expression of 774 genes. Classification of these genes indicate that co-treatment with I3C and bortezomib primarily inhibits the multistep development of cancer, consistent with the GO gene enrichment dataset (data not shown). Validation of our microarray data by qRT-PCR and Western blot analysis in both OVCAR3 and OVCAR5 cells showed that target genes involved in cell cycle control (e.g. *CDKN1A*, *CDK1*), apoptosis (e.g. *BCL2L1*, *BCL10*) and signal transduction (e.g. *DUSP1*, *NFkBIB*) were significantly deregulated (Fig. 32 and data not shown).

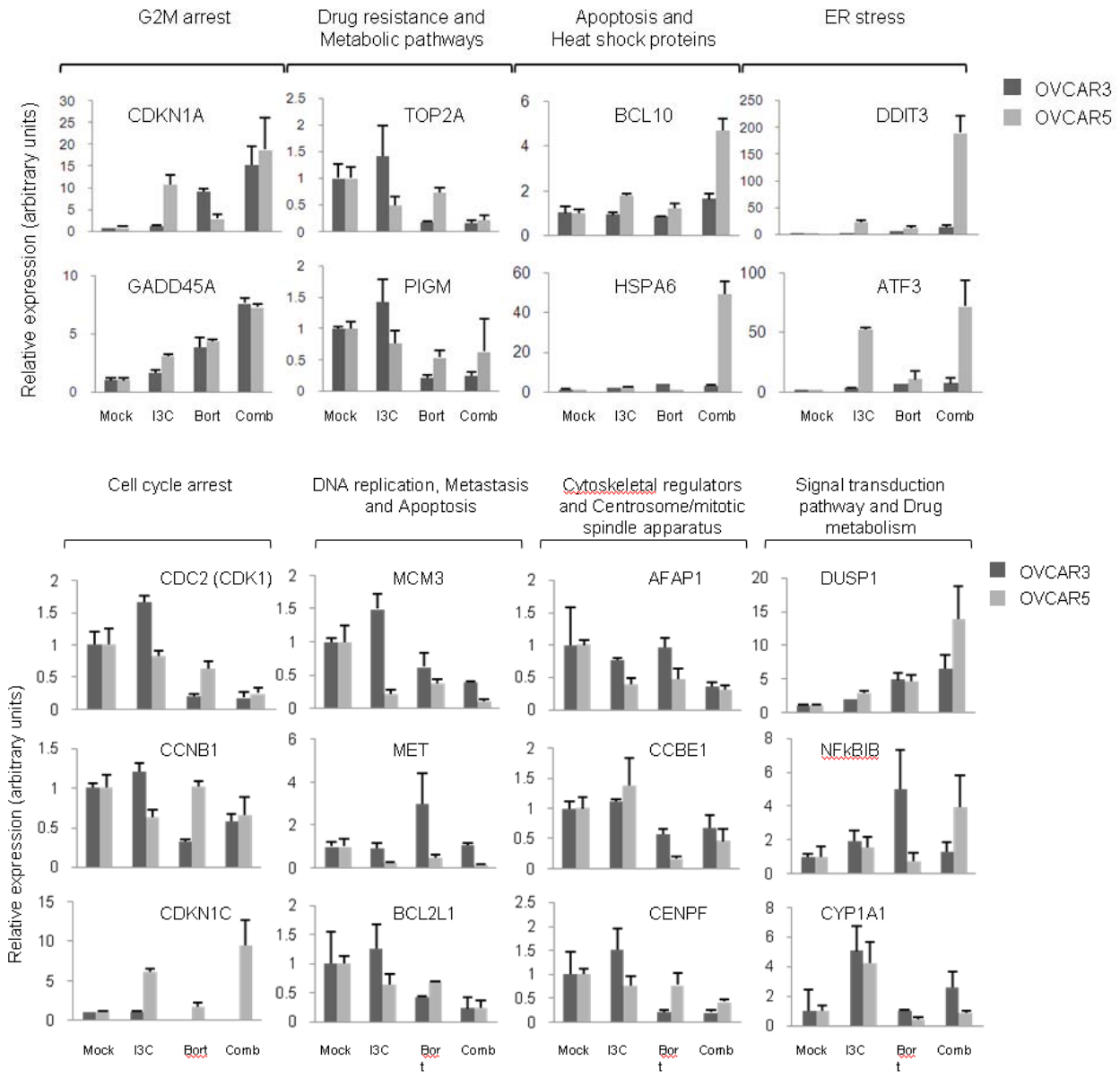

Figure 32. Quantitative RT-PCR of candidate target genes identified by microarray analysis categorized by function. Target gene validation was also performed in OVCAR3 cells treated with vehicle (mock), 270 µM I3C, 18.8 nM bortezomib or in combination for 24 h.

Moreover, metastasis (e.g. *MET*, *SNAI1*), angiogenesis, and adhesion target genes showed altered expression (Fig. 32). Notably, co-treatment with I3C and bortezomib appeared to downregulate *TOP2A* and *ABCC4*, target genes that are typically associated with chemoresistance. Consistent with our microarray data, qRT-PCR showed that *TOP2A* was severely downregulated (Fig. 32), a result that was reproducible by Western analysis in OVCAR3 cells but not in OVCAR5 cells (Fig. 33), suggesting that these effects are transient and/or evident only at the transcriptional level.

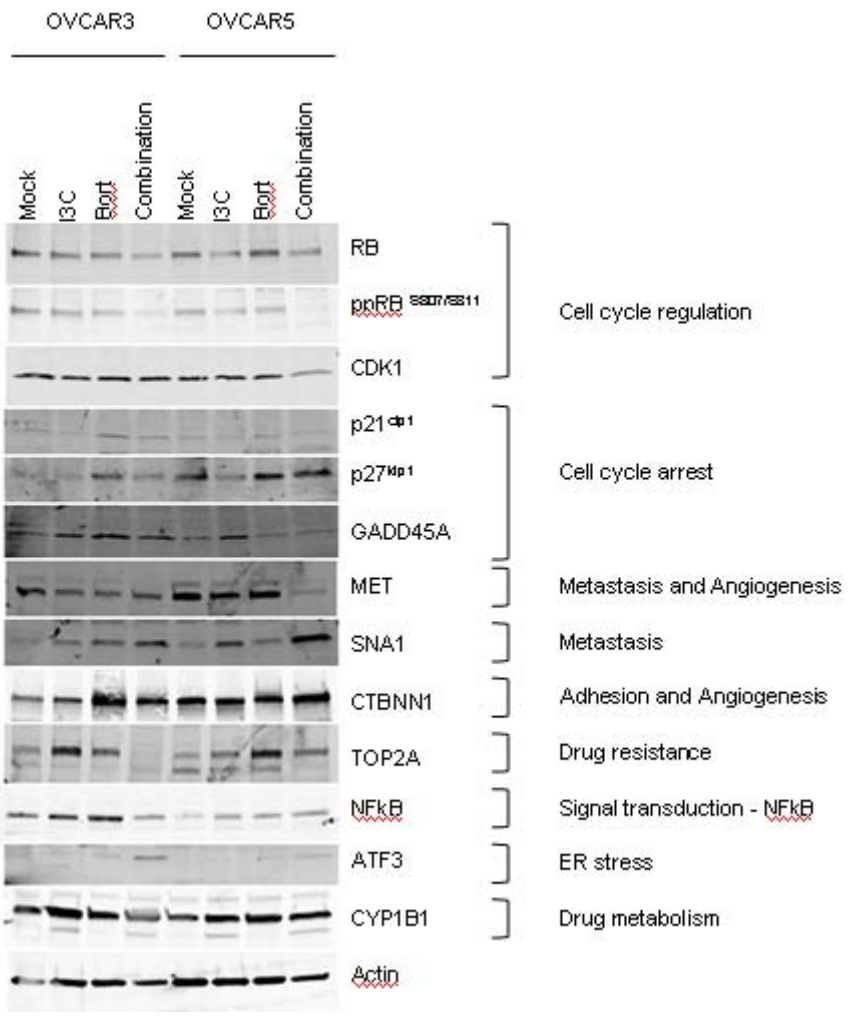

Figure 33. Western blot demonstrating effects of I3C, bortezomib, and combination treatment on protein levels categorized by function. Actin was used as a loading control.

Besides promoting cell death and inhibiting cancer progression, the combination of I3C and bortezomib deregulated other biological processes including ER stress, protein folding, centrosome and mitotic spindle apparatus, carcinogen metabolism, metabolic pathways, and cytoskeletal regulators. Representative target genes (e.g. *DDIT3*, *HSPA6*, *CENPF*) from each of these processes were validated by qRT-PCR with the majority of them demonstrating regulation as determined by microarray analysis (Fig. 32).

Overall, we found that co-treatment with I3C and bortezomib causes widespread gene deregulation that impinges on multiple pathways ultimately resulting in cell death (Fig. 34).

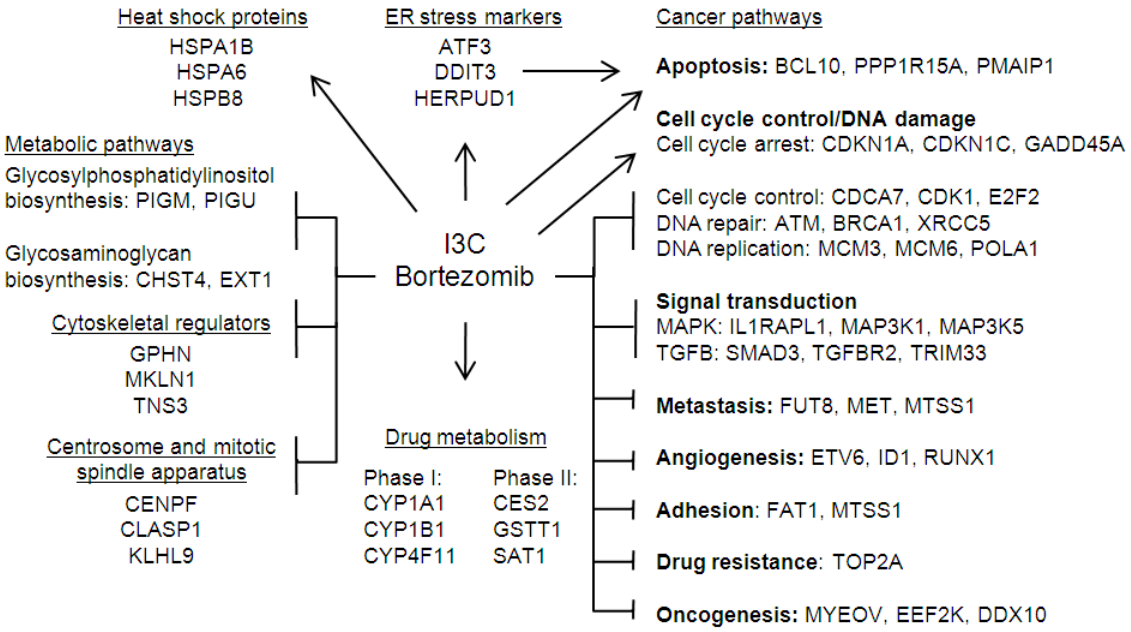

Figure 34. Pleiotropic effect of I3C and bortezomib on multiple biological processes. Representative target genes with log-fold changes >1.5 or <-1.5 ($p<0.0025$) are shown.

This data has particular relevance in light of recent phase II data demonstrating limited single-agent activity of bortezomib in recurrent ovarian cancer [6]. The finding that I3C, a natural dietary phytochemical found in cruciferous vegetables, synergistically sensitizes ovarian cancer cells to the cytotoxic effects of bortezomib may lead to a novel therapeutic combination.

This data were published in an original article, “Indole-3-Carbinol synergistically sensitizes ovarian cancer cells to Bortezomib treatment” in the *British Journal of Cancer* in 2012 [7].

Task 7: siRNA experiments against cyclin E and SKP2 using ovarian cancer cell lines that overexpress both proteins

Small interfering RNAs (siRNAs) against cyclin E and SKP2 were purchased from Sigma Aldrich and introduced into the OVCAR3 cell line (which expressed high endogenous levels of cyclin E and SKP2). We were able to achieve partial knock-down of protein expression levels of the two targets (figure 35). However, we found the cells with cyclin E knock-down to grow poorly and to be a poor experimental system for further manipulation, such as treatment with drugs. Furthermore, we were initially interested in SKP2 as a target for inhibition in tumors that overexpress cyclin E. Based on the negative data generated in task 6 (no difference in cell proliferation in cells expressing different levels of cyclin E when treated with the proteasome inhibitor bortezomib) and the generation of only partial knock-down of SKP2 levels, we did not pursue further experiments with these cells.

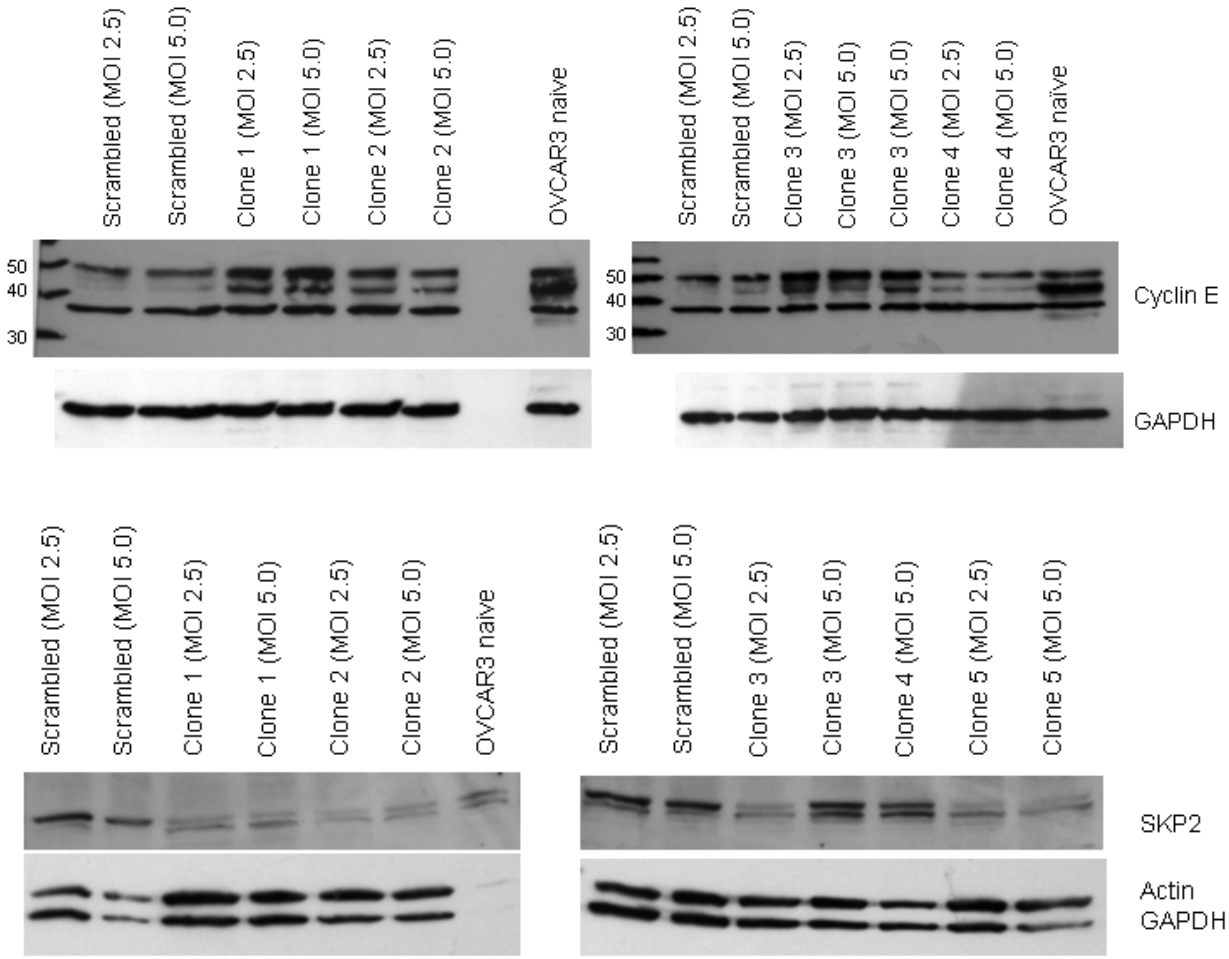

Figure 35. Small interfering RNA inhibition of cyclin E (upper panel) and SKP2 in OVCAR3 ovarian cancer cells. Western blotting data demonstrate partial knock-down of the two target proteins.

Task 8: In vivo tumor xenograft experiments

To examine the effect of I3C and bortezomib *in vivo*, we monitored the tumor growth of OVCAR5 tumor xenografts in nude mice treated with I3C and/or bortezomib. Six-week-old female nude mice were obtained from Charles River Laboratories (Wilmington, MA, USA) and maintained according to IACUC guidelines. Mice were inoculated subcutaneously in both flanks with an equal volume of 8×10^6 OVCAR5 cells and matrigel (Becton Dickinson) in a total volume of 200 µl. Mice were randomly divided into 4 treatment groups with 4 mice per group (8 tumors). Treatments were as follows: vehicle (control); I3C alone (20 mg/kg); bortezomib alone (1 mg/kg) and the drug combination (20 mg/kg I3C with 1 mg/kg bortezomib). Treatment was given intraperitoneally twice weekly starting 4 d post-inoculation. Tumor size was measured

twice weekly with a caliper and tumor volume was calculated as follows: L x W^2, where L = length and W = width. Data were expressed relative to the initial tumor volume 4 d post-inoculation. The initial tumor volume was set to 1 for each treatment group.

Although treatment with I3C or bortezomib alone initially induced tumor regression (Fig. 36A), these mice relapsed after prolonged treatment (≥31 d post-treatment. However, the combination of I3C and bortezomib significantly inhibited tumor growth (Fig. 36A) compared to control animals (64.6% tumor reduction, *P*<0.001) or individual treatment with I3C (47.6% tumor reduction, *P*=0.007) or bortezomib (35.9% tumor reduction, *P*=0.029) by the final day of treatment, consistent with our *in vitro* results. Indeed, the final weight (65.4% tumor reduction in I3C/bortezomib combination vs control, *P*=0.053) and appearance of the tumors post-treatment were consistent with the measurements obtained from earlier time points (Fig. 36B-D).

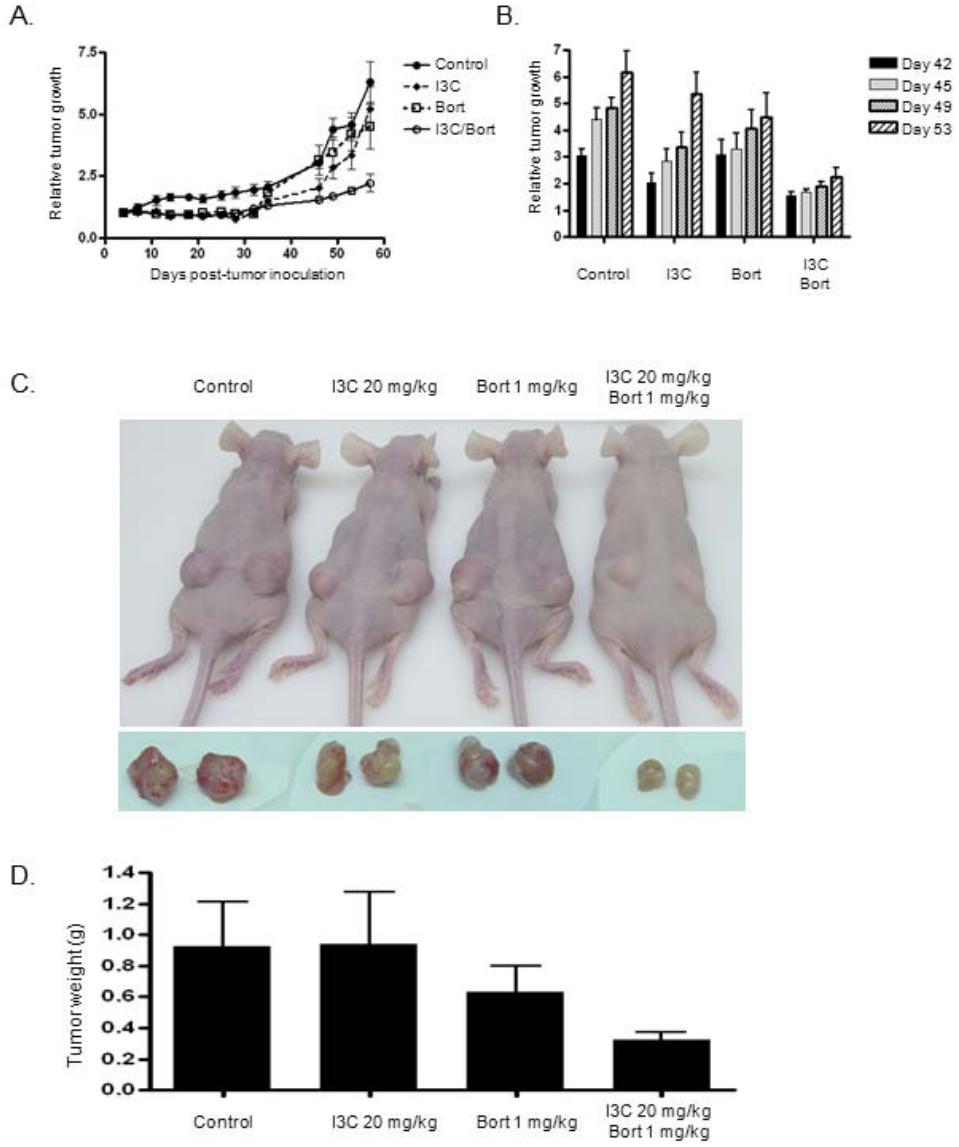

Figure 36. I3C and bortezomib co-treatment inhibit human ovarian tumor xenografts in nude mice. **A**, Relative tumor growth of OVCAR5 xenografts treated with vehicle (control), 20 mg/kg I3C, 1 mg/kg bortezomib or in combination measured from 0 to 53 d post-treatment or **B**, measured 42, 45, 49 and 53 d post-treatment. The data shown represent the mean ± SEM (n=8). **C**, Representative tumor images of control- (vehicle), I3C- and bortezomib-treated mice pre- and post-dissection, with corresponding **D**, tumor weight 53 d post-treatment. The data shown represent the mean ± SEM (n=8).

Task 9: Data analysis and manuscript generation and grant preparation

Data analysis has been on-going and has driven the experimental processes, with re-evaluation of hypotheses and generation of additional experiments to address the evolving data. Data from specific aim 3 were presented in poster format at the 2010 AACR meeting in Washington DC and published in the *British Journal of Cancer* in 2011 (see appendix) [7]. A review article on ovarian cancer biomarkers was published during the first year by myself and a mentor on this award, Beth Karlan (see appendix) [8]. Dr. Karlan provided me with the opportunity to write this review to further support my academic and career development activities related to ovarian cancer research.

KEY RESEARCH ACCOMPLISHMENTS

- We found synergistic cytotoxicity of I3C and bortezomib in ovarian cancer cell lines with differing levels of cyclin E expression. These findings provide a potential novel therapeutic option in the treatment of ovarian cancer expressing high or low levels of cyclin E. This may have particular clinical relevance in light of recent phase II clinical data showing limited activity of bortezomib as a single-agent in recurrent ovarian or peritoneal carcinomas.
- We have infected ovaries from K5-TVA transgenic, P53 conditional mutant mice with RCAS viruses causing overexpression of various oncogenes (oncogenic P53, cyclin E, myc, K-ras, AKT). This did not result in transformation of ovarian surface epithelial cells into epithelial ovarian carcinoma. We repeated the experiments with p53 -/- null mice but did not see transformation of OSE cells with the RCAS experiments. We adjusted our experimental technique to use pBabe retroviral transfection, rather than RCAS infection. Our positive control (overexpression of myc and K-ras) is now working with the pBabe vector and we have experiments on-going to determine the oncogenic potential for cyclin E overexpression.
- We performed IHC and FISH analysis for *CCNE1* expression in clinical ovarian cancer samples. These data were matched to corresponding *CCNE1* gene expression values from microarray experiments on matched frozen tissue. We found correlation between the gene expression levels and the highest levels of cyclin E protein expression and *CCNE1* gene amplification.
- We examined gene expression profiles among cyclin E overexpressing ovarian cancers and found the co-expressed genes to be drivers of the cell cycle rather than neighboring genes on the *CCNE1* gene locus.

REPORTABLE OUTCOMES

- Taylor-Harding B, Agadjanian H, Nassanian H, Berenson JR, Miller C, Karlan BY, Orsulic S, **Walsh CS**. The natural dietary phytochemical Indole-3-Carbinol (I3C) sensitizes ovarian cancer cells to the proteasome inhibitor

bortezomib. Abstract presented as poster at the American Association for Cancer Research meeting in Washington D.C., April 2010

- **Walsh CS**, Karlan BY. Molecular signatures of ovarian cancer: from detection to prognosis. Mol Diagn Ther 14(1):13-22, 2010 [8]
- Taylor-Harding B, Agadjanian H, Nassanian H, Kwon S, Guo X, Miller C, Karlan BY, Orsulic S, **Walsh CS**. Indole-3-Carbinol (I3C) synergistically sensitizes ovarian cancer cells to bortezomib treatment. *Br J Cancer.* 2012 Jan 17;106(2):333-43. Epub 2011 Dec 13. PMID: 22166800 [7]

CONCLUSION

At the genetic level, ovarian cancer is characterized by a large degree of genetic instability. High copy-number amplification at the *CCNE1* (cyclin E) gene locus is the single most notable recurrent change, occurring in about 20% of tumors. We have hypothesized that *CCNE1* gene amplification is an initiating event in the carcinogenic process of a subset of epithelial ovarian cancers. We have further hypothesized that this subset of tumors can be treated with specific targeted therapies, based on the biology of cyclin E overexpression.

During the three years of this award, we have made progress towards testing our hypothesis of cyclin E-induced ovarian cancer initiation in a mouse model. We successfully crossed the K5-TVA mice with P53 conditional mutant mice to generate a model for introduction of genetic changes to ovarian surface epithelial cells. We constructed the vectors to introduce full-length cyclin E and a truncated low molecular weight isoform of cyclin E and other collaborating genetic events into the mouse model. Our initial attempts to cause transformation of normal mouse ovarian surface epithelial cells through introduction of various oncogenic drivers were not successful. We hypothesized that the mouse model, which utilizes a p53 conditional mutant that is reported to function as a dominant negative protein, is not completely suppressing p53 activity, allowing for cells to undergo apoptosis under oncogenic stress. We made modifications to our model and crossed the K5-TVA mice with p53 null mice and repeated the experiment. We continued to experience difficulties with this system and did not see transformation, even with our positive control (overexpression of myc and K-ras). We made an additional modification to use the retroviral pBabe vector rather than the RCAS system for further experiments. With this modification, we were able to get our positive control (overexpression of myc and K-ras) to work. Our experiments are on-going to determine whether cyclin E overexpression can cause a similar transformation of ovarian surface epithelial cells.

In testing for a targeted response of cyclin E-overexpressing cells, we have demonstrated that the proteasome inhibitor bortezomib does not affect ovarian cancer cells through a cyclin E-mediated pathway. However, based on the biology of low molecular weight cyclin E isoforms, we found a natural dietary phytochemical called Indole-3-Carbinol (I3C) that disrupts cyclin E processing through the inhibition of the elastase enzyme. When combining I3C with bortezomib, we found I3C to synergistically sensitize ovarian cancer cells to bortezomib. This was true of various ovarian cancer

cell lines, irrespective of the cyclin E expression levels. The mechanism of synergy was explored through microarray and validation studies. Co-treatment caused gene expression changes affecting carcinogenesis, chemoresistance, endoplasmic reticulum stress, cytoskeletal regulation, and other metabolic pathways. These findings have translational potential as bortezomib as a single-agent was found to have minimal activity in a phase II treatment trial of recurrent ovarian cancer. This finding could re-introduce bortezomib to the therapeutic armamentarium against ovarian cancer if the results replicate in humans.

REFERENCES

[1] Wingate H, Bedrosian I, Akli S, et al. The low molecular weight (LMW) isoforms of cyclin E deregulate the cell cycle of mammary epithelial cells. Cell Cycle 2003;2(5):461-6.
[2] Orsulic S, Li Y, Soslow RA, et al. Induction of ovarian cancer by defined multiple genetic changes in a mouse model system. Cancer Cell 2002;1(1):53-62.
[3] Kido M, Shibuya M. Isolation and characterization of mouse ovarian surface epithelial cell lines. Pathol Res Pract 1998;194(10):725-30.
[4] Uddin S, Ahmed M, Bavi P, et al. Bortezomib (Velcade) induces p27Kip1 expression through S-phase kinase protein 2 degradation in colorectal cancer. Cancer Res 2008;68(9):3379-88.
[5] Nguyen HH, Aronchik I, Brar GA, et al. The dietary phytochemical indole-3-carbinol is a natural elastase enzymatic inhibitor that disrupts cyclin E protein processing. Proc Natl Acad Sci U S A 2008;105(50):19750-5.
[6] Aghajanian C, Blessing JA, Darcy KM, et al. A phase II evaluation of bortezomib in the treatment of recurrent platinum-sensitive ovarian or primary peritoneal cancer: a Gynecologic Oncology Group study. Gynecol Oncol 2009;115(2):215-20.
[7] Taylor-Harding B, Agadjanian H, Nassanian H, et al. Indole-3-carbinol synergistically sensitises ovarian cancer cells to bortezomib treatment. Br J Cancer 2011;106(2):333-43.
[8] Walsh CS, Karlan BY. Molecular signatures of ovarian cancer: from detection to prognosis. Mol Diagn Ther 2010;14(1):13-22.

The Natural Dietary Phytochemical Indole-3-Carbinol (I3C) Sensitizes Ovarian Cancer Cells to the Proteasome Inhibitor Bortezomib through Inhibition of Cyclin E Activity

Barbie Taylor-Harding[1], Hasmik Agadjanian[1], Hoorig Nassanian[1], James R. Berenson[2], Carl Miller[1], Beth Y. Karlan[1], Sandra Orsulic[1], and Christine Walsh[1]

[1]Women's Cancer Research Institute at the Samuel Oschin Comprehensive Cancer Institute, Cedars-Sinai Medical Center, Los Angeles, CA

[2]Institute for Myeloma & Bone Cancer Research, Oncotherapeutics, West Hollywood, CA

Background

Epithelial ovarian cancer (EOC) remains the leading cause of gynecologic cancer mortality. Cyclin E deregulation is an important initial event in a subset of EOCs associated with poor outcome. The proteasome inhibitor bortezomib has been shown to inhibit the growth of both ovarian and colorectal tumor cell lines through upregulation of p27, indicating its potential therapeutic role in the subset of ovarian cancers that overexpress cyclin E. As many as five low molecular weight (LMW) isoforms of cyclin E exist in cancer tissues, while only the 50-kDa cyclin E form is expressed in normal tissues. These LMW isoforms are generated via proteolysis of the normal 50-kDa cyclin E form by elastase. Proteolytic activity of elastase can be selectively inhibited by indole-3-carbinol (I3C), a natural component of Brassica vegetables and potent anticarcinogen. Considering the specific inhibitory properties of I3C and bortezomib in the processing and potential expression of cyclin E, respectively, we hypothesize that ovarian cancers overexpressing cyclin E may demonstrate an enhanced response to targeted combination therapy with I3C and bortezomib.

Methods

Viability of OVCAR3 and OVCAR5 human ovarian cancer cells ± I3C and ± bortezomib for 48 h was assessed by MTT assays.

Synergy between I3C and bortezomib was determined using isobologram analysis using Calcusyn software; combination indices (CI)<1.0 are considered synergistic.

FACS analysis of Annexin V and propidium iodide (PI) stained cells was used to discriminate between early and late apoptosis in OVCAR3 and OVCAR5 cells treated with ± I3C and ± bortezomib for 24 h.

Western blotting was used for protein expression analysis of OVCAR3 and OVCAR5 cells treated with ± I3C and ± bortezomib for 24 h.

Real-time PCR was used for gene expression analysis.

Results

OVCAR3 Cells Express High Levels of Cyclin E Compared to OVCAR5 Cells

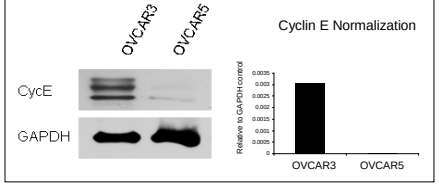

OVCAR3 Cells are More Chemosensitive to Individual Treatment with I3C and Bortezomib Compared to OVCAR5 Cells

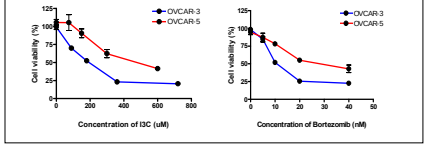

Synergistic Cytotoxicity of I3C and Bortezomib in Both OVCAR3 and OVCAR5 Cells

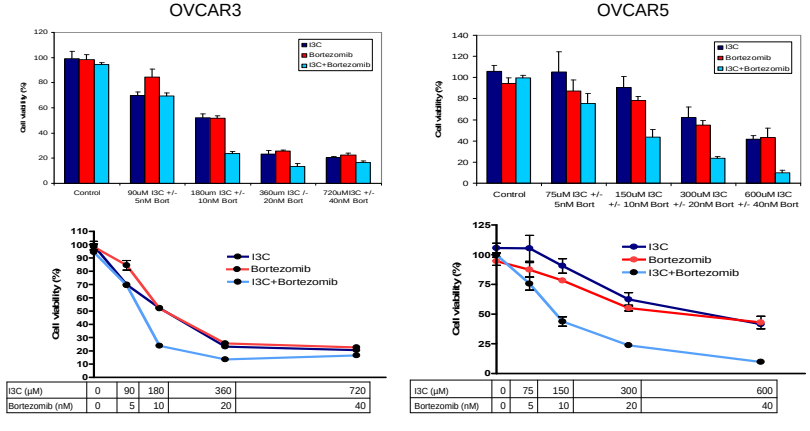

Greater Synergy of I3C and Bortezomib in OVCAR5 Cells Compared to OVCAR3 Cells

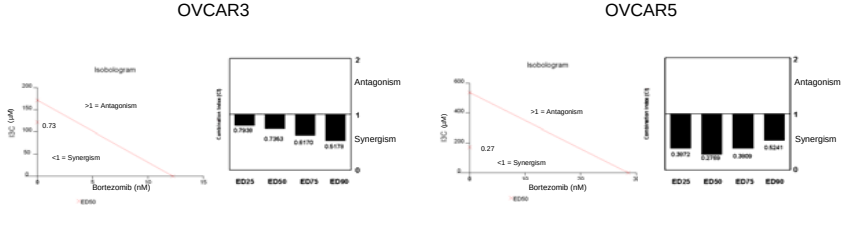

I3C and Bortezomib Enhance Apoptosis

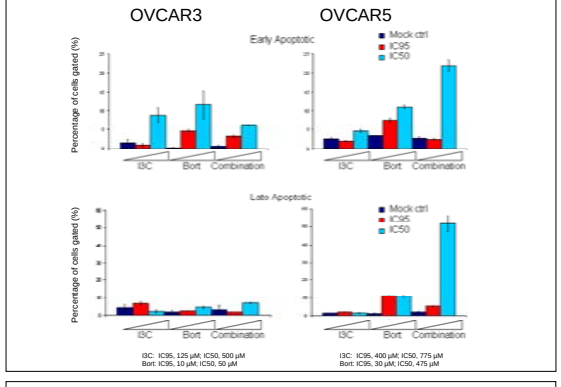

I3C and Bortezomib Alter Cell Cycle Protein Expression

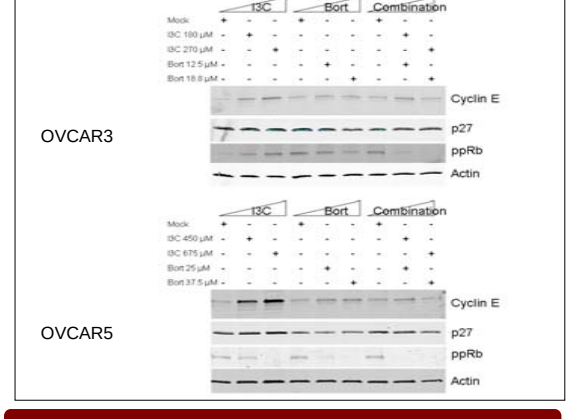

Translational Potential

Our data demonstrate synergistic cytotoxicity of I3C and bortezomib, through premature apoptosis and impairment of cell cycle progression. Our findings support a possible therapeutic role for I3C and bortezomib in the treatment of ovarian cancers expressing high or low levels of cyclin E.

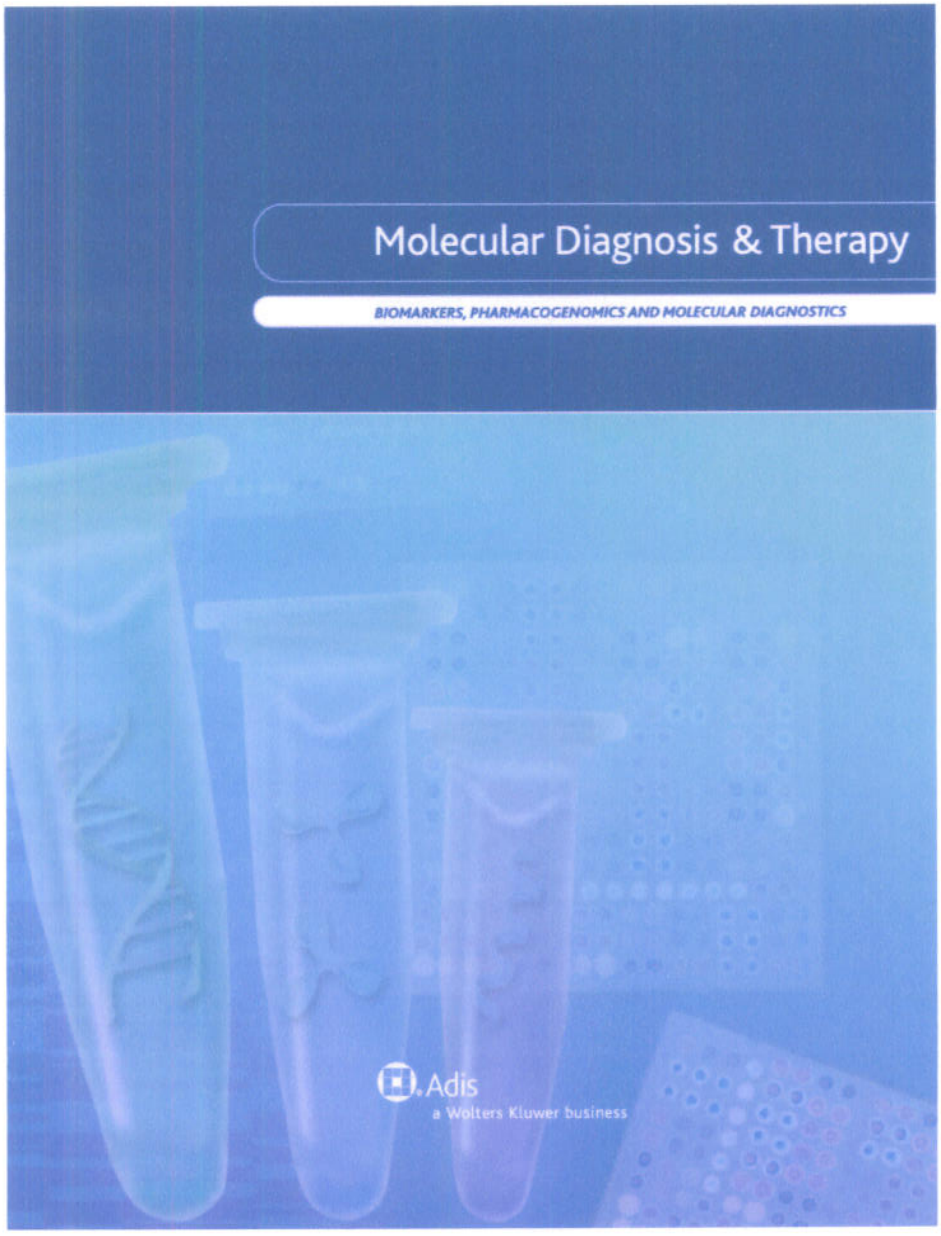

REVIEW ARTICLE

Mol Diagn Ther 2010; 14 (1): 13-22
1177-1062/10/0001-0013/$49.95/0

Molecular Signatures of Ovarian Cancer

From Detection to Prognosis

Christine S. Walsh and *Beth Y. Karlan*

Cedars-Sinai Medical Center, Los Angeles, California, USA

Contents

Abstract

The search for an effective screening test for the early detection of ovarian cancer has been intensive. Transvaginal ultrasound and the serum biomarker cancer antigen 125 (CA125) have been used clinically for decades in high-risk populations despite the lack of evidence demonstrating efficacy. More recently, new technologies have identified novel biomarker panels that attempt to improve on the performance of currently available modalities. Some of these tests report superior performance characteristics (sensitivity, specificity, positive predictive value) when compared with CA125 testing alone. Based on early encouraging studies, two commercial ovarian cancer screening products were recently marketed to the public and medical community. They were both withdrawn after concerns were raised by the US FDA and the scientific community regarding their validation and efficacy. There is no clear and established pipeline for the development and approval of these types of tests, and the FDA is working to fill in a large regulatory gap. In order to minimize the potential for public harm, an ovarian cancer screening test will need to be appropriately tested before being made available to the general population. In this review, we discuss the current state of biomarker development for the early detection of ovarian cancer and explore the continuing challenges to realizing this goal.

An effective means for the early detection of ovarian cancer is a much sought-after goal, yet remains an unmet need. The vast majority of ovarian cancers are diagnosed by clinical symptoms at advanced stages, when the chance of surviving beyond 5 years is approximately 30%. Only one-third of ovarian cancers are diagnosed at an early stage, when the 5-year survival is 90%.[1] This disparity in survival statistics has provided strong motivation to find a means for earlier diagnosis and detection before symptoms develop. Current efforts are heavily focused on biomarkers, including single markers, marker patterns over time, and marker panels. In this review, we will discuss the current state and challenges toward finding an effective screening test for ovarian cancer.

1. Challenges to Early Ovarian Cancer Detection

Ovarian cancer is notoriously difficult to diagnose. The ovaries are tucked away in the pelvis and are relatively

inaccessible; in addition, they can give rise to a broad spectrum of pathology with great genetic and molecular heterogeneity. Epithelial ovarian cancers comprise the histologic subtypes that are responsible for the majority of ovarian cancer deaths. The papillary serous histologic subtype represents 70% of epithelial ovarian cancers and is one of the most lethal.[2] The quest toward the discovery of an effective screening test for this challenging clinical condition has been marked with numerous difficulties. Among the greatest of the challenges are (i) the lack of information about a detectable preclinical stage; (ii) the low prevalence of the disease; and (iii) the inability to easily biopsy the ovary.

The single most important criterion to allow for effective early detection of a disease through screening is the presence of a detectable preclinical stage of sufficient duration during the development of the disease.[3] Until recently, very little was known about the natural biology underlying the development of papillary serous ovarian cancers. The length of time from a localized tumor to widely disseminated disease had not been defined, and prior screening studies demonstrating the development of advanced-stage cancers within 6–12 months of a negative screen suggested that this time interval was relatively short.[4-6]

However, a new study now suggests that serous cancers spend >4 years as *in situ* or early-stage cancers and approximately 1 year as advanced-stage cancers before they become clinically apparent.[7] These estimates were derived from a model of growth and progression, based on data from occult serous tumors found at the time of prophylactic bilateral salpingo-oophorectomy in high-risk *BRCA1* (breast cancer 1, early onset) mutation carriers. This model further estimates that occult serous tumors have a diameter of <3 mm and spend >90% of the duration of the window of opportunity for early detection at a diameter of <9 mm. By the time a tumor has reached 3 cm in diameter, >50% have already metastasized to stage III or IV. Therefore, to have an impact on mortality reduction, the authors suggest that a screening test in an average-risk population would need to detect a 4 mm tumor to achieve 80% sensitivity.[7] These data are encouraging because they suggest that a preclinical stage of sufficient duration exists for one of the most deadly types of ovarian cancer. However, our currently available tests are not yet sensitive enough for detection of these subcentimeter lesions.

The second major challenge to the development of a widely applicable screening test is the low prevalence of ovarian cancer in the general population.[8] Ovarian cancer remains a relatively uncommon disease, affecting approximately 1 in 2500 postmenopausal women in the US. In this low-prevalence setting, a screening test would need to achieve near-perfect specificity in order to minimize the potential harm resulting from false-positive results.[9] For example, a test with a sensitivity of 99%, or a false-positive rate of 1%, would subject 25 of 2500 healthy women to the worry, anxiety, and risks of additional follow-up procedures resulting from a positive screen that falsely suggests the presence of ovarian cancer. Even a hypothetical test with an extremely high specificity of 99.6% and a sensitivity of 75% would achieve a positive predictive value (PPV) of only 10% and would result in the diagnostic evaluation and work-up of ten women for every one with ovarian cancer. This seemingly high trade-off has been suggested to be an acceptable goal for this low-prevalence condition.[10]

The third major challenge to ovarian cancer screening is the inaccessibility of the ovaries to further diagnostic evaluation. The ovaries are not readily biopsied, and any positive result on an ovarian cancer screening test, either true or false, subjects that individual to invasive exploratory surgery. Furthermore, if we achieve the goal of developing a screening test that can detect subcentimeter ovarian tumors, the majority of which cannot be seen with gross evaluation at the time of surgery, the only rational evaluation would be bilateral salpingo-oophorectomy followed by meticulous pathologic evaluation of the specimen. The potential risks of such an invasive evaluation in healthy women as the result of a poor-performance screening test cannot be overstated.

2. Cancer Antigen 125

Cancer antigen 125 (CA125) was the first ovarian cancer biomarker to be described.[11,12] Although CA125 has demonstrated utility for monitoring established disease and response to treatment,[13] it performs poorly as a screening tool. Half of all early ovarian cancers, the presumed targets of early detection, would not be detected through the use of this serum biomarker.[14] In addition to the poor sensitivity of 50% for early-stage ovarian cancer, the specificity of CA125 is limited by the fact that many benign conditions cause false elevations of its levels.[15]

Despite the fact that CA125 has limited sensitivity and specificity as an early detection serum biomarker, it has been combined with transvaginal ultrasound in two large, randomized controlled trials of ovarian cancer screening.[16-18] The PLCO (Prostate, Lung, Colorectal, and Ovarian) Cancer Screening Trial is being conducted in the US by the National Institutes of Health (NIH).[19] The objective in the ovarian

cancer arm of the screening trial is to determine whether screening with both serum CA125 and transvaginal ultrasonography in healthy women aged 55–74 years reduces mortality from ovarian cancer. The trial is designed to detect a 30% reduction in mortality over 16 years of follow-up.

Mortality data from this trial will not be available for many more years, but the performance characteristics of serum CA125 and transvaginal ultrasound have been reported. In the prevalence screen (T0) of 28 826 women, a total of 1706 (5.9%) had abnormal results: 1338 (4.7%) had an abnormal ultrasound study; 402 (1.4%) had an abnormal CA125 level (≥35 units/mL); and 34 (0.1%) had abnormal results on both tests.[16] This baseline screen resulted in 570 oophorectomies being performed for 29 cancers (20 invasive, 9 low malignant potential) and 541 benign conditions, demonstrating the poor specificity of these tests. The PPV for invasive cancer was estimated at 1% for ultrasound, 3.7% for CA125, and 23.5% for the combination of the tests. However, only 9 of 29 (31%) of the invasive or borderline cancers were associated with abnormalities of both tests. Additionally, the majority of the invasive cancers (83%) detected by screening were stage III and IV.[16]

Over 3 additional years of annual screening (T1–T3), 89 invasive ovarian or peritoneal cancers were diagnosed.[17] Among these, only 60 (68%) were detected by screening. An additional 19 (21%) were detected in the interval between screenings, and 10 (11%) were detected in women that had never been screened. The PPV remained low, ranging from 1.0% to 1.3% over the 3 years, and the overall ratio of surgeries to screen-detected cancers remained high at 19 to 1.[17]

The high rate of surgery for benign conditions was largely due to false-positive screens on transvaginal ultrasound.[17] The ratio of surgeries to cancer was 44 to 1 at baseline T0, and then incrementally improved to 23 to 1 in the subsequent screening rounds, T1–T3. The ratio of surgeries to cancer was a more favorable 4.5 to 1 after a positive CA125 screen. However, the majority of cancers detected after a positive CA125 were late stage (89% of 27 cases were stage III/IV), while the majority of cancers detected after a positive transvaginal ultrasound screen were early stage (71% of 14 cases were stage I/II).[17]

The multicenter UKCTOCS (United Kingdom Collaborative Trial of Ovarian Cancer Screening) is the other ongoing large randomized controlled trial designed to assess the impact of ovarian cancer screening on mortality.[18] From 2001 to 2005, >200 000 postmenopausal women aged 50–74 years were randomized to a control arm or a screening arm. The screening arm was divided into two different strategies; an ultrasound-based screening approach (USS) or a multimodal screening approach (MMS). In the USS arm, subjects underwent screening with transvaginal ultrasound alone (and no serum CA125 measurement). In the MMS screening arm, serum CA125 levels were measured and assessed with a risk of ovarian cancer (ROC) algorithm. Instead of relying on a single threshold cut-off or static CA125 value, the ROC algorithm considers patient age, the absolute CA125 level, and the rate of CA125 level change to assign a level of risk.[20] Patients classified as low risk undergo repeat CA125 testing in 1 year. Individuals with a persistently intermediate-risk classification (which triggers a repeat CA125 in 12 weeks) or a high-risk classification are triaged to further evaluation with ultrasound. The performance of the ROC algorithm was first reported to have a sensitivity of 83%, a specificity of 99.7%, and PPV of 16% in the initial retrospective analysis.[20] In a subsequent prospective pilot study applying the algorithm to >6500 women, its performance maintained a specificity of 99.8% and PPV of 19%.[21]

The prevalence screen from the UKCTOCS found 59 invasive ovarian and tubal cancers (34 in MMS, 25 in USS) and 28 borderline tumors (8 in MMS, 20 in USS).[18] In contrast to the PLCO study, almost half of the invasive cancers (48%, or 28 of 59) were detected while at an early stage (I/II), with no difference in stage distribution seen between the two screening groups. Of the tumors, 44% (20 of 45) detected in the USS group were of low malignant potential. The high prevalence of benign adnexal masses and borderline tumors detected in the USS group led to a higher rate of repeat testing and surgeries and lower specificity in this screening arm. The rate of surgery to invasive cancer was 35 to 1 for the USS strategy compared with 2.9 to 1 for the MMS strategy, making the rate of surgery almost 9-fold higher in the USS arm.[18]

The performance characteristics of CA125 and transvaginal ultrasound in these two large randomized controlled trials are summarized in table I. Transvaginal ultrasound screening comes at a high cost of many invasive surgeries for benign or borderline tumors but may detect a higher rate of early-stage disease. This has also been demonstrated in prior ultrasound screening studies, which reported that 59–65% of cancers were detected at an early stage but with a similar high rate of false-positive screening results.[4,22,23] Both studies were consistent in demonstrating improved specificity of the serum biomarker over ultrasound imaging. However, the use of a static CA125 value has poor predictive ability in detecting early-stage disease, while the use of longitudinal assessments such as the ROC algorithm demonstrates better utility in picking up early-stage disease.

Whether any of these strategies has an impact on ovarian cancer mortality remains to be determined. In the PLCO trial,

Table I. Performance characteristics of serum cancer antigen 125 (CA125) and transvaginal ultrasound in two large randomized trials of ovarian cancer screening in the average-risk postmenopausal population

Performance characteristics	CA125			Transvaginal ultrasound		
	PLCO baseline T0[16]	PLCO annual T1–T3[17]	UKCTOCS MSS baseline[18]	PLCO baseline T0[16]	PLCO annual T1–T3[17]	UKCTOCS USS baseline[18]
Positive screen (%)	1.4	1.6–1.8	8.7	4.6	2.9–3.4	12
No. of borderline tumors	1	0, 1, 0	8	9	4, 0, 0	20
No. of invasive cancers	13	9, 13, 11	34	12	10, 6, 5	25
Proportion stage I/II (%)		11	47		71	50
No. of surgeries per 1 invasive cancer	4.5	4.5	2.9	44	23	35.2
Apparent sensitivity (%)			89.5			75
Specificity (%)			99.8			98.2
PPV (%)	3.2	2.1–2.7	35.1	0.9	0.7–1.1	2.8

MSS = multimodality screening strategy; **PLCO** = Prostate, Lung, Colorectal, Ovarian (Cancer Screening Trial); **PPV** = positive predictive value; **T0** = time 0, i.e. prevalence screen at baseline time 0; **T1–3** = time 1–3, i.e. incidence screen at years 1–3; **UKCTOCS** = United Kingdom Collaborative Trial of Ovarian Cancer Screening; **USS** = ultrasound screening strategy.

the stage distribution of the cancers detected by screening was not appreciably different than would be expected from clinical detection and, therefore, it would be surprising if this trial were to find an impact on mortality. The UKCTOCS demonstrated a shift in stage distribution toward earlier stages with screening. If there is a comparable decrease in ovarian cancer-specific mortality among the screened population, this might provide justification for screening in the general population with currently available technology.

3. Other Candidate Serum Biomarkers

The poor sensitivity and specificity of CA125 for preclinical disease has spurred an intensive search for alternatives that could more reliably herald the presence of early-stage cancers. Various serum markers have been evaluated through a candidate approach, either alone or in combination with CA125. Over 30 serum biomarkers have been analyzed, including autotoxin, CA15-3, CA72-4, CA19-9, claudin 3, human epididymis secretory protein 4 (HE4), human kallekreins, lipid-associated sialic acid, lipophosphatidic acid, macrophage colony-stimulating factor, matrix metalloproteinases (MMPs), mesothelin, osteopontin, OVX1, soluble epidermal growth factor receptor (EGFR), and vascular endothelial growth factor (VEGF).[10,24-29] When combined with CA125, some of these markers have demonstrated a slight improvement in sensitivity, compared with CA125 alone, when specificity is fixed at 97% or 98% (table II).

One of the most promising ovarian cancer biomarkers appears to be HE4, the protein product of the *WFDC2* gene.[36] Experiments using gene expression and cDNA microarray technologies found HE4 to be amplified in ovarian carcinomas but not in normal control tissues.[37,38] When compared with CA125, HE4 is better at detecting early-stage disease (improved sensitivity) and better at ruling out benign conditions (improved specificity).[39] HE4 has also been shown to complement CA125 when the two biomarkers are multiplexed together.[40] In postmenopausal women presenting with a pelvic mass, the dual marker combination of HE4 and CA125 can better classify patients into groups with a high or low risk of malignancy, with a sensitivity of 92.3% and a specificity of 75%.[41] In the context of early detection, a two-step screening algorithm that uses HE4 >1.8 ng/mL as step 1 followed by positive CA125, glycodelin, or plasminogen activator urokinase receptor (PLAUR) as step 2 achieves a sensitivity of 73.7% and a specificity of 93.7% for stage I/II disease.[34]

4. Biomarkers and Monitoring for Disease Recurrence

CA125 is widely used in clinical practice to monitor for ovarian cancer recurrence. Rising levels, even when remaining below the upper limit of normal (<35 U/mL), are highly predictive of disease recurrence.[42] A biomarker panel consisting of HE4, MMP7, and glycodelin was found to predict disease recurrence prior to elevation of CA125 in 56% of cases and in an equivalent timeframe to CA125 in 41% of cases, with a lead time ranging from 6 to 69 weeks.[34] In 2008, Allard et al.[43] presented data on the use of HE4 for monitoring patients with epithelial ovarian cancer. Among 80 patients with ovarian cancer, serial HE4 levels correlated with CT imaging

findings of recurrence in 76% of patients, and the addition of HE4 to CA125 led to a further increased correlation with clinical status (84%). These data are not yet published, but led to recent US FDA approval for Fujirebio Diagnostics, Inc. to market HE4 in combination with CA125 for the early detection of disease recurrence. However, the impact of early detection of disease recurrence on overall survival and quality of life has recently been called into question by the findings of a randomized controlled trial reported by Rustin et al.[44] in 2009.

5. Biomarker Discovery

The completion of the Human Genome Project has opened doors to a more global approach to biomarker discovery. Through the mechanisms of alternative splicing and post-translational modification, an estimated 30 000 genes lead to the production of 1.5 million protein products in our bodies, or approximately 50 protein products per gene.[45] High-throughput platforms allow for the profiling of thousands of potential

Table II. Performance of various serum biomarker panels in differentiating serum samples from ovarian cancer patients and various control populations

Studies	Screening method	Sensitivity (%)	Specificity (%)	Population tested
Petricoin et al., 2002[30]	SELDI-TOF	100	95	50 cancers (18 early), 66 benign
Zhang et al., 2004[31]	CA125	65	97	138 cancers,
	APOA1, TTR, inter-α trypsin inhibitor	74	97	63 controls
Skates et al., 2004[26]	CA125	45	98	60 early-stage cancers,
	CA125/CA72-4	67	98	98 controls
	CA125/CA72-4/M-CSF	70	98	
	CA125/CA72-4/M-CSF/CA15-3	65	98	
McIntosh et al., 2004[27]	CA125	78.8	98	53 cancers,
	CA125/mesothelin	86.5	98	43 benign, 220 controls
Gorelik et al., 2005[28]	CA125/IL-6/IL-8/VEGF/EGF	84	95	44 early-stage cancers,
	CA125/ IL-6/G-CSF/VEGF/EGF	86.5	93	37 benign, 45 controls
Mor et al., 2005[32]	Leptin, prolactin, osteopontin, IGF2	95	94	100 cancers, 106 controls
Visintin et al., 2008[33]	Leptin, prolactin, osteopontin, IGF2, MIF, CA125	95.3[a]	99.4[a]	Training set: 113 cancers, 181 controls Test set: 43 cancers, 181 controls
Havrilesky et al., 2008[34]	CA125, HE4, glycodelin, PLAUR, MUC1, PAI-1	80.5[b]	96.5[b]	200 cancers (133 stage I/II), 396 healthy controls
Shah et al., 2009[29]	CA125	78	98	143 cancers,
	HE4	68–82	98	124 benign,
	Mesothelin	31–44	98	344 controls
Amonkar et al., 2009[35]	CA125, CA19-9, EGFR, CRP, myoglobin, APOA1, APOC3, MIP1A, IL-6, IL-18, tenascin C	91.3	88.5	115 cancers, 93 benign, 24 controls, 13 non-ovarian cancers

a Combines training and test sets.

b Stage I/II.

APOA1 = apolipoprotein A1; **APOC3** = apolipoprotein C3; **CA** = cancer antigen; **CRP** = C-reactive protein; **EGF** = epidermal growth factor; **EGFR** = EGF receptor; **G-CSF** = granulocyte colony-stimulating factor; **HE4** = human epididymis protein 4; **IGF2** = insulin-like growth factor 2; **IL** = interleukin; **M-CSF** = macrophage colony-stimulating factor; **MIF** = macrophage migration inhibitory factor; **MIP1A** = macrophage inflammatory protein 1α (CCL3); **MUC1** = mucin 1; **PAI-1** = plasminogen activator inhibitor (also known as SERPINE1); **PLAUR** = plasminogen activator, urokinase receptor; **SELDI-TOF** = surface-enhanced laser desorption/ionization time of flight; **TTR** = transthyretin; **VEGF** = vascular endothelial growth factor.

biomarkers or of the entire serum proteome in a single experiment, enabling scientists to break out of the confines of the candidate biomarker approach, which relies on biological inference.

Proteomic technologies have been applied to the discovery of biomarkers that distinguish the sera of ovarian cancer patients from their healthy counterparts. Two general approaches have been utilized. In the first approach, surface-enhanced laser desorption/ionization time of flight (SELDI-TOF) and mass spectroscopy are used to profile proteins in serum according to the size and net electrical charge of each of the individual proteins. Proteins are bound to a protein array, a laser desorbs and ionizes the proteins from the bound surfaces, and the time of flight of the protein fragments is translated into a spectrum of peaks. The peptides responsible for the discriminatory peaks can be further sequenced to identify the serum proteins.[46] In the second approach, a panel of known markers can be assayed through more traditional techniques, such as antibody microarrays or enzyme-linked immunosorbent assay (ELISA). Multiplex platforms have been developed that allow for the assessment of multiple markers with a very small volume of serum.

In a high-profile 2002 Lancet publication resulting from collaboration between researchers from the NIH, the FDA and a private firm, Correlogic Systems, Inc., a proteomics study using SELDI-TOF and mass spectrometry demonstrated 100% sensitivity and 95% specificity for correctly classifying the sera from 50 women with ovarian cancer and 66 healthy controls.[30] Mass spectrometry revealed discriminatory peaks that could differentiate samples as being from a cancer patient or a control, using proprietary pattern-recognition software. Although these results were based on a small set of stored and frozen serum samples, the findings rippled through the mass media and created a sensation.

However, enthusiasm waned when the initial results could not be replicated.[47,48] Major criticisms of the study emerged, including the possibility of bias related to artifacts in sample collection, storage, and processing; the nature of the clinical samples used; the mass spectrometry instrument; and the bioinformatics analysis.[48,49] Reanalysis of the raw data by a different set of investigators led to the conclusion that the discriminatory peaks between cancer and control sera were doubtful in the setting of substantial, non-biologic experimental bias, including experimental noise due to matrix effects.[47,49] Furthermore, the PPV of 94% claimed in the study was an artificially inflated value that reflected the high prevalence of ovarian cancer in an enriched study population.[50,51] The lack of identification of the peptides associated with the discriminatory peaks was regarded as a further flaw.[52]

The original authors acknowledged the problem of unacceptable week-to-week and machine-to-machine variability with the Cipergen ProteinChip™ Biomarker System-II mass spectrometer, which was the low-resolution platform used in the original 2002 publication.[30] In a follow-up study, the high-resolution hybrid quadrupole time-of-flight mass spectrometer was found to yield a superior classification pattern with 100% sensitivity and 100% specificity in the classification of sera from 68 cancers and 43 healthy controls.[53] This report was published in 2004, but it is unclear where Correlogic plans to go with proteomic peak profiling at this time.

More recent publications from the company demonstrate a shift in strategy toward evaluating the levels of known analytes in the sera of patients with ovarian cancer or benign conditions.[35,54] The analytes cover a broad range of biologic activities and include cancer antigens, hormones, clotting factors, tissue modeling factors, lipoprotein constituents, proteases and protease inhibitors, markers of cardiovascular risk, growth factors, cytokines/chemokines, soluble forms of cell signaling receptors, and inflammatory and acute-phase reactants. Using a bead-based approach, the levels of 204 molecules were measured simultaneously in sera from 147 patients with ovarian cancer and 147 patients with benign ovarian pathology.[54] By generating a receiver operating characteristic curve for each analyte, the area under the curve (AUC) values were compared with that of an uninformative marker (AUC 0.5).

The analyte with the highest AUC value was CA125, with an AUC of 0.906. Analytes with AUC values between 0.756 and 0.701 included C-reactive protein, soluble EGFR, interleukin (IL)-10, IL-8, connective tissue growth factor, haptoglobin, and tissue inhibitor of metalloproteinase 1 (TIMP1). These markers largely represented inflammatory markers and acute-phase reactants that were upregulated in ovarian cancer sera. All 26 informative autoimmune and infectious disease markers were downregulated in ovarian cancer samples, suggesting a possible overall immune compromise in these patients.[54]

The 204-marker panel included 35 that had been proposed as potentially useful markers for ovarian cancer in prior studies. Only 12 of these 35 (apolipoprotein A1 [APOA1], CA125, CA19-9, C-reactive protein [CRP], EGFR, haptoglobin, IL-6, IL-8, ferritin, leptin, tumor necrosis factor-α, and VEGF) were dysregulated in this study.[54] The most discriminatory markers included the well-studied CA125, in addition to markers of inflammation (CRP), cell cycle mediators (EGFR), angiogenic factors (VEGF), and extracellular matrix regulators (TIMP1).[54]

Only five markers had statistically dysregulated levels in early-stage I and II cancers, including CA125, CA19-9, CRP, creatine kinase-MB, and EGFR. This is in contrast to

40 markers that were found to be dysregulated in late stage III and IV cancers. There was no single diagnostic marker that emerged as informative. The results underscore the heterogeneity of ovarian carcinogenesis and the inability of any single marker to capture the diversity of disease.

The 204-analyte panel was further studied in 91 stage I data sets and an equivalent number of controls, resulting in the identification of an 11-analyte panel that appeared to be informative for all stages and common subtypes of ovarian cancer.[35] The panel was composed of CA125, CA19-9, EGFR, CRP, myoglobin, APOA1, apolipoprotein C3 (APOC3), macrophage inflammatory protein 1α (MIP1A; also known as CCL3), IL-6, IL-18, and tenascin C. When applied to a test set of 245 samples, the panel was found to have 91.3% sensitivity and 88.5% specificity.[35] Correlogic has recently completed a blinded, prospective clinical validation study, the results of which are forthcoming.

Other studies using proteomics technologies have defined additional biomarker panels. An approach using the Cipergen ProteinChip™, SELDI-TOF and mass spectrometry identified a panel that includes transthyretin (TTR), β-hemoglobin, APOA1, and transferrin.[55,56] An independent group using the Ciphergen ProteinChip™ identified a three-marker panel containing APOA1, TTR, and inter-α-trypsin inhibitor.[31] This panel reported 74% sensitivity for ovarian cancer detection at a fixed specificity of 97% (table II).

In another well-publicized effort conducted by investigators at Yale University, a panel of four biomarkers was identified through an antibody microarray screening method called cytokine rolling-circle amplification microarray. This panel, including leptin, prolactin, osteopontin, and insulin-like growth factor 2, performed with a sensitivity of 95% and specificity of 95% in differentiating the sera from 100 patients with ovarian cancer and 106 controls.[32] In an attempt to further improve the specificity, two additional markers, macrophage migration inhibitory factor (MIF) and CA125, were added to the panel. A multiplex, bead-based, immunoassay system was used to evaluate the six-marker panel in a training set (113 ovarian cancers, 181 controls) and a test set (43 ovarian cancers, 181 controls). The performance of this panel was reported to have a sensitivity of 95.3% and a specificity of 99.4%.[33] However, this 'final model' provided an overinflated assessment of the test's performance, as observations were combined from the training and test sets.[57] The reported PPV of 99.3% in this study was also falsely elevated. A recalculation to a low-prevalence setting would more accurately represent the PPV at only 6.5%.[58,59] The study was further criticized, as the samples used were not representative of those targeted through screening, with only 13 samples coming from patients with stage I cancers.[58] These criticisms are relevant, as the more favorable results were used as justification to bring an ovarian cancer screening test prematurely to the market.

6. Regulatory Issues

The pace of biomarker discovery and the attempts to rapidly bring non-validated products to the market prematurely have exposed a large regulatory gap. OvaCheck® was an ovarian cancer product that was widely anticipated to come on the market in 2004 when one of the two laboratories licensed to perform the test began distributing marketing materials.[60] The data on this Correlogic Systems, Inc. product was reported in a 2002 Lancet publication,[30] but the results were never replicated or validated, causing the FDA to step in. In February 2004, the FDA sent a letter to the CEO of Correlogic Systems, Inc. indicating that the agency was aware the company was "contemplating or has begun the commercial distribution" of the test. In March 2004, the FDA sent letters to Quest Diagnostics Inc. and Laboratory Corporation of America (LabCorp), the two laboratories licensed to conduct the tests, stating that "because the nature of this test is not clear from the materials we have reviewed, we are uncertain if your ovarian cancer offering will be subject to regulation only by the Clinical Laboratory Improvement Amendments of 1988 (CLIA), or whether it may also require premarket review by FDA under the Federal Food, Drug, and Cosmetic Act."[60] Prior to this notification, it had been assumed that the product could be defined as a laboratory-developed 'home brew' test that would be overseen by the less stringent Centers for Medicare and Medicaid's CLIA rules. The FDA subsequently released a draft guidance that considers *in vitro* diagnostic multivariate index assays as medical devices that fall under its regulatory guidance and that require premarket approval.

Despite this new guidance by the FDA, in June 2009, LabCorp began marketing OvaSure™ based on the results of the six-marker panel published by the Yale University group in 2008.[33] The FDA responded by sending a letter to LabCorp in August 2009, stating that "we believe you are offering a high-risk test that has not received adequate clinical validation and may harm the public health." OvaSure™ was then withdrawn from the market.

7. Biomarker Development and Clinical Use

Currently, there are no approved biomarkers for the early detection of ovarian cancer, nor are there clear pipelines for the transfer of a test to the marketplace. It has been suggested that a

comprehensive biomarker pipeline should contain six essential components: (i) candidate discovery; (ii) qualification; (iii) verification; (iv) research assay optimization; (v) biomarker validation; and (vi) commercialization.[61] Candidate biomarkers identified in the discovery phase undergo 'qualification' to confirm the differential expression in diseased and normal samples and 'verification' to confirm sensitivity and to begin to assess specificity when studied in a broader range of samples that capture the heterogeneity of the population to be tested. A high-throughput assay that can be applied to many samples is developed in the 'research assay optimization' phase and tested in the target population in the 'validation' phase. Finally, the assay is refined to meet the rigorous standards required for clinical tests in the 'commercialization' stage.[61] The test should ultimately be assessed in three different populations: a retrospective collection of stored specimens that includes prediagnostic samples from women with early-stage disease; a prospective screening study; and a cancer control study to ultimately determine if the test reduces the population burden of disease.[62]

To date, CA125 is the only marker that is being tested in the general postmenopausal screening population. Publications testing other biomarkers and panels have been limited to retrospective populations highly enriched for ovarian cancer. The performance of these panels in a more general population with a low prevalence of disease has not yet been determined. The specificity and PPV of these tests in the general population will be of paramount importance in limiting the morbidity arising from false-positive results. Further, the randomized controlled trial remains the gold-standard method for determining the effect of a screening test on cancer-specific mortality. New approaches that will allow for assessment of the costs and benefits of screening in a more efficient and timely fashion are needed.[62]

Three additional points require consideration in the translation of current biomarker discovery into clinical use. The first consideration is the control group. Some studies have developed assays based on differential expression of various serum components between ovarian cancer patients and those with benign ovarian pathology, while other studies have used normal healthy subjects as the controls. Studies that have used sera from both types of controls have found different performance characteristics of the test, depending on whether the control population had benign pathology or normal ovaries.[63] This has a bearing on the appropriate clinical application of the assay. An assay that was developed using benign ovarian pathology as the control population would be better suited to assess the risk of malignancy in the setting of a confirmed pelvic mass. In contrast, an assay that was developed with a normal control population would be more appropriate to offer as a screening study to the general population.

The second issue to consider is case selection in these studies. These serum biomarker panels were developed using clinically diagnosed ovarian cancers as the cases, many of which were late stage. These samples are not representative of those that would be the targets of screening. To find a test that is truly appropriate for early detection, biomarker discovery would be more appropriately performed using the serum samples collected from patients *prior to* the clinical discovery of disease. This is where banked samples from the participants of prospective studies, such as the PLCO trial or the UKCTOCS, will become invaluable.

Finally, current biomarker panels are largely composed of markers that reflect a patient's systemic reaction to cancer rather than those that capture the unique proteins secreted by the tumor.[49] Tumor-specific markers circulate at concentrations that are orders of magnitude lower than the proteins that can be measured by current mass spectrometry technology.[7,49,64] With our current technology, proteins secreted from millimeter-sized tumors could be detected only if secreted at high rates and with zero background, which is an unrealistic condition.[65] The signal from proteins secreted by subcentimeter-sized tumors are drowned out by the much more abundant proteins secreted in response to inflammation, infection, and malnutrition.[49] Cancer-specific antigens, such as CA125 or prostate-specific antigen (PSA), are detected only when tumors typically reach a size in the many-centimeter range.[65]

8. Conclusion

Ovarian cancer is responsible for the highest fatality rate among the gynecologic malignancies, and there is great interest in defining a screening test that would allow for early detection. As ovarian cancers are complex and heterogeneous, no single biomarker will be able to detect all histologic subtypes or stages. Biomarker panels have reported excellent performance characteristics (sensitivity, specificity, PPV) but have not yet undergone appropriate validation. As a positive result leads to invasive diagnostic testing and potential for harm, the specificity of an ovarian cancer screening test needs to be close to 100% to limit the number of false-positive results. Appropriate validation of a test is critical, as a test could result in more harm than good when applied to a healthy population. Current biomarker panels measure acute-phase reactants and markers of inflammation rather than protein products secreted by tumors. The identification of unique cancer proteins or products will require advances in current technology. The identification

of biomarkers that herald the presence of subcentimeter lesions will require a change in case selection at the biomarker discovery phase. More work is required before we will realize the goals of early detection of ovarian cancer: to discover lesions when they are localized and curable; to prevent mortality; and to reduce morbidity and cost.[62]

Acknowledgments

This work was supported by career development awards to Christine Walsh from the Department of Defense Ovarian Cancer Research Program (award contract no. W81XWH-1-0209; log no. OC080179) and the American Society of Clinical Oncology (ASCO) Cancer Foundation Career Development Award. Any opinions, findings, and conclusions expressed in this material are those of the authors and do not necessarily reflect those of the ASCO or the ASCO Cancer Foundation. This work was also supported by the American Cancer Society California Division Early Detection Professorship to Beth Karlan (grant no. SIOP-06-258-01-CCE).

The funding organizations had no role in the design and conduct of the study; collection, management, analysis, and interpretation of the data; and preparation, review, or approval of the manuscript.

The authors have no conflicts of interest directly relevant to the content of this review.

References

1. Heintz AP, Odicino F, Maisonneuve P, et al. Carcinoma of the ovary: FIGO 6th annual report on the results of treatment in gynecological cancer. Int J Gynaecol Obstet 2006; 95 Suppl. 1: S161-92
2. Hogg R, Friedlander M. Biology of epithelial ovarian cancer: implications for screening women at high genetic risk. J Clin Oncol 2004; 22 (7): 1315-27
3. Wilson JMG, Junger G. Principles and practice of screening for disease: public health papers. Geneva: WHO, 1968
4. van Nagell Jr JR, DePriest PD, Reedy MB, et al. The efficacy of transvaginal sonographic screening in asymptomatic women at risk for ovarian cancer. Gynecol Oncol 2000; 77 (3): 350-6
5. Fishman DA, Cohen L, Blank SV, et al. The role of ultrasound evaluation in the detection of early-stage epithelial ovarian cancer. Am J Obstet Gynecol 2005; 192 (4): 1214-21; discussion 1221-2
6. Liede A, Karlan BY, Baldwin RL, et al. Cancer incidence in a population of Jewish women at risk of ovarian cancer. J Clin Oncol 2002; 20 (6): 1570-7
7. Brown PO, Palmer C. The preclinical natural history of serous ovarian cancer: defining the target for early detection. PLoS Med 2009; 6 (7): e1000114 [online]. Available from URL: http://www.plosmedicine.org/article/info%3Adoi%2F10.1371%2Fjournal.pmed.1000114 [Accessed 2009 Nov 30]
8. Skates SJ, Xu FJ, Yu YH, et al. Toward an optimal algorithm for ovarian cancer screening with longitudinal tumor markers. Cancer 1995; 76 (10 Suppl.): 2004-10
9. Brawley OW, Kramer BS. Cancer screening in theory and in practice. J Clin Oncol 2005; 23 (2): 293-300
10. Jacobs IJ, Menon U. Progress and challenges in screening for early detection of ovarian cancer. Mol Cell Proteomics 2004; 3 (4): 355-66
11. Bast Jr RC, Feeney M, Lazarus H, et al. Reactivity of a monoclonal antibody with human ovarian carcinoma. J Clin Invest 1981; 68 (5): 1331-7
12. Bast Jr RC, Klug TL, St John E, et al. A radioimmunoassay using a monoclonal antibody to monitor the course of epithelial ovarian cancer. N Engl J Med 1983; 309 (15): 883-7
13. Goonewardene TI, Hall MR, Rustin GJ. Management of asymptomatic patients on follow-up for ovarian cancer with rising CA-125 concentrations. Lancet Oncol 2007; 8 (9): 813-21
14. Woolas RP, Xu FJ, Jacobs IJ, et al. Elevation of multiple serum markers in patients with stage I ovarian cancer. J Natl Cancer Inst 1993; 85 (21): 1748-51
15. Moss EL, Hollingworth J, Reynolds TM. The role of CA125 in clinical practice. J Clin Pathol 2005; 58 (3): 308-12
16. Buys SS, Partridge E, Greene MH, et al. Ovarian cancer screening in the Prostate, Lung, Colorectal and Ovarian (PLCO) Cancer Screening Trial: findings from the initial screen of a randomized trial. Am J Obstet Gynecol 2005; 193 (5): 1630-9
17. Partridge E, Kreimer AR, Greenlee RT, et al. Results from four rounds of ovarian cancer screening in a randomized trial. Obstet Gynecol 2009; 113 (4): 775-82
18. Menon U, Gentry-Maharaj A, Hallett R, et al. Sensitivity and specificity of multimodal and ultrasound screening for ovarian cancer, and stage distribution of detected cancers: results of the prevalence screen of the UK Collaborative Trial of Ovarian Cancer Screening (UKCTOCS). Lancet Oncol 2009; 10 (4): 327-40
19. Prorok PC, Andriole GL, Bresalier RS, et al. Design of the Prostate, Lung, Colorectal and Ovarian (PLCO) Cancer Screening Trial. Control Clin Trials 2000; 21 (6 Suppl.): 273-309S
20. Skates SJ, Menon U, MacDonald N, et al. Calculation of the risk of ovarian cancer from serial CA-125 values for preclinical detection in postmenopausal women. J Clin Oncol 2003; 21 (10 Suppl.): 206-10
21. Menon U, Skates SJ, Lewis S, et al. Prospective study using the risk of ovarian cancer algorithm to screen for ovarian cancer. J Clin Oncol 2005; 23 (31): 7919-26
22. Sato S, Yokoyama Y, Sakamoto T, et al. Usefulness of mass screening for ovarian carcinoma using transvaginal ultrasonography. Cancer 2000; 89 (3): 582-8
23. DePriest PD, Gallion HH, Pavlik EJ, et al. Transvaginal sonography as a screening method for the detection of early ovarian cancer. Gynecol Oncol 1997; 65 (3): 408-14
24. Bast Jr RC. Status of tumor markers in ovarian cancer screening. J Clin Oncol 2003; 21 (10 Suppl.): 200-5
25. Rapkiewicz AV, Espina V, Petricoin III EF, et al. Biomarkers of ovarian tumours. Eur J Cancer 2004; 40 (17): 2604-12
26. Skates SJ, Horick N, Yu Y, et al. Preoperative sensitivity and specificity for early-stage ovarian cancer when combining cancer antigen CA-125II, CA 15-3, CA 72-4, and macrophage colony-stimulating factor using mixtures of multivariate normal distributions. J Clin Oncol 2004; 22 (20): 4059-66
27. McIntosh MW, Drescher C, Karlan B, et al. Combining CA 125 and SMR serum markers for diagnosis and early detection of ovarian carcinoma. Gynecol Oncol 2004; 95 (1): 9-15
28. Gorelik E, Landsittel DP, Marrangoni AM, et al. Multiplexed immunobead-based cytokine profiling for early detection of ovarian cancer. Cancer Epidemiol Biomarkers Prev 2005; 14 (4): 981-7
29. Shah CA, Lowe KA, Paley P, et al. Influence of ovarian cancer risk status on the diagnostic performance of the serum biomarkers mesothelin, HE4, and CA125. Cancer Epidemiol Biomarkers Prev 2009; 18 (5): 1365-72
30. Petricoin EF, Ardekani AM, Hitt BA, et al. Use of proteomic patterns in serum to identify ovarian cancer. Lancet 2002; 359 (9306): 572-7
31. Zhang Z, Bast Jr RC, Yu Y, et al. Three biomarkers identified from serum proteomic analysis for the detection of early stage ovarian cancer. Cancer Res 2004; 64 (16): 5882-90
32. Mor G, Visintin I, Lai Y, et al. Serum protein markers for early detection of ovarian cancer. Proc Natl Acad Sci U S A 2005; 102 (21): 7677-82
33. Visintin I, Feng Z, Longton G, et al. Diagnostic markers for early detection of ovarian cancer. Clin Cancer Res 2008; 14 (4): 1065-72
34. Havrilesky LJ, Whitehead CM, Rubatt JM, et al. Evaluation of biomarker panels for early stage ovarian cancer detection and monitoring for disease recurrence. Gynecol Oncol 2008; 110 (3): 374-82

35. Amonkar SD, Bertenshaw GP, Chen T-H, et al. Development and preliminary evaluation of a multivariate index assay for ovarian cancer. PLoS One 2009; 4 (2): e4599 [online]. Available from URL: http://www.plosone.org/article/info%3Adoi%2F10.1371%2Fjournal.pone.0004599 [Accessed 2009 Nov 30]

36. Bouchard D, Morisset D, Bourbonnais Y, et al. Proteins with whey-acidic-protein motifs and cancer. Lancet Oncol 2006; 7 (2): 167-74

37. Ono K, Tanaka T, Tsunoda T, et al. Identification by cDNA microarray of genes involved in ovarian carcinogenesis. Cancer Res 2000; 60 (18): 5007-11

38. Welsh JB, Zarrinkar PP, Sapinoso LM, et al. Analysis of gene expression profiles in normal and neoplastic ovarian tissue samples identifies candidate molecular markers of epithelial ovarian cancer. Proc Natl Acad Sci U S A 2001; 98 (3): 1176-81

39. Moore RG, Brown AK, Miller MC, et al. The use of multiple novel tumor biomarkers for the detection of ovarian carcinoma in patients with a pelvic mass. Gynecol Oncol 2008; 108 (2): 402-8

40. Hellstrom I, Raycraft J, Hayden-Ledbetter M, et al. The HE4 (WFDC2) protein is a biomarker for ovarian carcinoma. Cancer Res 2003; 63 (13): 3695-700

41. Moore RG, McMeekin DS, Brown AK, et al. A novel multiple marker bioassay utilizing HE4 and CA125 for the prediction of ovarian cancer in patients with a pelvic mass. Gynecol Oncol 2009; 112 (1): 40-6

42. Santillan A, Garg R, Zahurak ML, et al. Risk of epithelial ovarian cancer recurrence in patients with rising serum CA-125 levels within the normal range. J Clin Oncol 2005; 23 (36): 9338-43

43. Allard J, Somers E, Theil R, et al. Use of a novel biomarker HE4 for monitoring patients with epithelial ovarian cancer [abstract no. 5535]. J Clin Oncol 2008; 26 (15S): 5535 [online]. Available from URL: http://meeting.ascopubs.org/cgi/content/abstract/26/15_suppl/5535 [Accessed 2009 Nov 30]

44. Rustin GJ, van der Burg ME, on behalf of MRC and EORTC Collaborators. A randomized trial in ovarian cancer (OC) of early treatment of relapse based on CA125 level alone versus delayed treatment based on conventional clinical indicators (MRC OV05/EORTC 55955 trials) [abstract no. 1]. J Clin Oncol 2009; 27 (18S): 1 [online]. Available from URL: http://meeting.ascopubs.org/cgi/content/abstract/27/18S/1 [Accessed 2009 Nov 30]

45. Meri S, Baumann M. Proteomics: posttranslational modifications, immune responses and current analytical tools. Biomol Eng 2001; 18 (5): 213-20

46. Sellers TA, Yates JR. Review of proteomics with applications to genetic epidemiology. Genet Epidemiol 2003; 24 (2): 83-98

47. Sorace JM, Zhan M. A data review and re-assessment of ovarian cancer serum proteomic profiling. BMC Bioinformatics 2003; 4: 24 [online]. Available from URL: http://www.biomedcentral.com/1471-2105/4/24 [Accessed 2009 Nov 30]

48. Baggerly KA, Morris JS, Coombes KR. Reproducibility of SELDI-TOF protein patterns in serum: comparing datasets from different experiments. Bioinformatics 2004; 20 (5): 777-85

49. Diamandis EP. Analysis of serum proteomic patterns for early cancer diagnosis: drawing attention to potential problems. J Natl Cancer Inst 2004; 96 (5): 353-6

50. Rockhill B. Proteomic patterns in serum and identification of ovarian cancer [letter]. Lancet 2002; 360 (9327): 169; author reply 170-1

51. Pearl DC. Proteomic patterns in serum and identification of ovarian cancer [letter]. Lancet 2002; 360 (9327): 169-70; author reply 170-1

52. Diamandis EP. Proteomic patterns in serum and identification of ovarian cancer [letter]. Lancet 2002; 360 (9327): 170; author reply 170-1

53. Conrads TP, Fusaro VA, Ross S, et al. High-resolution serum proteomic features for ovarian cancer detection. Endocr Relat Cancer 2004; 11 (2): 163-78

54. Bertenshaw GP, Yip P, Seshaiah P, et al. Multianalyte profiling of serum antigens and autoimmune and infectious disease molecules to identify biomarkers dysregulated in epithelial ovarian cancer. Cancer Epidemiol Biomarkers Prev 2008; 17 (10): 2872-81

55. Kozak KR, Amneus MW, Pusey SM, et al. Identification of biomarkers for ovarian cancer using strong anion-exchange ProteinChips: potential use in diagnosis and prognosis. Proc Natl Acad Sci U S A 2003; 100 (21): 12343-8

56. Kozak KR, Su F, Whitelegge JP, et al. Characterization of serum biomarkers for detection of early stage ovarian cancer. Proteomics 2005; 5 (17): 4589-96

57. McIntosh M, Anderson G, Drescher C, et al. Ovarian cancer early detection claims are biased [letter]. Clin Cancer Res 2008; 14 (22): 7574; author reply 7577-9

58. Coates RJ, Kolor K, Stewart SL, et al. Diagnostic markers for ovarian cancer screening: not ready for routine clinical use [letter]. Clin Cancer Res 2008; 14 (22): 7575-6; author reply 7577-9

59. Greene MH, Feng Z, Gail MH. The importance of test positive predictive value in ovarian cancer screening [letter]. Clin Cancer Res 2008; 14 (22): 7574; author reply 7577-9

60. Wagner L. A test before its time? FDA stalls distribution process of proteomic test. J Natl Cancer Inst 2004; 96 (7): 500-1

61. Rifai N, Gillette MA, Carr SA. Protein biomarker discovery and validation: the long and uncertain path to clinical utility. Nat Biotechnol 2006; 24 (8): 971-83

62. Etzioni R, Urban N, Ramsey S, et al. The case for early detection. Nat Rev Cancer 2003; 3 (4): 243-52

63. Nosov V, Su F, Amneus M, et al. Validation of serum biomarkers for detection of early-stage ovarian cancer. Am J Obstet Gynecol 2009; 200 (6): 639.e1-5

64. Diamandis EP. Point: proteomic patterns in biological fluids. Do they represent the future of cancer diagnostics? Clin Chem 2003; 49 (8): 1272-5

65. Lutz AM, Willmann JK, Cochran FV, et al. Cancer screening: a mathematical model relating secreted blood biomarker levels to tumor sizes. PLoS Med 2008; 5 (8): e170 [online]. Available from URL: http://www.plosmedicine.org/article/info%3Adoi%2F10.1371%2Fjournal.pmed.0050170 [Accessed 2009 Nov 30]

Correspondence: Dr *Christine S. Walsh*, Department of Obstetrics and Gynecology, Cedars-Sinai Medical Center, 8700 Beverly Blvd., Suite 160W, Los Angeles, CA 90048, USA.
E-mail: walshc@cshs.org

British Journal of Cancer (2012) 106, 333 – 343

www.bjcancer.com

Indole-3-carbinol synergistically sensitises ovarian cancer cells to bortezomib treatment

B Taylor-Harding[1], H Agadjanian[1], H Nassanian[1], S Kwon[2], X Guo[2], C Miller[1], BY Karlan[1,3], S Orsulic[1] and CS Walsh[*,1,3]

[1]Women's Cancer Program and Division of Gynecologic Oncology, Burns and Allen Research Institute, Cedars-Sinai Medical Center, 8700 Beverly Boulevard, Los Angeles, CA 90048, USA; [2]Medical Genetics Institute, Cedars-Sinai Medical Center, 8700 Beverly Boulevard, Los Angeles, CA 90048, USA; [3]Department of Obstetrics and Gynecology, David Geffen School of Medicine, University of California at Los Angeles, Los Angeles, CA 90095, USA

BACKGROUND: Bortezomib is a proteasome inhibitor with minimal clinical activity as a monotherapy in solid tumours, but its combination with other targeted therapies is being actively investigated as a way to increase its anticarcinogenic properties. Here, we evaluate the therapeutic potential of co-treatment with bortezomib and indole-3-carbinol (I3C), a natural compound found in cruciferous vegetables, in human ovarian cancer.

METHODS: We examined the effects of I3C, bortezomib and cisplatin in several human ovarian cancer cell lines. Synergy was determined using proliferation assays and isobologram analysis. Cell cycle and apoptotic effects were assessed by flow cytometry. The mechanism of I3C and bortezomib action was determined by RNA microarray studies, quantitative RT–PCR and western blotting. Antitumour activity of I3C and bortezomib was evaluated using an OVCAR5 xenograft mouse model.

RESULTS: I3C sensitised ovarian cancer cell lines to bortezomib treatment through potent synergistic mechanisms. Combination treatment with bortezomib and I3C led to profound cell cycle arrest and apoptosis as well as disruptions to multiple pathways, including those regulating endoplasmic reticulum stress, cytoskeleton, chemoresistance and carcinogen metabolism. Moreover, I3C and bortezomib co-treatment sensitised ovarian cancer cells to the standard chemotherapeutic agents, cisplatin and carboplatin. Importantly, *in vivo* studies demonstrated that co-treatment with I3C and bortezomib significantly inhibited tumour growth and reduced tumour weight compared with either drug alone.

CONCLUSION: Together, these data provide a novel rationale for the clinical application of I3C and bortezomib in the treatment of ovarian cancer.

British Journal of Cancer (2012) **106,** 333–343. doi:10.1038/bjc.2011.546 www.bjcancer.com
Published online 13 December 2011

Keywords: ovarian cancer; indole-3-carbinol (I3C); bortezomib; chemosensitivity; synergy; xenograft tumours

Ovarian cancer is the most lethal of gynaecologic malignancies, largely due to the late stage at diagnosis and development of chemoresistance after initial platinum- and paclitaxel-based combination chemotherapy. Treatment of patients with intrinsic or acquired chemoresistance represents a major clinical challenge (Bast *et al*, 2009). Furthermore, the molecular mechanisms underlying the aggressive biology of these tumours are poorly understood. This suggests that more effective therapeutic agents are needed to improve the treatment outcome of patients associated with biologically aggressive ovarian tumours, poor survival and chemoresistance (Etemadmoghadam *et al*, 2009; Nakayama *et al*, 2010). Strategies that overcome drug resistance and exploit pathways involved in tumourigenesis are attractive treatment options.

Bortezomib, the first-in-class proteasome inhibitor, has anticancer properties through wide-ranging mechanisms such as disruption of the cell cycle, promotion of apoptosis, and inhibition of proliferation and angiogenesis (Boccadoro *et al*, 2005). In both ovarian and colorectal tumour cell lines, bortezomib has been shown to inhibit cellular growth through upregulation of $p27^{kip1}$ and induction of apoptosis (Uddin *et al*, 2008, 2009; Bruning *et al*, 2009), suggesting a possible therapeutic role for bortezomib in ovarian cancer. Several phase I clinical trials have evaluated the dose-limiting toxicities and maximum tolerated dose of bortezomib when combined with chemotherapeutic agents in ovarian cancer (Aghajanian *et al*, 2005; Cresta *et al*, 2008; Ramirez *et al*, 2008). However, a recent phase II study demonstrated minimal clinical activity of bortezomib as a single-agent treatment in recurrent platinum-sensitive ovarian or primary peritoneal cancer (Aghajanian *et al*, 2009). Currently, bortezomib is FDA approved and licensed for the treatment of multiple myeloma and mantle cell lymphoma, but it has generally not been an effective monotherapy in solid tumours. Combination of bortezomib with novel targeted agents has emerged as a treatment strategy that could broaden its clinical efficacy (Wright, 2010). We hypothesised that the combination of bortezomib with another agent could result in an effective treatment strategy for epithelial ovarian cancer.

Indole-3-carbinol (I3C) is a natural compound present in cruciferous vegetables, such as broccoli and cabbage. *In vitro* and *in vivo* studies demonstrate that I3C exhibits chemopreventive

*Correspondence: Dr CS Walsh; E-mail: walshc@cshs.org
Received 10 October 2011; accepted 18 November 2011; published online 13 December 2011

and anticancer properties in a variety of cancers, especially those that are hormonally responsive (Chinni *et al*, 2001; Rahman *et al*, 2006; Weng *et al*, 2008). Like bortezomib, I3C demonstrates anticarcinogenic properties through multiple mechanisms, including the induction of apoptosis, G1 cell cycle arrest, activation of the endoplasmic reticulum (ER) stress response and reversal of multidrug resistance (Weng *et al*, 2008). Previous studies have demonstrated a potential benefit of I3C in the treatment of high-risk breast cancer, vulvar intraepithelial neoplasia and recurrent respiratory papillomatosis, while clinical trials of I3C are ongoing in cervical and prostate cancer (Rosen and Bryson, 2004; Reed *et al*, 2005; Naik *et al*, 2006). With the exception of a single study of I3C in human ovarian cancer cells (Raj *et al*, 2008), no further reports have investigated the biological effects nor clinical benefits of I3C in ovarian cancer.

Both I3C and bortezomib have been shown to target a broad spectrum of signalling pathways, which are likely to contribute to their ability to sensitise cells to apoptosis. Considering their potent anticarcinogenic properties and pleiotropic effects, we investigated the sensitivity of ovarian cancer cells and tumour xenografts to I3C and bortezomib combination treatment. In this report, we provide the first evidence that I3C and bortezomib work synergistically against ovarian cancer by promoting apoptosis, upregulating enzymes required for carcinogen metabolism, inducing ER stress, deregulating metabolic pathways, inhibiting carcinogenesis and reducing chemoresistance. These data provide support for the further investigation of I3C and bortezomib combination treatment in epithelial ovarian carcinoma.

MATERIALS AND METHODS

Cell culture and reagents

Human ovarian carcinoma cell lines OVCAR3, OVCAR5, OVCAR8, A2780, SKOV3, 3A, HEY and CAOV3 cells were purchased from American Type Culture Collection (Manassas, VA, USA). Cells were cultured in DMEM (MediaTech, Manassas, VA, USA) supplemented with 10% FBS, 100 U ml^{-1} penicillin and 100 μg ml^{-1} streptomycin. Cell lines were cultured at 37°C and with 5% CO_2 in a humidified atmosphere. Bortezomib (Velcade) was purchased from LC Laboratories (Woburn, MA, USA). Indole-3-carbinol, cisplatin and carboplatin were purchased from Sigma-Aldrich (St Louis, MO, USA). The following antibodies were used: RB, phospho-RB$^{S807/S811}$, GADD45A, MET, SNAI1, CTBNN1, TOP2A and NFkB (Cell Signaling Technology, Danvers, MA, USA); CDK1, CYP1B1, p21^{cip1} and p27^{kip1} (Santa Cruz Biotechnology, Santa Cruz, CA, USA); ATF3 (Abcam, Cambridge, MA, USA); Actin (Sigma-Aldrich) and GAPDH (Fitzgerald, Acton, MA, USA). The following reagents and secondary antibodies were used in western blot analysis: Odyssey blocking buffer and Infrared IRDye-labelled secondary antibodies (LI-COR Biosciences, Lincoln, NE, USA).

Proliferation assays

Cells (4×10^3 per 100 μl per well) were plated in 96-well plates. After an overnight incubation, cells were treated with I3C, bortezomib, cisplatin or carboplatin at the indicated concentrations. After 48-h post-drug treatment, MTS/PMS solution (MTT Assay, Promega, Madison, WI, USA) was added according to the manufacturer's instructions and the absorbance recorded at 490 nm on an Ultramark-EX Microplate spectrophotometer (BioRad, Hercules, CA, USA) (Figure 1). For cisplatin and carboplatin experiments (Figure 2), we used a luminescent-based assay (CellTiter-Glo Luminescent Cell Viability Assay, Promega) for increased sensitivity. After 48-h post-drug treatment, CellTiter-Glo reagent was added to each well according to the manufacturer's protocol. Luminescence was measured on a Veritas microplate luminometer (Turner BioSystems, Sunnyvale, CA, USA) after 15 min. IC50 values were determined and used for the evaluation of drug interactions. Multiple independent experiments were performed in triplicate, and data were expressed as a relative percentage compared with the untreated control group set at 100%.

Flow cytometry

Cells (5×10^5) were plated into 100-mm tissue culture plates. After an overnight incubation, I3C and bortezomib were added at the indicated concentrations and samples were harvested 24 h post treatment. For cell cycle analysis, samples were fixed in 70% ethanol and subsequently treated with propidium iodide (PI) (Sigma-Aldrich) and RNase A (Sigma-Aldrich). Samples were analysed for PI incorporation with a Becton Dickinson FACScan (Franklin Lakes, NJ, USA) using ModFit LT software (Verity Software House, Topsham, ME, USA). For the apoptosis assay, cells were co-stained with annexin V and PI according to the manufacturer's protocol (Annexin V-FITC Apoptosis Detection Kit, BD Biosciences, San Jose, CA, USA), followed by flow cytometric analysis using CellQuest version 3.1 software (BD Biosciences) to gate viable, early and late apoptotic cells. The results generated were from multiple independent experiments performed in triplicate. A total of 10 000 events were collected for final analysis.

Isobologram analysis

Synergy between I3C and bortezomib was studied as previously described (Taylor-Harding *et al*, 2010). To calculate the combined effects of the drugs, the combination index (CI) isobologram method was used (Chou and Talalay, 1984). Assessment of synergy was performed using CalcuSyn software (Biosoft, Cambridge, UK). Combination index values <1, $=1$ and >1 indicate synergy, additivity and antagonism, respectively.

Western blot analysis

Western blot was performed as previously described (Taylor-Harding *et al*, 2010) with the following modifications. The membrane was blocked for 1 h with Odyssey blocking buffer (LI-COR Biosciences) and immunoblotted with primary antibody overnight at 4°C in blocking buffer supplemented with 0.1% Tween-20. After washing in TBST (0.1% Tween-20 in TBS), the membrane was probed with Infrared IRDye-labelled secondary antibody (LI-COR Biosciences) (1:10 000 dilution) in blocking buffer with 0.1% Tween-20 for 1 h. After washing, the membrane was visualised using the Odyssey Infrared Imager (LI-COR Biosciences).

Quantitative RT–PCR (qRT–PCR)

Total RNA was isolated with TriReagent (Molecular Research Center, Cincinnati, OH, USA) and purified with the RNeasy kit (Qiagen, Germantown, MD, USA). Complementary DNA was generated by reverse transcription with Superscript III (Invitrogen, Carlsbad, CA, USA) and oligo dT priming. Quantitative RT–PCR was performed on the BioRad iCycler using QuantiTect SYBR Green (BioRad) according to the manufacturer's protocol. The results generated were from two independent experiments performed in triplicate. Quantitation was calculated by the comparative method ($2^{-\Delta\Delta Ct}$) and data expressed relative to cells treated with vehicle (mock) set to 1. Primer sequences used in qRT–PCR are listed in Supplementary Table S1.

Microarray gene expression profiling

OVCAR5 cells were treated with vehicle, 37.5 nM bortezomib, 675 μM I3C, or with I3C and bortezomib in combination for 24 h.

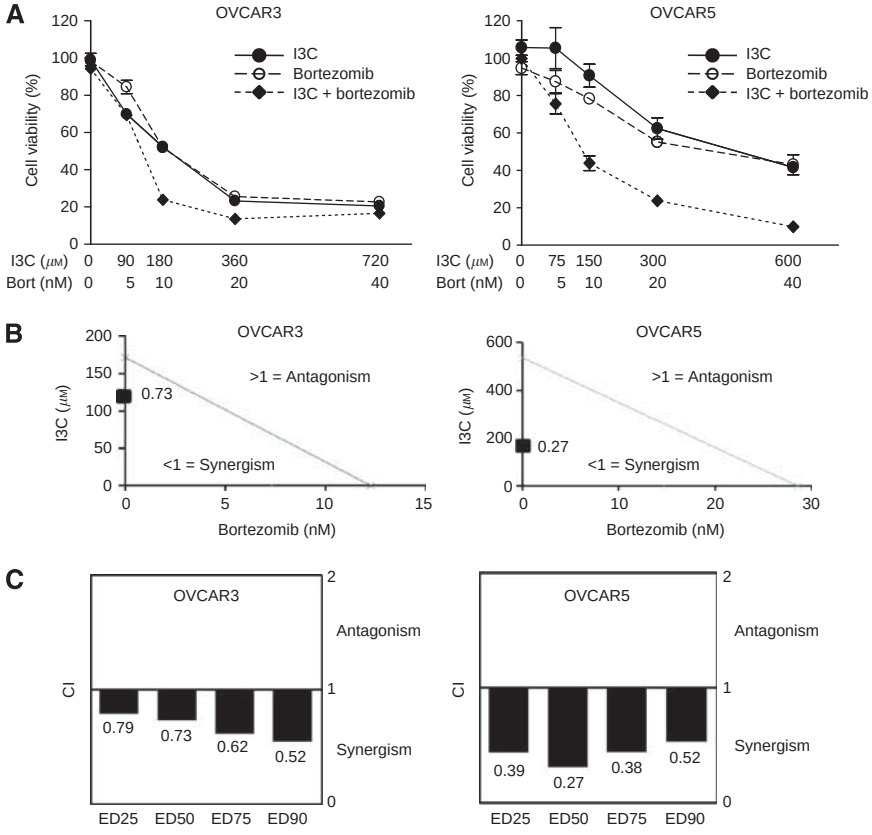

Figure 1 Indole-3-carbinol and bortezomib exhibit synergistic cytotoxicity in OVCAR3 and OVCAR5 cells. (**A**) Dose-dependent cytotoxicity of I3C, bortezomib and their combination. OVCAR3 and OVCAR5 cells were treated with I3C and bortezomib at the indicated concentrations for 48 h. Cell viability was measured as described in Materials and Methods. The data shown represent the mean ± s.e.m. ($n = 3$). (**B**) Isobologram analysis of combination I3C with bortezomib used in equipotent concentrations in OVCAR3 and OVCAR5 cells. The line designates the CI where CI = 1 (additive effect). Combination index < 1 indicates synergism and CI > 1 represents antagonism. The combination data points (CI = 0.73 for OVCAR3 and CI = 0.27 for OVCAR5) calculated by CalcuSyn software indicate synergism at ED50. (**C**) The CI values of combination I3C and bortezomib at a range of EDs. TheCI values at ED25, ED50, ED75 and ED90 indicate a synergistic interaction between I3C and bortezomib in OVCAR3 and OVCAR5 cells.

Three independent experiments were performed for a total of four triplicate conditions (12 samples). Total RNA was isolated as described for qRT–PCR analysis and the quality of RNA confirmed using an Agilent 2100 bioanalyzer (Santa Clara, CA, USA). Probe labelling, microarray hybridisation, washing and scanning were carried out as per manufacturer's instructions (Illumina, San Diego, CA, USA). Twelve samples were used to probe the Illumina HumanHT-12 v4 Expression BeadChip containing 47 231 human gene transcripts.

Microarray data normalisation and analysis

Quality control of the microarray expression data was performed using the lumi R package (Du *et al*, 2008). We applied the lumiT function with a default setting to check the assumption of a constant variance. Variance-stabilising transformation was performed when needed. To remove systematic variation of non-biological origin, the data were normalised via the lumiN function, which performs quantile normalisation. Quality control of the normalised data was performed using the lumiQ function in the lumi R package. To identify differentially expressed genes, the cleaned data were analysed using the eBayes function in limma R package (Smyth, 2005). An empirical Bayes method to shrink the probe-wise sample variances towards a common value was utilised. Genes that had FDR adjusted P-values <0.01 were selected as differentially expressed. Among these, the top 1000 significantly altered genes ($P<0.0025$) were analysed. The selected genes were then compared with the Gene Ontology (GO) database using the Fisher's exact test, assuming a hypergeometric distribution, to evaluate gene set enrichment. The GOstats R package (Falcon and Gentleman, 2007) was utilised for the gene set enrichment analysis.

In vivo tumour xenograft studies

Six-week-old female nude mice were obtained from Charles River Laboratories (Wilmington, MA, USA) and maintained according to IACUC guidelines. Mice were inoculated subcutaneously in both flanks with an equal volume of 8×10^6 OVCAR5 cells and matrigel (Becton Dickinson) in a total volume of 200 μl. Mice were randomly divided into four treatment groups with four mice per group (eight tumours). Treatments were as follows: vehicle (control); I3C alone (20 mg kg^{-1}); bortezomib alone (1 mg kg^{-1}) and the drug combination (20 mg kg^{-1} I3C with 1 mg kg^{-1} bortezomib). Treatment was given intraperitoneally twice weekly starting 4 days post inoculation. Tumour size was measured twice weekly with a caliper, and tumour volume was calculated as follows: $L \times W^2$, where L = length and W = width. Data were expressed relative to the initial tumour volume 4 days post inoculation. The initial tumour volume was set to 1 for each treatment group.

Statistical analysis

Data were analysed using a two-tailed Student's t-test. A P-value of <0.05 was considered statistically significant.

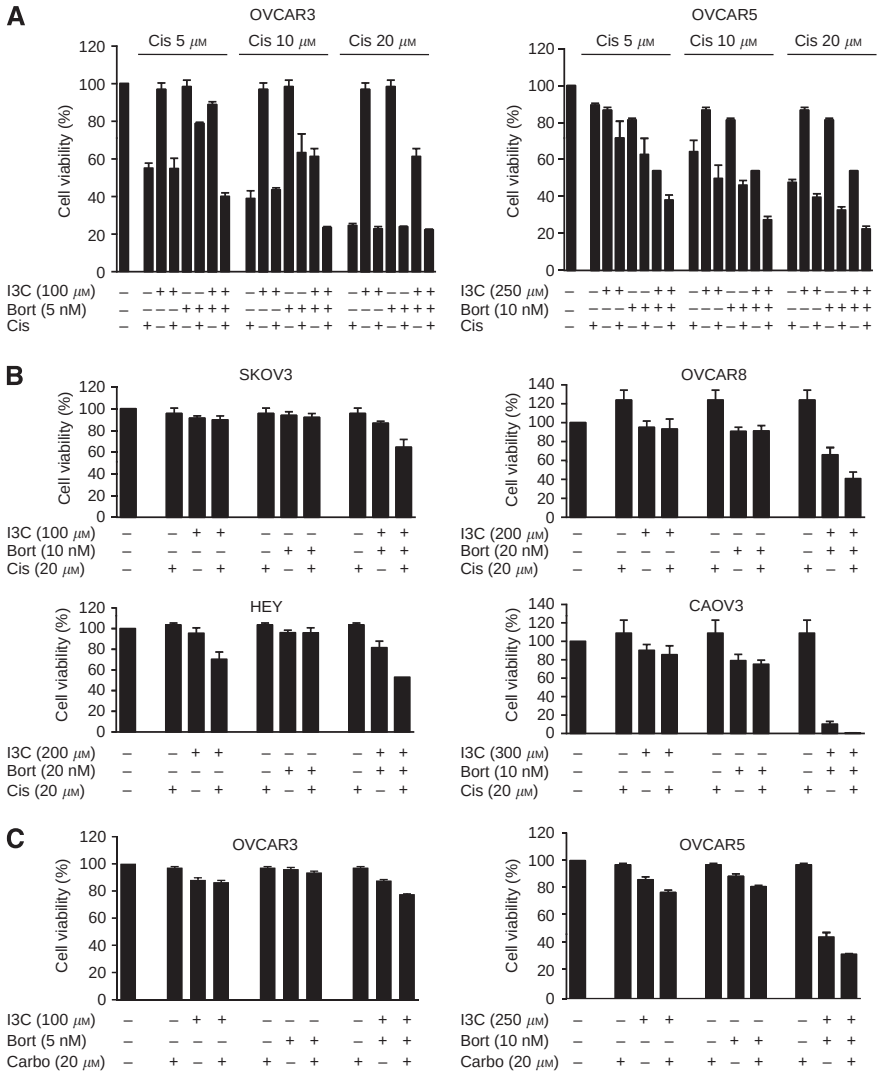

Figure 2 Indole-3-carbinol and bortezomib combination sensitises ovarian cancer cells to platinum-based chemotherapeutic agents. (**A**) OVCAR3 and OVCAR5 cells were treated with I3C, bortezomib, cisplatin or (**C**) carboplatin at the indicated concentrations for 48 h. Cell viability was measured as described in Materials and Methods. The data shown represent the mean ± s.e.m. ($n = 3$). (**B**) SKOV3, OVCAR8, HEY and CAOV3 cells were treated with I3C, bortezomib and cisplatin as in (**A**). The data shown represent the mean ± s.e.m. ($n = 3$).

RESULTS

Synergistic cytotoxicity between I3C and bortezomib

To determine whether I3C and bortezomib exhibit a combined effect in ovarian cancer cells, we examined the effect of individual and combination treatment with I3C and bortezomib after 48-h exposure using the MTT assay. To ensure that the contributing effects from each drug was equivalent, the IC50 for each drug was determined and serial dilutions were generated based on the IC50 of each drug providing a 1:1 equipotent I3C/bortezomib ratio. We found that the drug combination caused greater inhibition of cellular proliferation than either drug alone in OVCAR3 and OVCAR5 cells (Figure 1A), an effect that was reproducible in a panel of ovarian cancer cell lines (Figure 2B and data not shown). To determine whether I3C and bortezomib interact synergistically, isobologram analysis was performed. This analysis provides a CI value that measures the degree of interaction between two or more drugs, where a CI <1 and a CI >1 indicates synergism and antagonism, respectively (Chou and Talalay, 1984). A CI of 0.73 and 0.27 was identified for OVCAR3 and OVCAR5 cells, respectively, when the effective dose (ED) of both agents inhibited cell viability by 50% (Figure 1B). Irrespective of high cytotoxicity (90% inhibition, ED90) or low cytotoxicity (25% inhibition, ED25), the CI values remained below 1, indicating that synergism occurs independently of the equipotency levels of I3C and bortezomib (Figure 1C). Our data demonstrate that I3C and bortezomib exhibit a robust synergistic interaction in ovarian cancer cells, particularly in OVCAR5 cells.

I3C and bortezomib combination sensitises ovarian cancer cells to standard platinum-based chemotherapeutic agents

To determine whether I3C and bortezomib could sensitise cells to cisplatin, we treated OVCAR3 and OVCAR5 cells with subtoxic doses of equipotent I3C and bortezomib with increasing concentrations of cisplatin. We found that combination I3C and bortezomib could sensitise cells to cisplatin in a dose-dependent manner (Figure 2A). To ensure that this effect was not limited to these cell lines, we tested a panel of ovarian cancer cell lines with equipotent concentrations of I3C and bortezomib plus cisplatin. Interestingly, we found that in all six cell lines tested, co-treatment

with I3C and bortezomib conferred sensitivity to cisplatin (Figure 2B and data not shown). To further explore the cytotoxic effects of I3C and bortezomib with conventional platinum-based chemotherapeutics, we examined the effect of carboplatin with I3C and bortezomib in OVCAR3 and OVCAR5 cells. Similarly, co-treatment with I3C and bortezomib could sensitise cells to carboplatin (Figure 2C) suggesting that I3C and bortezomib can increase the antitumour effects of standard platinum-based chemotherapeutic agents.

I3C and bortezomib combination enhances apoptosis

To determine whether the cytotoxic effects of I3C and bortezomib were due to apoptosis, annexin V and PI co-staining was performed followed by flow cytometric analysis. As the cytotoxic effects of I3C and bortezomib were evident at 24 h, we determined the effects on apoptosis at this time point to assess for direct effects. To evaluate the apoptotic effects of equipotent doses of I3C and bortezomib, the IC10 for each drug was established for OVCAR3 and OVCAR5 cells, which provided an initial concentration that caused minimal (10%) cytotoxicity. The IC10 for I3C in OVCAR3 and OVCAR5 were 180 and 450 μM, respectively, which induced apoptosis in both cell lines (Figure 3, upper panels). Raising the IC10 concentration by 1.5 fold increased apoptosis in a dose-dependent manner. The IC10 for bortezomib in OVCAR3 and OVCAR5 cells were 12.5 and 25 nM, respectively. Increasing concentrations of bortezomib similarly induced apoptosis in a dose-dependent manner (Figure 3, middle panels). When OVCAR3 and OVCAR5 cells were treated with combination I3C and bortezomib, a dose-dependent increase in apoptosis was observed compared with using either drug alone (Figure 3, lower panels). Specifically, we found that OVCAR3 cells treated with maximum doses of I3C/bortezomib increased apoptosis by 31.3% and 26.9% compared with I3C or bortezomib alone, respectively. OVCAR5 cells treated with maximum doses of I3C/bortezomib increased apoptosis by 57.8% and 56.8% compared with I3C or bortezomib alone, respectively. These data indicate that I3C and bortezomib induce apoptosis, and that the drug combination significantly enhances this effect, especially in OVCAR5 cells.

I3C and bortezomib combination induces cell cycle arrest

To determine whether the cytotoxic effects of I3C and bortezomib could be attributed to alterations in the cell cycle, OVCAR3 and OVCAR5 cells were treated with I3C and bortezomib for 24 h and subjected to PI flow cytometric analysis. Identical drug concentrations used for the annexin V/PI apoptosis assay were used for cell cycle analysis. We found that in OVCAR3 cells, increasing concentrations of I3C reduced the percentage of cells in G1 (Figure 4A), whereas I3C induced a G1 arrest at maximal concentration (675 μM) in OVCAR5 cells (Figure 4B). Increasing bortezomib concentrations induced a G2-M arrest in both OVCAR3 and OVCAR5 cells, although this effect was more pronounced in OVCAR5 cells (Figures 4A and B). In both OVCAR3 and

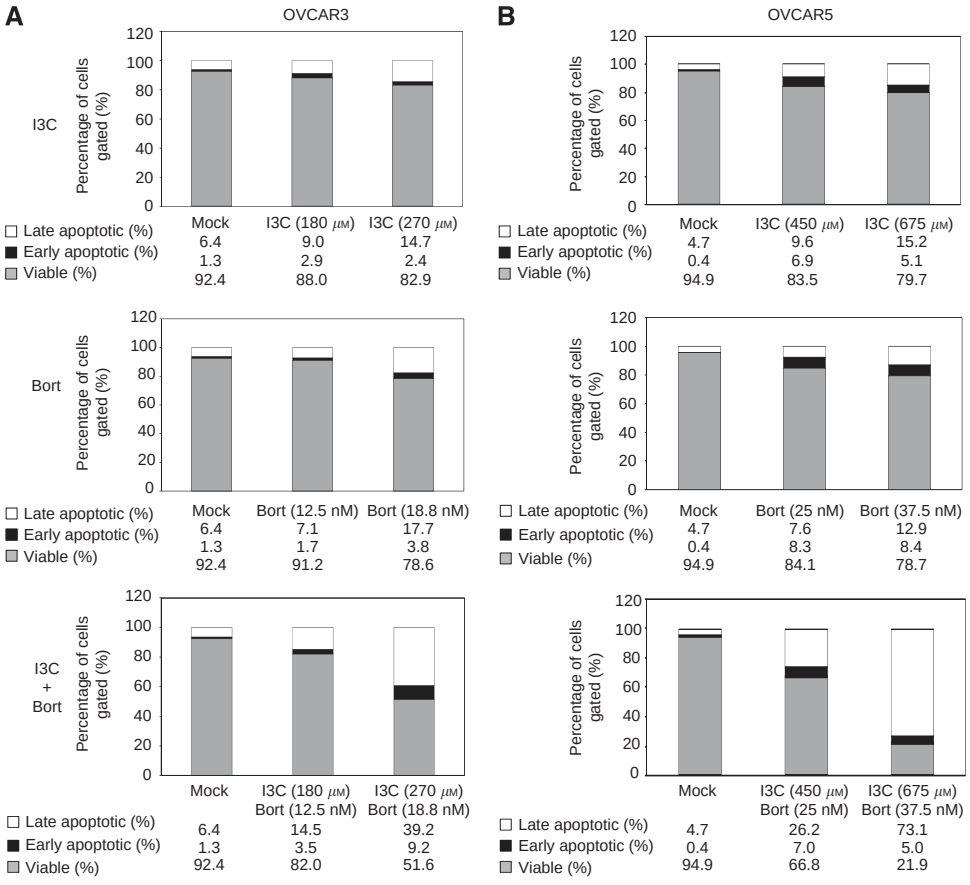

Figure 3 Indole-3-carbinol and bortezomib enhance apoptosis in OVCAR3 and OVCAR5 cells. (**A**) OVCAR3 and (**B**) OVCAR5 cells were treated with I3C, bortezomib or their combination for 24 h at the indicated concentrations. The cells were subsequently co-stained with annexin V and PI, and viable (annexin V-negative and PI-negative), early apoptotic (annexin V-positive and PI-negative) and late apoptotic (annexin V-positive and PI-positive) cells were distinguished by flow cytometric analysis. The stacked bar graph represents the mean percentage of viable (grey), early apoptotic (black) and late (white) apoptotic cells from a triplicate experiment.

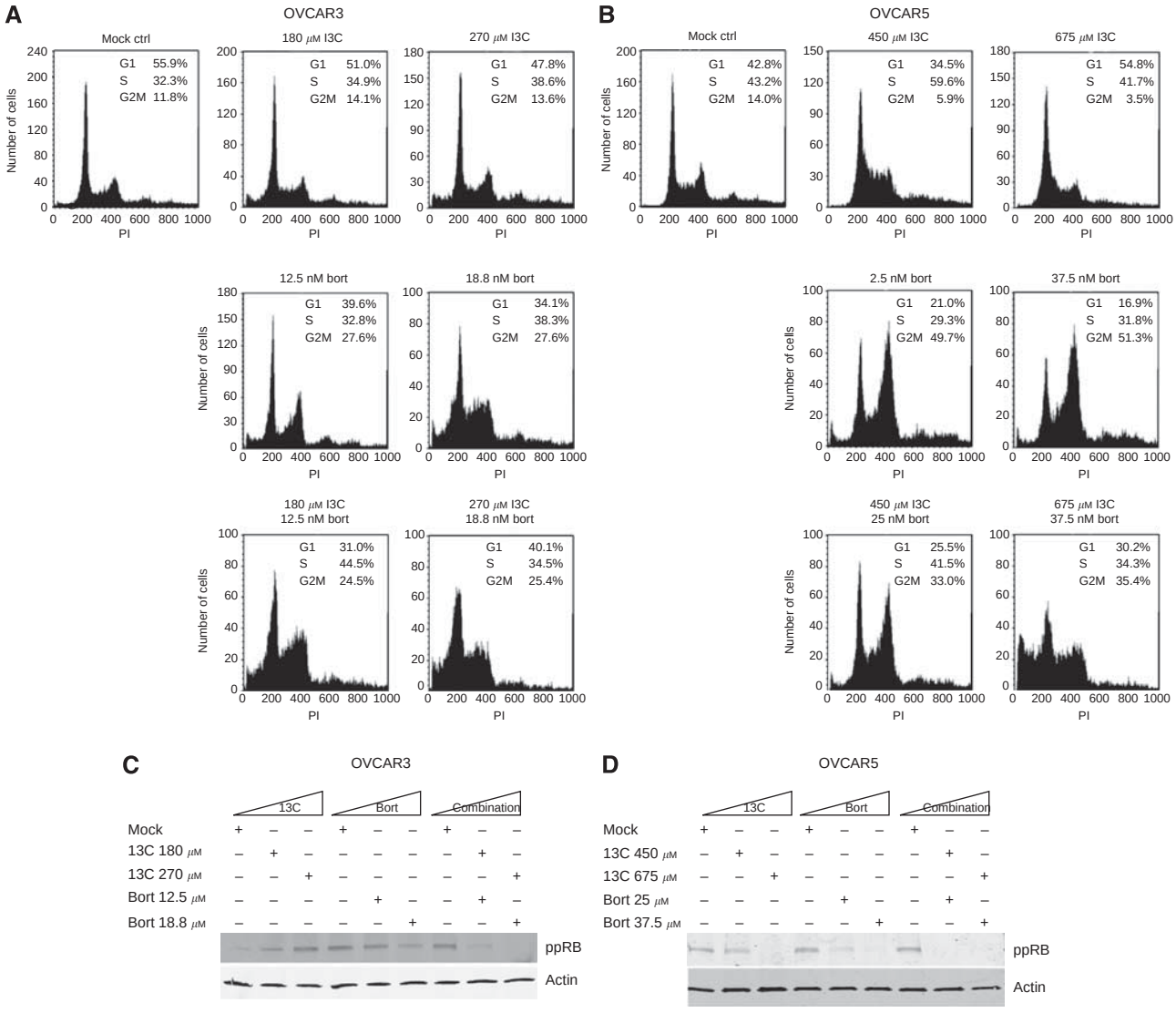

Figure 4 Indole-3-carbinol and bortezomib cause cell cycle arrest in OVCAR3 and OVCAR5 cells. (**A**) OVCAR3 and (**B**) OVCAR5 cells were treated with I3C, bortezomib or in combination for 24 h at the indicated concentrations. Cells were fixed and stained with PI followed by flow cytometric analysis for DNA content as described in Materials and Methods. A representative DNA histogram is shown for each condition. The mean percentage of cells from a triplicate experiment is indicated for cells in G1-, S- and G2-M-phase for each condition. (**C**) OVCAR3 and (**D**) OVCAR5 cells were treated with I3C, bortezomib or in combination as in (**A**) and (**B**), respectively. Whole-cell extracts were isolated and immunoblotted with the indicated antibodies. Actin was used as a loading control.

OVCAR5 cells, co-treatment with I3C and bortezomib shifted the cell cycle towards G2-M in a dose-dependent manner (Figures 4A and B). Additionally, OVCAR5 cells treated with combination I3C and bortezomib at maximum concentration exhibited a significant sub-G1 peak indicative of apoptosis (Figure 4B, bottom right), consistent with the elevated levels of apoptosis observed in annexin V/PI assays (Figure 3B, bottom right). These data suggest that while individual treatment with I3C and bortezomib have different effects on cell cycle distribution that appear to be context-dependent, the combination of these agents commonly impede the cell cycle by exerting a G2-M arrest.

In parallel, we sought to determine whether co-treatment with I3C and bortezomib may elicit a cell cycle arrest at the G1-S boundary. Co-treatment with increasing I3C and bortezomib severely reduced the levels of phosphorylated RB compared with using either drug alone (Figures 4C and D). This suggests that I3C and bortezomib can prevent RB phosphorylation and maintain RB in an active repressive state thereby blocking the cell cycle at the G1-S transition.

I3C and bortezomib combination affects multiple pathways important for cancer progression

To determine the mechanism responsible for the synergistic effect of I3C and bortezomib, we performed RNA microarray analysis. Considering that both the apoptotic and synergistic effects of I3C and bortezomib were more robust in OVCAR5 cells compared with OVCAR3 cells at equipotent doses, we selected OVCAR5 cells for microarray analysis. We treated OVCAR5 cells with vehicle (mock), 675 μM I3C, 37.5 nM bortezomib or combination for 24 h, identical to the maximum concentrations used for our apoptosis and cell cycle studies. Subsequent microarray analysis of replicate samples from triplicate experiments shared similar gene expression patterns that clustered together in the dendrogram (Figure 5A) demonstrating the high reproducibility of our results.

We focused on significantly altered genes ($P<0.0025$) with log-fold changes >1.5 (upregulated) or <-1.5 (downregulated). While I3C treatment has significantly more differentially expressed genes (216 genes) in common with co-treatment compared with

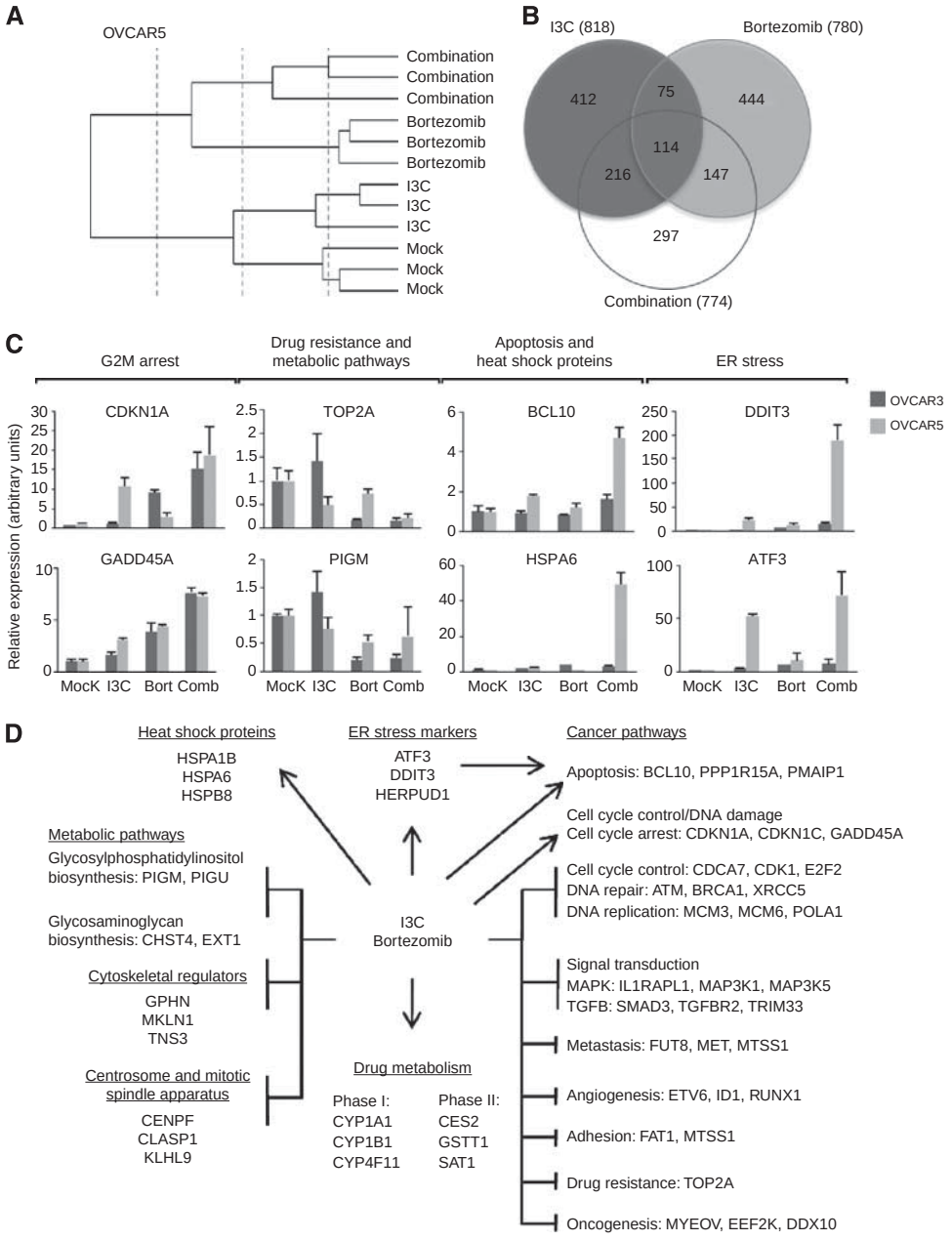

Figure 5 Indole-3-carbinol and bortezomib combination inhibits carcinogenesis, reduces chemoresistance, upregulates ER stress markers, deregulates metabolic pathways and causes widespread gene deregulation in OVCAR3 and OVCAR5 cells. OVCAR5 cells were treated with vehicle (mock), 675 μM I3C, 37.5 nM bortezomib or in combination for 24 h with subsequent RNA isolation and microarray gene expression analysis. (**A**) A dendrogram presentation of the data from triplicate experiments indicate that replicate samples cluster together. (**B**) Venn diagram representing overlap between I3C and bortezomib treatment. Target genes with log-fold changes >0.4 or <-0.4 ($P<0.0025$) are presented. (**C**) Quantitative RT–PCR of candidate target genes identified by microarray analysis categorised by function. Target gene validation was also performed in OVCAR3 cells treated with vehicle (mock), 270 μM I3C, 18.8 nM bortezomib or in combination for 24 h. (**D**) Pleiotropic effect of I3C and bortezomib on multiple biological processes. Representative target genes with log-fold changes >1.5 or <-1.5 ($P<0.0025$) are shown.

bortezomib (147 genes), the majority is unique to the combination condition (297 genes) (Figure 5B). In total, I3C/bortezomib treatment altered the expression of 774 genes. Classification of these genes indicate that co-treatment with I3C and bortezomib induces gene expression changes in multiple pathways, particularly carcinogenesis (Supplementary Table S2), consistent with the GO gene enrichment dataset (data not shown). Validation of our microarray data by qRT–PCR and western blot analysis in both OVCAR3 and OVCAR5 cells showed that target genes involved in cell cycle control (e.g., *CDKN1A* and *CDK1*), apoptosis (e.g., *BCL2L1* and *BCL10*) and signal transduction (e.g., *DUSP1* and *NFkBIB*) were significantly deregulated (Figure 5C, Supplementary Figure S1 and data not shown). Moreover, metastasis (e.g., *MET* and *SNAI1*), angiogenesis and adhesion target genes showed altered expression (Supplementary Figure S1 and Supplementary Table S2). Notably, co-treatment with I3C and bortezomib appeared to downregulate *TOP2A* and *ABCC4*, target genes that are typically associated with chemoresistance. Consistent with our microarray data, qRT–PCR showed that *TOP2A* was severely downregulated (Figure 5C), a result that was reproducible by

western analysis in OVCAR3 cells but not in OVCAR5 cells (Supplementary Figure S1B), suggesting that these effects are transient and/or evident only at the transcriptional level.

Besides promoting cell death and inhibiting cancer progression, the combination of I3C and bortezomib deregulated other biological processes including ER stress, protein folding, centrosome and mitotic spindle apparatus, carcinogen metabolism, metabolic pathways and cytoskeletal regulators (Supplementary Table S2). Representative target genes (e.g., *DDIT3*, *HSPA6* and *CENPF*) from each of these processes were validated by qRT–PCR with the majority of them demonstrating regulation as determined by microarray analysis (Figure 5C and Supplementary Figure S1A).

Overall, we found that co-treatment with I3C and bortezomib causes widespread gene deregulation that impinges on multiple pathways ultimately resulting in cell death (Figure 5D). A summary of target genes both related to and identified by microarray analysis were confirmed by qRT–PCR and western analysis (Supplementary Table S3).

I3C and bortezomib co-treatment inhibits the growth of OVCAR5 tumour xenografts in nude mice

To examine the effect of I3C and bortezomib *in vivo*, we monitored the tumour growth of OVCAR5 tumour xenografts in nude mice treated with I3C and/or bortezomib. Initially, we performed a dose-finding study to establish the tolerable dosages of I3C and bortezomib (see Supplementary Methods for details and Supplementary Figure S2). Based on our dose-finding data, we randomly assigned mice to the following four treatment groups: vehicle (control); I3C ($20\,mg\,kg^{-1}$); bortezomib ($1\,mg\,kg^{-1}$) or combination treatment ($20\,mg\,kg^{-1}$ I3C with $1\,mg\,kg^{-1}$ bortezomib). Although treatment with I3C or bortezomib alone initially induced tumour regression (Figure 6A), these mice relapsed after prolonged treatment ($\geqslant 31$ days post treatment). In contrast, the combination of I3C and bortezomib significantly inhibited tumour growth (Figure 6A) compared with control animals (64.6% tumour reduction, $P<0.001$) or individual treatment with I3C (47.6% tumour reduction, $P=0.007$) or bortezomib (35.9% tumour reduction, $P=0.029$) by the final day of treatment, consistent with our *in vitro* results. Indeed, the final weight (65.4% tumour reduction in I3C/bortezomib combination *vs* control, $P=0.053$) and appearance of the tumours post treatment were consistent with the measurements obtained from earlier time points (Figures 6B–D). Moreover, we found that co-treatment with reduced bortezomib levels ($0.5\,mg\,kg^{-1}$) inhibited tumour growth and increasing levels of I3C significantly potentiated bortezomib-induced tumour regression in a dose-dependent manner, emphasising the synergistic effect of these two drugs (Supplementary Figure S2).

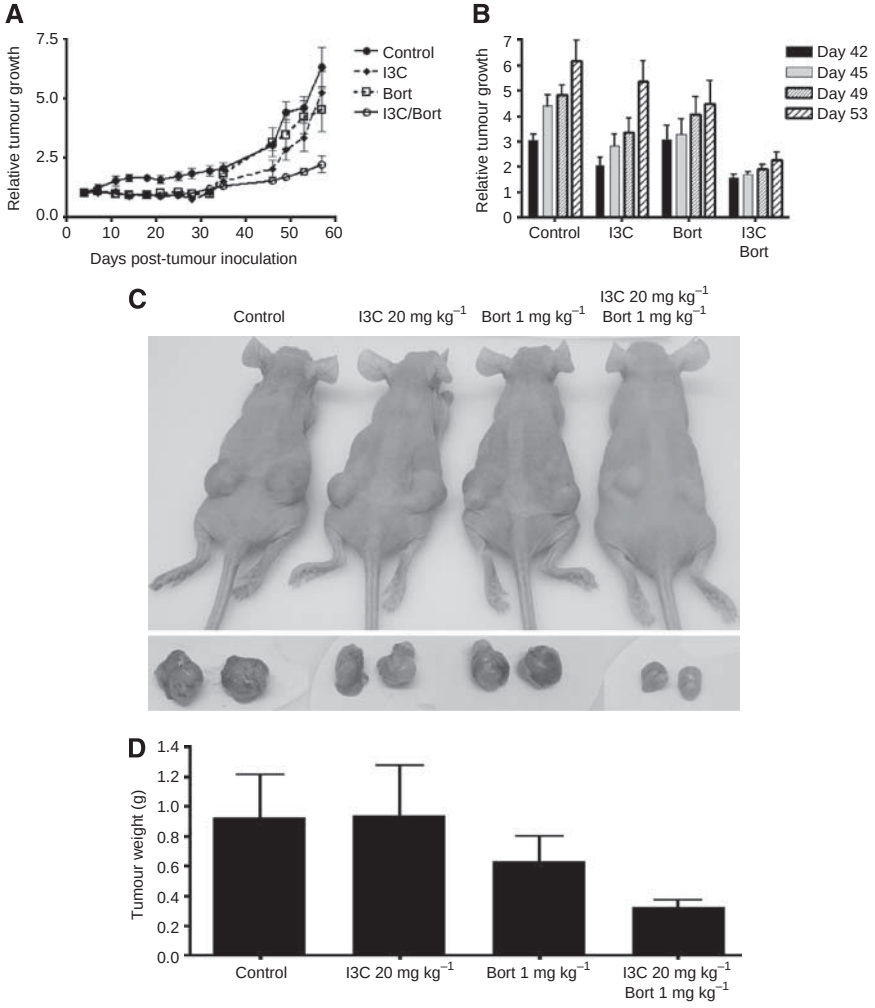

Figure 6 Indole-3-carbinol and bortezomib co-treatment inhibit human ovarian tumour xenografts in nude mice. (**A**) Relative tumour growth of OVCAR5 xenografts treated with vehicle (control), $20\,mg\,kg^{-1}$ I3C, $1\,mg\,kg^{-1}$ bortezomib or in combination measured from 0 to 53 days post treatment or (**B**) measured 42, 45, 49 and 53 days post treatment. The data shown represent the mean ± s.e.m. ($n=8$). (**C**) Representative tumour images of control-(vehicle), I3C- and bortezomib-treated mice pre and post dissection, with corresponding (**D**) tumour weight 53 days post treatment. The data shown represent the mean ± s.e.m. ($n=8$).

DISCUSSION

Ovarian cancer is a highly heterogeneous disease involving the deregulation of multiple genes and pathways commonly evaded by gene- or pathway-specific agents (Donninger *et al*, 2004; Landen *et al*, 2008). We rationalised that targeted therapeutics that can overcome drug resistance and exploit pathways involved in tumourigenesis may be beneficial in the treatment of ovarian cancer. Here, we have shown that the combination of potent anticarcinogens, I3C and bortezomib, inhibits several signalling pathways and exerts antiproliferative and apoptotic effects in ovarian cancer cells, consistent with the individual properties of these drugs. Microarray analysis and validation studies showed that combination I3C and bortezomib induces pleiotropic effects reflecting its use as a multi-targeted combination therapy. We have extended the limited data of I3C treatment in ovarian cancer and found that I3C and bortezomib combination demonstrate synergistic cytotoxicity through additionally influencing chemoresistance, metastasis, cytoskeletal regulation, ER stress, carcinogen metabolism and metabolic pathways. Importantly, we show that I3C and bortezomib co-treatment inhibits tumour growth *in vivo*. Collectively, these data provide the first evidence that combining I3C with bortezomib is effective and may demonstrate a clinical benefit in the management of ovarian cancer.

In our study, we found that inhibition of carcinogenesis-associated pathways was the main mechanism of combination I3C/bortezomib-induced cytotoxicity, particularly through inhibition of cell proliferation, DNA replication and promotion of cell cycle arrest, consistent with our findings *in vivo*. Additionally, deregulation of the cell cycle was extended to centrosome and mitotic spindle apparatus inactivation. As many of the target genes altered by combination I3C and bortezomib were involved in cell cycle control, we explored whether the mechanism of these drugs may act through a common cell-cycle-related factor. Given that I3C and bortezomib inhibit the cyclin E pathway using independent mechanisms (Nguyen *et al*, 2008; Uddin *et al*, 2008, 2009; Bruning *et al*, 2009), we considered whether overexpression of cyclin E would cause an enhanced response to combination therapy. However, synergy was more robust in low-cyclin-E-expressing OVCAR5 cells compared with OVCAR3 cells, implying that the mechanism of I3C and bortezomib is cyclin-E-independent, and that other biological pathways are responsible for the effects seen with this drug combination.

Indeed, I3C and bortezomib combination induced apoptosis and inhibited several signal transduction pathways that promote cell survival, including MAPK, TGFβ, NFkB and PI3K-AKT. Co-treatment with these two agents also affected metastasis and tumour suppressor genes (TSGs). One metastasis-associated gene, *MET*, is a proto-oncogene that was downregulated both at the RNA and protein level consistent with our microarray analysis. MET promotes tumour growth, angiogenesis and activates multiple cell survival signalling pathways (Xiao *et al*, 2001; Birchmeier *et al*, 2003; Derksen *et al*, 2003; Garcia *et al*, 2007). Aberrant MET activation occurs in many human cancers, correlates with poor prognosis, and is considered an important candidate for targeted therapy (Kaposi-Novak *et al*, 2006; Comoglio *et al*, 2008; Liu *et al*, 2008). However, we also identified and confirmed the upregulation of SNAI1, which promotes tumour growth and metastasis in various solid tumours, including ovarian (Jin *et al*, 2010). Several TSGs were deregulated including *CCBE1*. Interestingly, *CCBE1* is a new TSG candidate that was upregulated in our microarray dataset and is frequently inactivated in ovarian cancer (Barton *et al*, 2010). Several biotransformation enzymes required for carcinogen detoxification were upregulated in our microarray dataset similar to treatment with I3C in prostate cancer cells (Li *et al*, 2003). Metabolic enzymes required for post-translational modifications were deregulated, including downregulation of *PIGM*, a gene encoding a glycosylphosphatidylinositol biosynthetic enzyme required for growth in yeast (Maeda *et al*, 2001; Kim *et al*, 2007). Among the validated targets, ER stress (*DDIT3* and *ATF3*) and heat shock proteins (*HSPA6*) were the most severely upregulated. This is typically observed in cells undergoing cellular stress (Santoro, 2000), and is preceded by ER stress and DDIT3-induced apoptosis (Zimmermann *et al*, 2000; Fribley and Wang, 2006). We also found that chemoresistance-associated genes *TOP2A* (cell-cycle-regulated gene) and *ABCC4* (multidrug-resistant gene) were both downregulated, although the latter was just above the log-fold threshold (-1.47). TOP2A is upregulated in chemoresistant ovarian and hepatocellular tumours, and correlates with reduced survival (Ju *et al*, 2009; Wong *et al*, 2009), implying that I3C/bortezomib treatment may circumvent drug resistance. Consistent with this, our data also demonstrated that I3C/bortezomib treatment sensitised cells to standard platinum-based chemotherapeutic agents.

From a clinical perspective, these findings in conjunction with our I3C/bortezomib-induced tumour regression data provide compelling evidence for the potential treatment of patients that succumb to platinum-resistant disease. Future studies that address whether I3C/bortezomib treatment can potentiate the effects of cisplatin and carboplatin *in vivo* or additional *in vivo* studies that compare I3C/bortezomib treatment with standard combination chemotherapy (e.g., cisplatin/paclitaxel) could highlight the advantage of this novel drug combination.

We acknowledge several limitations of our study. First, we selected a single cell line and time point to determine the mechanism of I3C and bortezomib action. Overlap of the target genes from an additional OVCAR3 microarray study may have narrowed down the most essential target genes/pathways required for I3C and bortezomib action. As the cytotoxic effect of I3C and bortezomib was rapid (24 h), a compilation of gene expression profiles from earlier time points may provide more insight into the mechanism of these combined agents in ovarian cancer, similar to the study performed with I3C in prostate cancer cells at three time points (Li *et al*, 2003). Second, we primarily focused on target genes that had log-fold changes >1.5 or <-1.5. According to our arbitrary cutoff, 189 genes were significantly deregulated in our microarray analysis that failed to meet the log-fold ratio criteria. This suggests that additional target genes/pathways that confer subtle changes in gene expression may contribute to the deleterious effects of I3C and bortezomib. Third, bortezomib resistance is a significant problem despite clinical success in patients with myeloma and mantle cell lymphoma (Ruschak *et al*, 2011). Perhaps using alternative, irreversible proteasome inhibitors in combination with I3C may demonstrate comparable or improved effects.

In summary, this is the first study to describe the synergistic effects of combination I3C and bortezomib in ovarian cancer. The ability of this combination of agents to inhibit tumour growth *in vivo*, sensitise cells to standard chemotherapeutic agents, promote apoptosis and interfere with genes affecting multiple pathways important for cancer progression supports the utility of I3C and bortezomib in the treatment of ovarian cancer.

ACKNOWLEDGEMENTS

We thank Dr Vincent Funari and Yuan Xue from Cedars-Sinai Genomics Core for microarray gene expression profiling, Patricia Lin from Cedars-Sinai Flow Cytometry Core Facility for technical assistance, Dr Phillip Koeffler's laboratory for assistance with the CalcuSyn software and Dr Ruprecht Wiedemeyer for technical advice. This work was supported by career development awards to CSW from the Department of Defense Ovarian Cancer Research Program (award contract no. W81XWH-1-0209; log no. OC080179)

and the UCLA Clinical and Translational Science Institute (CTSI) Scholars Program. SO is supported by the Grant RSG-10-252-01-TBG from the American Cancer Society. The funding organisations had no role in the design and conduct of the study, collection, management, analysis and interpretation of the data, and preparation, review or approval of the manuscript.

Conflict of interest

The authors declare no conflict of interest.

Supplementary Information accompanies the paper on British Journal of Cancer website (http://www.nature.com/bjc)

REFERENCES

Aghajanian C, Blessing JA, Darcy KM, Reid G, DeGeest K, Rubin SC, Mannel RS, Rotmensch J, Schilder RJ, Riordan W; Gynecologic Oncology Group (2009) A phase II evaluation of bortezomib in the treatment of recurrent platinum-sensitive ovarian or primary peritoneal cancer: a Gynecologic Oncology Group study. *Gynecol Oncol* **115:** 215 – 220

Aghajanian C, Dizon DS, Sabbatini P, Raizer JJ, Dupont J, Spriggs DR (2005) Phase I trial of bortezomib and carboplatin in recurrent ovarian or primary peritoneal cancer. *J Clin Oncol* **23:** 5943 – 5949

Barton CA, Gloss BS, Qu W, Statham AL, Hacker NF, Sutherland RL, Clark SJ, O'Brien PM (2010) Collagen and calcium-binding EGF domains 1 is frequently inactivated in ovarian cancer by aberrant promoter hypermethylation and modulates cell migration and survival. *Br J Cancer* **102:** 87 – 96

Bast Jr RC, Hennessy B, Mills GB (2009) The biology of ovarian cancer: new opportunities for translation. *Nat Rev Cancer* **9:** 415 – 428

Birchmeier C, Birchmeier W, Gherardi E, Vande Woude GF (2003) Met, metastasis, motility and more. *Nat Rev Mol Cell Biol* **4:** 915 – 925

Boccadoro M, Morgan G, Cavenagh J (2005) Preclinical evaluation of the proteasome inhibitor bortezomib in cancer therapy. *Cancer Cell Int* **5:** 18

Bruning A, Burger P, Vogel M, Rahmeh M, Friese K, Lenhard M, Burges A (2009) Bortezomib treatment of ovarian cancer cells mediates endoplasmic reticulum stress, cell cycle arrest, and apoptosis. *Invest New Drugs* **27:** 543 – 551

Chinni SR, Li Y, Upadhyay S, Koppolu PK, Sarkar FH (2001) Indole-3-carbinol (I3C) induced cell growth inhibition, G1 cell cycle arrest and apoptosis in prostate cancer cells. *Oncogene* **20:** 2927 – 2936

Chou TC, Talalay P (1984) Quantitative analysis of dose-effect relationships: the combined effects of multiple drugs or enzyme inhibitors. *Adv Enzyme Regul* **22:** 27 – 55

Comoglio PM, Giordano S, Trusolino L (2008) Drug development of MET inhibitors: targeting oncogene addiction and expedience. *Nat Rev Drug Discov* **7:** 504 – 516

Cresta S, Sessa C, Catapano CV, Gallerani E, Passalacqua D, Rinaldi A, Bertoni F, Viganò L, Maur M, Capri G, Maccioni E, Tosi D, Gianni L (2008) Phase I study of bortezomib with weekly paclitaxel in patients with advanced solid tumours. *Eur J Cancer* **44:** 1829 – 1834

Derksen PW, de Gorter DJ, Meijer HP, Bende RJ, van Dijk M, Lokhorst HM, Bloem AC, Spaargaren M, Pals ST (2003) The hepatocyte growth factor/Met pathway controls proliferation and apoptosis in multiple myeloma. *Leukemia* **17:** 764 – 774

Donninger H, Bonome T, Radonovich M, Pise-Masison CA, Brady J, Shih JH, Barrett JC, Birrer MJ (2004) Whole genome expression profiling of advance stage papillary serous ovarian cancer reveals activated pathways. *Oncogene* **23:** 8065 – 8077

Du P, Kibbe WA, Lin SM (2008) Lumi: a pipeline for processing Illumina microarray. *Bioinformatics* **24:** 1547 – 1548

Etemadmoghadam D, deFazio A, Beroukhim R, Mermel C, George J, Getz G, Tothill R, Okamoto A, Raeder MB, Harnett P, Lade S, Akslen LA, Tinker AV, Locandro B, Alsop K, Chiew YE, Traficante N, Fereday S, Johnson D, Fox S, Sellers W, Urashima M, Salvesen HB, Meyerson M, Bowtell D, AOCS Study Group (2009) Integrated genome-wide DNA copy number and expression analysis identifies distinct mechanisms of primary chemoresistance in ovarian carcinomas. *Clin Cancer Res* **15:** 1417 – 1427

Falcon S, Gentleman R (2007) Using GOstats to test gene lists for GO term association. *Bioinformatics* **23:** 257 – 258

Fribley A, Wang CY (2006) Proteasome inhibitor induces apoptosis through induction of endoplasmic reticulum stress. *Cancer Biol Ther* **5:** 745 – 748

Garcia S, Dales JP, Charafe-Jauffret E, Carpentier-Meunier S, Andrac-Meyer L, Jacquemier J, Andonian C, Lavaut MN, Allasia C, Bonnier P, Charpin C (2007) Overexpression of c-Met and of the transducers PI3K, FAK and JAK in breast carcinomas correlates with shorter survival and neoangiogenesis. *Int J Oncol* **31:** 49 – 58

Jin H, Yu Y, Zhang T, Zhou X, Zhou J, Jia L, Wu Y, Zhou BP, Feng Y (2010) Snail is critical for tumor growth and metastasis of ovarian carcinoma. *Int J Cancer* **126:** 2102 – 2111

Ju W, Yoo BC, Kim IJ, Kim JW, Kim SC, Lee HP (2009) Identification of genes with differential expression in chemoresistant epithelial ovarian cancer using high-density oligonucleotide microarrays. *Oncol Res* **18:** 47 – 56

Kaposi-Novak P, Lee JS, Gomez-Quiroz L, Coulouarn C, Factor VM, Thorgeirsson SS (2006) Met-regulated expression signature defines a subset of human hepatocellular carcinomas with poor prognosis and aggressive phenotype. *J Clin Invest* **116:** 1582 – 1595

Kim YU, Ashida H, Mori K, Maeda Y, Hong Y, Kinoshita T (2007) Both mammalian PIG-M and PIG-X are required for growth of GPI14-disrupted yeast. *J Biochem* **142:** 123 – 129

Landen Jr CN, Birrer MJ, Sood AK (2008) Early events in the pathogenesis of epithelial ovarian cancer. *J Clin Oncol* **26:** 995 – 1005

Li Y, Li X, Sarkar FH (2003) Gene expression profiles of I3C- and DIM-treated PC3 human prostate cancer cells determined by cDNA microarray analysis. *J Nutr* **133:** 1011 – 1019

Liu X, Yao W, Newton RC, Scherle PA (2008) Targeting the c-MET signaling pathway for cancer therapy. *Expert Opin Investig Drugs* **17:** 997 – 1011

Maeda Y, Watanabe R, Harris CL, Hong Y, Ohishi K, Kinoshita K, Kinoshita T (2001) PIG-M transfers the first mannose to glycosylphosphatidylinositol on the lumenal side of the ER. *EMBO J* **20:** 250 – 261

Naik R, Nixon S, Lopes A, Godfrey K, Hatem MH, Monaghan JM (2006) A randomized phase II trial of indole-3-carbinol in the treatment of vulvar intraepithelial neoplasia. *Int J Gynecol Cancer* **16:** 786 – 790

Nakayama N, Nakayama K, Shamima Y, Ishikawa M, Katagiri A, Iida K, Miyazaki K (2010) Gene amplification CCNE1 is related to poor survival and potential therapeutic target in ovarian cancer. *Cancer* **116:** 2621 – 2634

Nguyen HH, Aronchik I, Brar GA, Nguyen DH, Bjeldanes LF, Firestone GL (2008) The dietary phytochemical indole-3-carbinol is a natural elastase enzymatic inhibitor that disrupts cyclin E protein processing. *Proc Natl Acad Sci USA* **105:** 19750 – 19755

Rahman KW, Li Y, Wang Z, Sarkar SH, Sarkar FH (2006) Gene expression profiling revealed survivin as a target of 3,3′-diindolylmethane-induced cell growth inhibition and apoptosis in breast cancer cells. *Cancer Res* **66:** 4952 – 4960

Raj MH, Abd Elmageed ZY, Zhou J, Gaur RL, Nguyen L, Azam GA, Braley P, Rao PN, Fathi IM, Ouhtit A (2008) Synergistic action of dietary phyto-antioxidants on survival and proliferation of ovarian cancer cells. *Gynecol Oncol* **110:** 432 – 438

Ramirez PT, Landen Jr CN, Coleman RL, Milam MR, Levenback C, Johnston TA, Gershenson DM (2008) Phase I trial of the proteasome inhibitor bortezomib in combination with carboplatin in patients with platinum- and taxane-resistant ovarian cancer. *Gynecol Oncol* **108:** 68 – 71

Reed GA, Peterson KS, Smith HJ, Gray JC, Sullivan DK, Mayo MS, Crowell JA, Hurwitz A (2005) A phase I study of indole-3-carbinol in women: tolerability and effects. *Cancer Epidemiol Biomarkers Prev* **14:** 1953 – 1960

Rosen CA, Bryson PC (2004) Indole-3-carbinol for recurrent respiratory papillomatosis: long-term results. *J Voice* **18:** 248 – 253

Ruschak AM, Slassi M, Kay LE, Schimmer AD (2011) Novel proteasome inhibitors to overcome bortezomib resistance. *J Natl Cancer Inst* **103:** 1007 – 1017

Santoro MG (2000) Heat shock factors and the control of the stress response. *Biochem Pharmacol* **59:** 55 – 63

Smyth GK (2005) Limma: linear models for microarray data. In *Bioinformatics and Computational Biology Solutions using R and*

Bioconductor, Gentleman R, Carey V, Dudoit S, Irizarry R, Huber W (eds) pp 397 – 420. Springer: New York

Taylor-Harding B, Orsulic S, Karlan BY, Li AJ (2010) Fluvastatin and cisplatin demonstrate synergistic cytotoxicity in epithelial ovarian cancer cells. *Gynecol Oncol* **119:** 549 – 556

Uddin S, Ahmed M, Bavi P, El-Sayed R, Al-Sanea N, AbdulJabbar A, Ashari LH, Alhomoud S, Al-Dayel F, Hussain AR, Al-Kuraya KS (2008) Bortezomib (velcade) induces p27Kip1 expression through S-phase kinase protein 2 degradation in colorectal cancer. *Cancer Res* **68:** 3379 – 3388

Uddin S, Ahmed M, Hussain AR, Jehan Z, Al-Dayel F, Munkarah A, Bavi P, Al-Kuraya KS (2009) Bortezomib-mediated expression of p27Kip1 through S-phase kinase protein 2 degradation in epithelial ovarian cancer. *Lab Invest* **89:** 1115 – 1127

Weng JR, Tsai CH, Kulp SK, Chen CS (2008) Indole-3-carbinol as a chemopreventive and anti-cancer agent. *Cancer Lett* **262:** 153 – 163

Wong N, Yeo W, Wong WL, Wong NL, Chan KY, Mo FK, Koh J, Chan SL, Chan AT, Lai PB, Ching AK, Tong JH, Ng HK, Johnson PJ, To KF (2009) TOP2A overexpression in hepatocellular carcinoma correlates with early age onset, shorter patients survival and chemoresistance. *Int J Cancer* **124:** 644 – 652

Wright JJ (2010) Combination therapy of bortezomib with novel targeted agents: an emerging treatment strategy. *Clin Cancer Res* **16:** 4094 – 4104

Xiao GH, Jeffers M, Bellacosa A, Mitsuuchi Y, Vande Woude GF, Testa JR (2001) Anti-apoptotic signaling by hepatocyte growth factor/Met via the phosphatidylinositol 3-kinase/Akt and mitogen-activated protein kinase pathways. *Proc Natl Acad Sci USA* **98:** 247 – 252

Zimmermann J, Erdmann D, Lalande I, Grossenbacher R, Noorani M, Furst P (2000) Proteasome inhibitor induced gene expression profiles reveal overexpression of transcriptional regulators ATF3, GADD153 and MAD1. *Oncogene* **19:** 2913 – 2920